Sensing for Offal Grading and Enablement of Automation

PROJECT CODE:	**2016-1003**
PREPARED BY:	AgResearch Ltd
DATE SUBMITTED:	10 August 2018
DATE PUBLISHED:	XXX
PUBLISHED BY:	AgResearch Ltd

The Australian Meat Processor Corporation acknowledges the matching funds provided by the Australian Government to support the research and development detailed in this publication.

TABLE OF CONTENTS

1.0 EXECUTIVE SUMMARY

Offal inspection requires both internal (excision and/or palpitation) and external (visual) activities. Therefore an automated offal inspection station must offer both internal and external inspection mechanisms. It must also differentiate between tissues and surface cells (fat, moisture and linings). This suggests that a single type of sensor is unlikely to offer sufficient efficacy to fully identify and inspect offal.

This project seeks to simplify this complex problem by using several sensors located in a multi-sensor tunnel. Each sensor obtains the ”piece” of inspection information for which that sensor is most suited, which are then merged to create a multi layered dataset (“image”) from which an overall inspection decision and/or robotic sorting decision is extracted. The project uses (a) X-ray images to inspect internally for cysts, lesions and pus and (b) hyperspectral imagers and RGB cameras (with UV and white light sources) to inspect surfaces for lesions, colour and contamination.

Further, these sensors produce high resolution images which would enable automatic selection, sorting and picking of the offal and allow information to be overlaid into a composite image for a human grader or auditor to assess. The sensors and techniques developed in this project may have future applications in carcase grading and identifying regions to be trimmed to remove contamination (including pre- and post-trim validation of the trim to minimize yield loses).

Reported here are two streams of work to progress the development of automatic offal inspection using multiple sensors, namely (a) a Freedom to Operate (FTO) search and (b) the development of prototype inspection algorithms using RGB digital cameras, Hyperspectral cameras and X-ray scanners.

Freedom to Operate (FTO) searches were conducted on multiple public databases including MLA’s and AMPC’s public publications, scientific and trade journals, patent databases and internet search engines. These searches identified the use of spectral technologies including vision, hyperspectral imaging, UV imaging, and single and dual energy X-ray in meat industry applications. None of the articles or patents examined advocated the use of multiple sensors to inspect offal for disease. Based on the FTO search undertaken, it appears that AMPC has FTO to develop and use hyperspectral imaging, DXA imaging and RGB-UV imaging sensors in a multi-sensor tunnel for the purpose of offal inspection. It is recommended that a watching brief be established to identify new patent publications and/or grants that may cause a new infringement.

The Inspection Algorithm Development stream comprised:

- Sourcing and/or assembling tunnel components (as separate sub-systems) which were taken to meat plants and used to capture spectral images of major offal components (liver, kidneys, lungs, heart) on a tray.
- Developing algorithms to import resultant “images” (spectral data), merge the images into datacubes, analyse the datacubes spectrally to predict tissue types and disease status, and assign pixels colour codes in a “results image”.

The “offal identification” algorithm demonstrated the ability of spectral devices to accurately classify tissue speedily even when tissue is partially obscured by other tissue. Some misclassifications were attributable to a function in the RGB camera and HSI imager that when disabled will further improve the accuracy of the algorithms. The “condemned offal” algorithms were able to differentiate between “healthy” and “diseased” tissue such as cirrhosis, facial eczema, abscesses, c. ovis, kidney necrosis and lung diseases, however diseases causing adhesion between tissues (e.g. pleurisy) were not “obvious” spectrally. Processing times are less than a few seconds.

This work identified risks associated with using default settings in manufacturer supplied interfaces in scientific work. Default control settings in the webcam and HSI imager automatically adjusted the cameras to maximize the brightness of each image depending on which combination of offal was on the tray. As spectral processing relies on the "spectra being the same for the same tissue", this impacted the accuracy of the algorithms. Controlling the settings for the webcam and HSI imager, including those for the aperture and exposure to fix the light sensitivity, has been recommended.

The RGB and HSI cameras have the disadvantage of only being able to "see" the upper surfaces (i.e. facing the camera). The X-ray scanner used cannot detect surface diseases easily. Thus, although the algorithms are satisfactory for classifying offal, consideration will need to be given to turning the offal to enable the RGB and HSI imagers to see thin surface defects hidden on the underside.

The X-ray unit uses dual energy X-ray absorptiometry (DEXA) optimised for baggage scanning. The spatial resolution is excellent and allowed very detailed internal structures to be observed. However, the low-high energy split does not discriminate well for organic materials (which preferentially absorb X-rays in the low energy range). It is recommended that detectors with better discriminate in the low energy ("organic") region be used. These may also allow the surface defects to be seen without touching the offal.

The DXA images provided 100% inspection of the offal. However with the unit used, the geometry between the generator, detectors and offal created parallax differences between the left and right sides of the images. This also meant that the DXA images could not be directly overlaid on to the RGB and HSI images. It was also recommended that a bespoke X-ray tunnel be designed and built that minimises the parallax with the X-ray image and between the X-ray and other imagers.

While the algorithms worked well on the dataset available, they have only been tested on a limited range of diseases and age of animals. Future work needs to extend this dataset.

The use of LED lighting for the visible and UV imaging with the webcam worked well and their continued use is recommended. NIR illumination was provided by halogen lights and are commonly used in NIR/HSI applications. However, they have disadvantages including: requiring very stable specialist DC power supply; needing several bulbs mounted well away from the offal in order to spread their light evenly; and having glass lens and running hot and therefore need isolating from water and people. NIR LEDs would be a more suitable illumination source and have a low profile. Purchase (or development) of an LED based NIR illumination system is recommended. This would allow both visible and NIR LEDs to be mounted within centimetres of the offal and is better suited to a tunnel application.

This project has demonstrated that multiple sensing technologies can identify and inspect offal internally and externally, and classify between organs fit for consumption and those needing to be condemned. The data can be captured, processed and action taken within a few seconds and would enable real time sorting in plants. The project also identified factors that need to be addressed, such as (a) using bespoke camera interfaces, (b) aligning sensor "views" (e.g. minimising parallax between the imaging technologies) and (c) sourcing "Meat Plant Suitable" sources of illumination.

2.0 INTRODUCTION

Grading currently requires a highly trained person who must concentrate for long periods while making rapid time-bound decisions relating to food safety, thus there are high labour costs and business risks associated with human graders.

Many sensors have been proposed for replacing humans in grading and evaluating carcases and offal. Grading inspection requires both internal (excision and/or palpitation) and external (visual) activities, yet few sensors are capable of both surface (reflective) and penetrative measurement. AgResearch has experience in many sensors and understands the advantages and shortcomings of these. For example, X-rays offer moderate definition images of internal attributes but cannot show surface attributes; NIR is an excellent sensor of chemical attributes of cells within a few mm of the surface but cannot penetrate further; UV is slightly penetrative but is more useful for detecting surface bacteria where fluorescent light emissions can be detected; and Hyperspectral images merge the best of NIR spectra and visual information albeit at the cost of requiring complex analytical techniques. Over the past decade, AgResearch has purchased commercially available examples of each of these sensors, built its internal analytical capability, and developed experience in merging data and images from multiple sensors into a coherent multi-sensor device able to operate in "harsh" (e.g. meat plant) environments. AgResearch has also learnt how to move from high resolution lab-based expensive equipment used to develop proof-of-concepts to lower cost, "good enough resolution" robust equipment suitable for in-plant use without compromising the overall ability to produce a meaningful result.

Grading is a complex problem which we propose to simplify by using specific sensors to obtain the "pieces" of grading information for which that sensor is most suited and then merge these pieces to create a multi layered image from which to extract an overall grading decision. These images will also be pixelated to a moderate resolution and could therefore be used to extract spatial information for enabling robotic sorting.

A successful project will deliver a robust automatic grading station delivering objective results in real-time while maintaining auditable data files. It would:

- replace human graders (reducing labour costs);
- never be tired or lose concentration (reduce business risk)
- maintain auditable data files on FIFO basis (reduce compliance risks and enhance customer's business risk)
- provide spatial data to enable future robotic manipulation of the offal and potentially carcases (productivity gains)

AgResearch has developed significant skills in applying spectral and imaging technologies to determining the composition and health of biological and organic materials in real world applications. Of relevance to this project are several projects using X-ray (1, 2), visible/RGB (confidential commercial), NIR/HSI (3, 4) and microwave (5, 6).

3.0 PROJECT OBJECTIVES

The objectives of the Sensing for Offal Grading and Enablement of Automation are:

3.1 Proof of Concept

3.1.1 Freedom to Operate

- A thorough literature search will be completed in MLA and AMPC Reports, Trade Journals and Academic Journals.
- A patent search will be conducted in Australia and PCT databases to establish Freedom to Operate. These searches will be collated and learnings incorporated into the Proof of Concept.

3.1.2 Offal Position on Tray Algorithms

- The spectral image data will be processed to identify the pieces of offal and their position on the tray.
- A successful outcome will be algorithms able to correctly identify the major pieces of offal and their spatial position using only data from the sensors.

3.2 Inspection Algorithms

- Data from the sensors above will be automatically extracted and processed in near real-time.
- The units will be located into a plant, offal from many animals scanned and their grading results recorded.
- Images associated with manually "condemned offal" (by AQIS/MPI) will be analysed to develop algorithms able to differentiate "good" from "condemned" material.
- A successful outcome for Stages 1 & 2 will be algorithms able to: (a) process merged data and report results within several seconds; (b) if sufficient data are available, to differentiate between "good" and "condemned" material; and (c) provide spatial data for the locations of the major offal pieces.

  Note: At this stage the sensors will not be integrated into one tunnel. This is especially the case for the x-ray machine which is subject to regulatory controls.

3.3 Proposed Next Steps

Stage 3: The project proposal outlined a subsequent project to integrate the sensors into an Integrated Sensor Tunnel for Commercial Installation. The integrated tunnel would be installed in a "demonstration plant" to be run in parallel with human graders.

- Images of offal (both healthy and condemned) would be extracted and used to refine the grading algorithms.
- The project team will work with AQIS/MPI to determine the performance criteria for regulatory approval to be used in plant, (Nominally this would be a similar false-positive and false-negative rates to human graders)

Stage 4: A commercialiser(s) will sell and support the device to Industry. They will also develop algorithms to grade other species. If approved by AMPC, AgResearch and the commercialisers will leverage knowledge developed in this project to develop a similar tool for carcase grading and/or trimming.

4.0 METHODOLOGY

4.1 Freedom to Operate Searches

Several searches were conducted to identify technologies and applications could (a) be used in this project and/or (b) that the outcomes of this project might infringe.

For the literature, internet and patent searches, the "non-invasive technologies" were restricted to commercially available technologies to ensure that technologies identified were purchasable and therefore available to this project and/or AMPC commercialisers. Thus the technologies nominated were:

- X-ray, DEXA (also DXA), CT (1)
- Vision (RGB) and UV fluorescence
- NIR and hyperspectral imaging (HSI) (2)
- MRI, NMR
- Ultrasound
- Microwave (3)

1. Hyperspectral X-ray scanners (greater than two energy levels) have current patents and cannot be used without a license. Therefore only DXA systems have been used in this project to date. (Refer patents US8000440; NZ548456; EU20141557)

2. Multi-spectral imagers (with several discrete and separated bands) are a sub-set of Hyperspectral imagers (with many contiguous bands)

3. Terahertz can be generated using high frequency microwave techniques (up to about 1000GHz, i.e. 1THz) or induced with lasers and diodes (> 1THz)

4.1.1 MLA and AMPC reports strategy, search terms and results

The MLA website report search page (https://www.mla.com.au/research-and-development/) and AMPC (www.ampc.com.au/research/reports) were accessed and searched for reports and case studies describing projects related to offal, inspection, and non-invasive measurement technologies.

The literature returned 10 hits relating the use of non-invasive technologies in MLA and/or AMPC projects. While these reports identify the usefulness of technologies such as vision, DEXA, NIR and IoT, there were no reports describing or advocating the use of multiple technologies to inspect red meat offal similar to this project.

4.1.2 Literature search strategy, search terms and results

Databases searched

The Biosis previews, CAB Abstracts, FSTA, Medline, Scopus and various websites were accessed and searched to identify non-invasive technologies used to inspect and/or grade offal after evisceration (i.e. not the carcase or "live animal"). While the search looked primarily for scientific uses of technologies, articles identifying commercially available inspection systems were also returned.

Search strings used

offal* adj21 (inspect OR inspection OR grade OR grading OR assessment OR assessing or surveillance); viscera adj21 (inspect OR inspection OR grade OR grading OR assessment OR assessing or surveillance); bovine or cow or cattle or sheep or beef or animal or goat or deer or ovine or cervine or caprine or pig or swine or porcine; "meat inspection")) AND (TITLE-ABSKEY (offal OR viscera

(bovine OR cow OR cattle OR sheep OR beef OR animal OR goat OR deer OR ovine OR cervine OR caprine OR pig OR swine OR porcine or poultry)) AND ((TITLE-ABS-KEY (offal OR viscera)) AND (TITLE-ABS-KEY (ultrasound OR microwave OR "ultra-sound"))

((TITLE-ABS-KEY (offal OR viscera)) AND (TITLE-ABS-KEY (mri OR nmr))) AND (TITLE-ABS-KEY (bovine OR cow OR cattle OR sheep OR beef OR animal OR goat OR deer OR ovine OR cervine OR caprine OR pig OR swine OR porcine or poultry

((TITLE-ABS-KEY (offal OR viscera)) AND (TITLE-ABS-KEY (nir OR hsi OR "hyperspectral imaging" or near infrared or near infra-red)

((TITLE-ABS-KEY (offal OR viscera)) AND (TITLE-ABS-KEY (rgb OR "uv fluorescence" or colo?r imaging or colo?r image/s

((TITLE-ABS-KEY (offal OR viscera)) AND (TITLE-ABS-KEY ("x-ray" OR dexa OR dxa OR ct or computed tomography))) AND (TITLE-ABS-KEY (bovine OR cow OR cattle OR sheep OR beef OR animal OR goat OR deer OR ovine OR cervine OR caprine OR pig OR swine OR porcine or poultry)

Results

The literature returned 137 hits (including some duplicates) of which twenty (no duplicates) reported the use of non-invasive technologies to inspect offal. Most commercially targeted applications related to poultry and no articles identified current use in a red meat plant. There were no articles advocating the use of multiple technologies to inspect red meat offal.

4.1.3 Internet search strategy, search terms and results

Search Engine used

This literature search was conducted by using Google Chrome search engine.

Search strategy and terms

The search was targeted at identifying non-invasive technologies used to inspect and/or grade offal after evisceration (i.e. not the carcase or "live animal"). While the search looked primarily for scientific uses of technologies, articles identifying commercially available inspection systems were also identified.

Results

Most returns related to websites of regulatory bodies (such as AQIS, MPI, FSIS) or NGOS (e.g. FAO) filling the top 20-30 returns. These sites disclosed their current regulatory environment and inspection procedures. None described the use of automated inspection for red meat, but its use for poultry was disclosed.

Commercial sites return information on offal handling equipment (trays, buggies etc.); foreign body and contamination detection (including Eagle FA; RGL (Sensortec); LOMA; Scott Automation; Cognex and Veritide).

No sites reported the use of combined technologies for use in inspecting ovine or bovine offal.

4.1.4 Patent search strategy, terms and results

Databases searched

The WIPO/PCT, USPTO and Australian Patent were searched

Search strategy and terms used

The databases were searched using a strategy of evolving the search terms based on the returns of the previous search to refine the results.

Results

Many patents were identified that used the technologies envisaged for offal inspection. Of these, only US 6,639,665 (and associated documents) and AU2002253987 (and associated patent family) had relevance. These patents related to using spectral technologies to detect fecal and ingesta contamination on meat. The reasons why these patents should not constitute an FTO issue were reported in the milestone report.

The patent search identified no patents with direct relevance to the concept of using multiple spectral sensors in a tunnel for the purpose of offal inspection. Based on the FTO search undertaken here, we do not foresee any FTO issues in the application of multiple spectral sensors in a tunnel for the purpose of offal inspection. Therefore, FTO should not constrain further development of multiple spectral sensors in a tunnel for the purpose of offal inspection. AMPC is advised that for a legally defensible position on freedom to operate, a patent attorney should be consulted.

4.2 Equipment

The sensors envisaged for an offal scanning tunnel were relocated to Ruakura and placed in housing that would enable suitable imaged to be obtained, as described below.

- ### 4.2.1 Light Boxes

Two light boxes were constructed using either (a) aluminum “profile” or (b) Chrome plated steel for the frames and corflute for the side panels. The surfaces of the aluminum and corflute internal to the box were painted with light and NIR absorbing matt black spray paint. While the materials of construction are not food grade, they were selected as short-term development options as they:

- Enabled adjustments (particularly height) to be made easily and quickly
- Were light and strong for transport and maneuverability
- Could be easily cleaned for hygiene before entering a processing area
- Could be made light proof

Figure 1: Ultraviolet and white light box (with curtain removed)

Figure 2: Hyperspectral Lightbox (with curtain retracted)

- ### 4.2.2 RGB and UV Imaging

Trays of offal were placed in the light box and illuminated with (a) white LED lights and then (b) UV LED lighting. Images were taken using a webcam inserted through the ceiling panel and saved to an external hard-drive for later analysis.

White LED: Two LED strip lights were sourced from Alibaba (manufacturer unknown) and mounted on the ceiling of the light box using height and angle adjustments to provide even light intensity across the area of the trays. These LEDs emitted a constant intensity stable light, whereas domestic LED lights (in NZ) use switch mode power supplies that create a “flicker” that is not seen by humans but is apparent as interference patterns in webcam images.

UV LED: Two strip lights, comprising 8 x 3W Ultraviolet LEDs with parabolic reflectors (Product Code 153.270, Tronios, Netherlands), were mounted on the lightbox’s ceiling and adjusted to provide even light intensity across the area of the trays.

Webcam: A Microsoft LifeCam Studio Webcam (Q2F-00017 Microsoft, USA) provides high resolution images from an inexpensive camera. Further these cameras allow images to be taken from a video stream, processed, saved and results written as data or images from within a single program. They do not require proprietary connection cables or software.

Triggers: Within this project switching light sources and triggering image capture was completed manually using a computer key, however the use of triggers and switching linked to plant operations (i.e. tray position) and/or location of trays in images are well known techniques in processing operations.

- ### 4.2.3 Hyperspectral Imaging

Trays of offal were placed in the light box and illuminated with halogen lights energized with a DC current supply. Six lights where mounted inside adjustable housings and set to provide diffuse visible (white) and NIR lighting across the tray area. Images were taken using a Snapshot hyperspectral camera inserted through two holes (left and right) in the ceiling panel and saved to an external hard-drive.

NIR Lighting: NIR bulbs (LMR16503KAL, 50W, 3000K; Hugo Lighting USA) have an aluminum coating on the rear surface which reflects the NIR wavelengths forward (c.f. dichroic coatings which allow much of the NIR energy (i.e. heat) to escape to the rear of the bulbs). Thus these bulbs project more NIR, but also more heat, onto the target which may impact the quality of the offal as illumination time increases. Halogen bulbs also have rise-times between switching on and achieving a consistent light intensity,and therefore they should not be turned off between images without risking an impact on image consistency.

Hyperspectral Imager: The Snapshot imager (MQ022HG-IM-SM5X5-NIR (Ximea, USA)) coupled with a 35mm lens (35mm/F1.65 67716 VIS-NIR (Edmund Optics, USA)) captures an image with 409 x 216 pixels with each pixel comprising intensity spectra for twenty five wavelength bands. This imager was selected as it provides images with good spatial resolution (0.7 mm x 0.7 mm at the focal length used in this project) with reasonable spectral resolution (25 bands with bandwidths of ~16nm) and acceptable capture speeds (~180 frames per second, fps).

Triggers: Prior to periods of data capture, the halogen lighting was switched on and allowed to stabilize for at least one minute and was not switched off. Capturing the HSI image was triggered manually but would be triggered by software in a commercial process.

- **4.2.4 X-ray**

The AgResearch owned x-ray machine was a bespoke unit designed to AgResearch specifications and built by Rapiscan (USA) for the purpose of scanning meat products in an export meat plant. A feature of this unit was that the imaging capability was designed to produce images with the parallax distributed evenly between the left and right sides of the center line. Unfortunately, this unit suffered a severe power spike and was rendered unusable and subsequently decommissioned.

Therefore within this Milestone, D-TX Ltd was contracted to provide access to a commercial X-ray baggage scanner Hi-Scan 6040i (Smith Heiman, USA & Germany) and transfer DEXA (Dual Energy X-ray Absorption) images of offal from this machine to AgResearch.

The Hi-Scan 6040i has a spatial resolution of 0.08 x 0.08mm. The unit is designed to: (a) capture pixels across the entire tunnel cross-sectional area while minimizing the number of detectors (pixels) used; (b) have images visually interpreted by a person, and therefore (c) was designed without concern for evenly distributing parallax. Thus DEXA images from these units cannot be directly overlaid onto the RGB or HSI images. These images do, however, show internal features in high definition.

Triggers: The Smiths unit triggers on an internal image processing algorithm that detects an object entering the X-ray beam and saves the DXA image to a file (that was subsequently transferred to a hard-drive and then the AgResearch server).

Figure 3: A Hi-Scan 6040i X-ray Scanner

- ### 4.2.5 Trays

Evaluation scans with stainless steel (SS) offal trays showed that at tray thicknesses this metal absorbs significant amounts of low energy X-rays and produces low intensity (dark) images. It also acted as a reflector (mirror) for light and NIR and saturated the devices diodes unless their sensitivity was reduced. Therefore, for the trials, food grade polypropylene trays were used to mitigate these issues.

To ensure that all images, irrespective of the spectral device, could be positively associated with the correct set of offal, the trays were coded such that a dot code (1 → 5 dots) would be visible in all images.

4.3 Plant Trials

- ### 4.3.1 Scanning in Abattoirs

The dual species Ruakura Abattoir was originally designated for the initial trials. This facility was selected for its proximity to AgResearch, number of animals processed and MPI inspection. However, during contracting, this facility changed ownership and converted to pork processing, and was therefore no longer accessible nor suitable for this project.

Access to Wally Smith Ltd (a Hamilton NZ micro-abattoir and home-kill facility) was then obtained and used for initial trial work. However the kill rate in this facility is very low and the offal is not inspected, thus "disease and defects" could not be verified to the images obtained.

- ### 4.3.2 Scanning in Export Plants

Access was granted to an ovine export plant and a bovine export plant in the North Island of New Zealand. The light boxes and x-ray unit were taken into processing rooms within these plants and assembled close to the processing lines. When diseases or other defects were identified by the Inspector, the offal was placed in plastic bags with a note (on a label) with the reason for condemnation and the offal made available for scanning. The condemned offal was transferred to the scanning area, placed in trays and imaged. The scanned offal was placed with "Condemned" material for rendering.

In export plants, animals are generally young and healthy, and therefore the condemned offal from an individual animal commonly comprises only one, or maybe two, organs. While these offal were scanned they did not challenge "offal identification" algorithms. Therefore offal from several animals were combined to create artificial offal sets with many tissue types and then scanned.

4.4 Inspection Algorithm Development

4.4.1 Overview

Software was written in Matlab (Mathworks Inc., USA) to classify the tissue in each pixel in an image using the spectral data associated with that pixel. The processing software:

- Imports the data from directories based on filenames
  - Imports the RBG and UV images, assembles them into a six layer hypercube
  - Imports the Hyperspectral images and assembles them into a 25 layer hypercube
  - Imports the DXA images and resolves them into their two low energy and high energy images.
- Processes the data spectrally to:
  - Remove the background tray
  - Predict the tissue scanned in each pixel using characteristic intensity levels in several key bands and create an associated results array [“image”] that colour codes the cells [pixels] according to the predicted tissue. This array is de-speckled using a simple image erosion and dilation algorithm.
  - Classify the tissue as acceptable or condemned and create an associated results array [“image”] that colour codes the cells [pixels] according to the predicted tissue and whether each pixel is associated with a “condemned tissue” or not.
- Outputs the results arrays as:
  - Images to a screen with sub-images for visual assessment and confirmation.
  - Saves the arrays to a directory (can be secured) associated with tray numbers and date/time stamps for auditing and review purposes

4.4.2 Processing Philosophy

Organ Classification: Organs can be easily identified within a single tray using just a few of wavelength intensities (analogous to colour brightness) in the images presented. However, to drive long term robustness in the algorithms, a restriction was enforced that the criteria defining “an organ” was to be consistently applied across all trays. This forced the criteria to become “within a range of several intensities across several bands”. Due to inherent variations across several images, some of these ranges overlapped and caused some pixels to be misclassified. The cause and impact is discussed further in the Discussion section. These result were presented as an image and visually assessed (see Table 1).

Disease Classification: This section of the algorithm assumes that the offal type is known from the organ classification step, and therefore the dataset was processed according to offal types. The datasets for each tissue were further assigned to either a development subset or a validation subset. The algorithms were developed in the development subset and then applied to the full data set for that offal type (i.e. both the development set and validation set). These result were presented as an image and visually assessed (see Table 2).

5.0 PROJECT OUTCOMES

5.1 Freedom to Operate

Freedom to Operate (FTO) searches were conducted on multiple public databases including MLA's publications, scientific and trade journals, patent databases and internet search engines by experienced searchers. These searches identified the use of spectral technologies including vision, hyperspectral imaging, UV imaging, and single and dual energy X-ray in meat industry applications. However, their use for offal inspection were generally for contaminant (fecal, ingesta and foreign body/metal) detection or composition (e.g. CL) using a single sensor operating in a particular spectral range. None of the articles or patents examined advocated the use of multiple sensors to inspect offal for disease.

Based on the FTO search undertaken, it appears that AMPC has FTO to develop and use hyperspectral imaging, DXA imaging and RGB-UV imaging sensors in a multi-sensor tunnel for the purpose of offal inspection. Care is still needed to ensure that incorporating other individual sensor technologies into this application, other than those nominated, does not infringe patents outside the scope of the FTO searches. AMPC was advised that for a legally defensible position on freedom to operate, a patent attorney should be consulted.

5.2 Inspection Algorithms

Data from fifteen trays with mixed offal on them were used to develop an algorithm that would classify tissue types. The Results Array for each tray were presented as false colour images and manually assessed for accuracy and scored on the number of offal correctly identified out of those present.

Table1: Assessment of the algorithm to correctly identify tissue types

Image	Comments	Tissues Correct	Tissues in Tray
1	The lungs and heart are correctly identified.	2	2
2	The lungs and heart are correctly identified. The diaphragm is also identified as "muscle"	3	3
3	The lungs, liver and gall bladder are correctly identified. The heart is partially identified (with small amount of magenta incorrectly allocated*)	3	4
4	The lung, diaphragm (silver-skin) are correctly identified. The heart is partially identified (with small amount of magenta incorrectly allocated.*)	2	3
5	The lungs and heart were correctly identified	2	2
6	The lung, diaphragm (silver-skin) are correctly identified. The heart is partially identified (with small amount of magenta incorrectly allocated.*)	2	3

7	The lungs are correctly identified (even though the lower lung is condemned material as seen in the yellow pixels in what should have been lung)	1	1
8	The lungs and diaphragm are correctly identified, the heart partially identified, however there is also a significant number of incorrect pixels.	2	3
9	The kidney, liver, lungs, gall bladder and heart are correctly identified. The diaphragm's silver-skin is identified, however the muscle tissue is not.	5	6
10	The heart and lung tissue is correctly identified but the diaphragm muscle is incorrectly assigned as lung.	3	4
11	The heart, diaphragm and lung are correctly identified.	3	3
12	The liver, gall bladder and lung are correctly identified. The heart is identified but with some pixels being incorrectly assigned as lung. The diaphragms silver skin is correctly identified but the muscle is incorrectly assigned as lung.	3	5
13	The lungs and diaphragm are correctly identified, the heart partially identified with some magenta.*	2	3
14	The lungs and heart are correctly identified. (Note the yellow pixels in the lung corresponding to the condemned tissue)	2	2
15	The liver, lungs and gall bladder [200,550] are correctly identified. The heart is correctly identified in the "Predicted Tissue" but some heart tissue is coloured dark green in the de-speckled image. (Note: Yellow in the lung and green in the liver corresponding to condemned tissue)	4	4
	Totals = 81%	39	48
* Assessing the areas of magenta associated with either "heart" or "liver" improves this result to 44/48 or 91.7% correct. The cause of this artifact is discussion in the body of the discussion			

Data from 76 trays of offal comprising mixed and single offal were processed and the outputs recorded in Appendix 10.2. The outputs were assessed against the recorded reason for being condemned and the assessment recorded in Table 2.

Table 2: Assessment of processing algorithms

Reason condemned	Number of samples available	Number correctly processed
Liver Cirrhosis	18	18
Liver Abscess	8	8
Liver cysts	3	3
Heart c. ovis	12	12
Lung	4	4
Kidney	6	6
Adhesion Diseases	14	0
Liver Fluke	2	2
Peritonitis	4	0
[Scanned for Offal ID development]	5	3
Sub-totals		
Condemned (other than below)	53	53
Pleurisy and Peritonitis	14	0
For "Offal ID" work (but also assessed)	5	3
Total	76	

Although on a limited dataset, these results suggest that spectral devices and processing are able to inspect offal. However work is needed to define a fingerprint spectra for pleurisy and peritonitis.

6.0 DISCUSSION

6.1 Freedom to Operate

The Freedom to Operate (FTO) searches were conducted in multiple databases including MLA and AMPC publications, journals databases, patent databases and internet search engines. The search terms used focused on the use of spectral technologies in meat industry applications generally, and offal in particular.

The results of the literature search in the journal databases, and MLA and AMPC databases are useful in establishing freedom to operate as of their date of publication, however they cannot be used to establish non-infringement of patents published prior to their date of publication. There were no publications identified that advocated the use of multi-spectral tunnel for use in offal inspection.

The patent search conducted did not identify any patents that AMPC would infringe using a combination of DXA, HSI, and RGB & UV imaging in a multi-sensor tunnel for offal. Thus the use of <u>THESE sensors in THIS application</u> has appears to have FTO. However, this position would need to be reassessed should:

- Other sensors be introduced as there may be a patent protecting the use of a new sensor (technology) in scanning offal.

For example, using a "monochromater and optical filters" [to capture hyperspectral images] is patented for meat scanning … but this is not one of the technologies used in this project.

- The scope of the application is extended as there may be a patent covering a technology used in this project in the new application.
  For example, UV has been patented for faecal and ingesta contamination on carcases in Australia …. But we are not looking specifically for faecal or ingesta contamination, and we are not scanning carcases.

- The tunnel be sold outside Australia, NZ, USA or EU.
  These jurisdictions were chosen as the major potential markets for the technology

The searches identified **US 6,639,665** (and associated documents) and **AU2002253987** (and associated patent family) which relate to using spectral technologies to detect fecal and ingesta contamination on meat. The reasons why these patents should not constitute an FTO issue are described in the Milestone report.

Disclaimer: While AMPC appears to have FTO to use multiple spectral sensors in a tunnel for the purpose of offal inspection, a legally defensible position on freedom to operate can only be established by a patent attorney.

6.2 Equipment

- ### 6.2.1 Cameras & Imagers

Colour similarities for different tissues and colour differences observed for the same tissue in different trays were observed in the RGB imager (See 6.3.1) and highlights an unexpected source of error. Post-scanning checks of the camera configuration file showed that a function in the RGB camera was automatically adjusting the recorded histogram to maximize the colour intensity and image brightness. Therefore large dark areas (e.g. liver) were automatically compensated for at the expense of other semi-dark pixels (e.g. moving heart into a darker intensity level in images with liver compared to those without liver present). This function negated the commonly used method of ensuring that areas of "white" (tray) and "dark" (painted floor) were in the field of view of the camera to establish the brightest and darkest pixels, thereby fixing the top and bottom intensities of the histogram range of the spectra. This function in the camera software can, and will be, turned off in the future to enforce a consistent colour intensity. In turn this will reduce the overlap of "criteria" in some spectral ranges and further improve the correct identification rate.

The HSI imager also had an automatic intensity adjustment, however as water dominates cells and absorption in the NIR spectrum, this impact was less severe.

- ### 6.2.2 Illumination

The use of LED lighting for the visible and UV imaging with the webcam was useful. Compared to halogen and incandescent lights, LEDs use less power (= low running costs), use lower voltage DC current (= lower HSE issues), provide more diffuse light and their intensity can be controlled. Their continued use is recommended.

The NIR illumination currently used in this project was provided by halogen lights and are commonly used in NIR/HSI applications. However, they have several disadvantages:

- They require significant amounts of very stable DC energy in order to produce a strong and spectrally stable light. Thus the DC power supply needs to be a specialist high current source with stable output (i.e. not a more commonly available switch mode unit).
- They tend to be tightly focused (compared to LED systems) and therefore need several bulbs mounted further away from the offal in order to spread their light more evenly. This compares to diffuse LED source which can be mounted within centimetres of the offal and is better suited to a tunnel.
- They have glass lens, run hot and therefore need isolating from water and people.

NIR LEDs would be a more suitable illumination source. While NIR LEDs exist, they have "holes" (low intensity) at several wavelengths, requiring several LEDs with overlapping wavelengths to be closely mounted and individually controlled to provide an even intensity across the range of wavelengths of interest. Purchase (or development) of an LED based NIR illumination system is recommended.

• 6.2.3 DEXA Imaging

The DXA images provided 100% inspection of the offal. However with the unit used, the geometry between the generator, detectors and offal created parallax differences between the left and right sides of the images. This also meant that the DXA images could not be directly overlaid on to the RGB and HSI images. While the defunct AGR DXA unit was designed to minimise the degree of parallax, baggage scanners are optimised for human interpretation of images. D-TX Ltd has the capability to design and build an X-ray tunnel that minimises the parallax within an image and also with any RGB and HSI camera in the tunnel. As they have been associated with this project, understand X-ray detectors and design, and are associated with a company with HSI and RGB expertise it is recommended that they be consulted regarding tunnel design and construction.

6.3 Algorithms

• 6.3.1 Offal Classification Algorithms

The results of fifteen trays holding "mixed offal" are shown in Appendix 10.1. These images have been assessed for the number of tissues correctly identified in Table 1.

The predicted tissue in each of the Prediction Sub-images (lower left and lower right) are colour coded:

Red	Heart (or muscle)
Grey	Fat or silver skin
Green	Lung
Magenta	Liver and Kidney (and sometimes heart)
Yellow	Background or "Tissue not of interest"

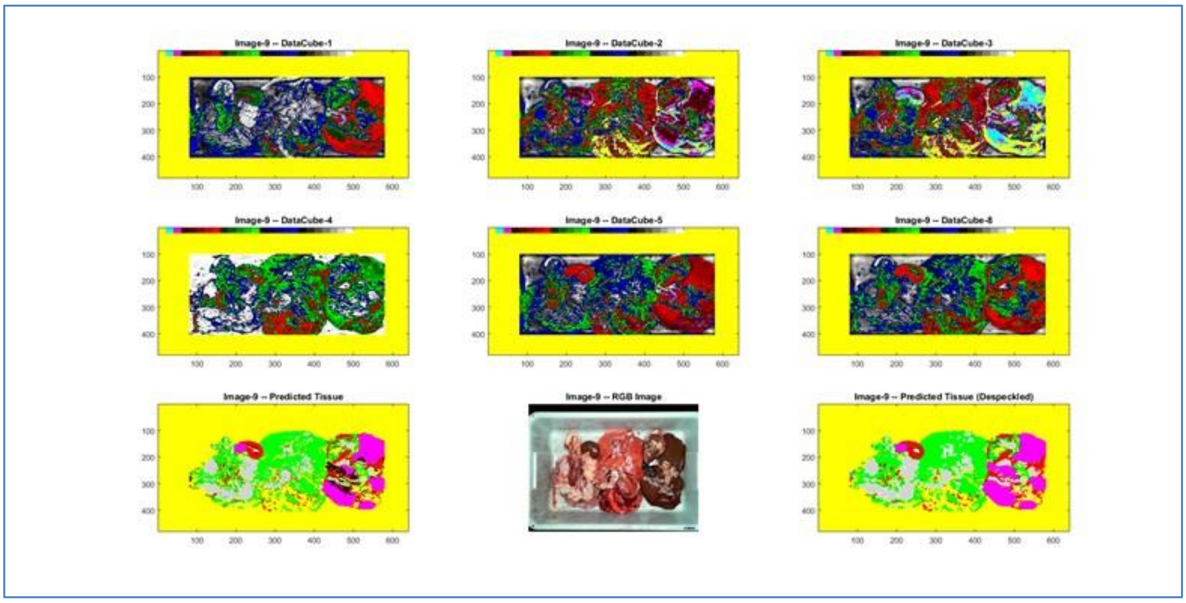

Image 4: Exemplar Algorithm Output

The offal identification algorithm correctly identified 39 of 48 pieces of offal across fifteen trays with 81% accuracy using **only spectral** processing. Although not perfect, this outcome demonstrates the efficacy of this technique compared to image processing, particularly when some of the offal is partially obscured by other tissue and therefore shape characteristics cannot be used.

The observance of magenta pixels appearing in heart tissue demonstrates the negative impact of the "one criteria fits all" regime (especially when camera settings change between images. See 6.2.1). For example, in Images 3, 4, 6, 8 and 13 some pixels associated with "heart" appear with intensities of yellow and aqua in DataCube3 & DataCube4, but these colours are also associated with "liver" in Images 3, 9, 12 and 15. Thus the algorithm fails to differentiate these using only spectral processing. A simple pixel count and threshold algorithm would establish the size of the "magenta offal" and therefore the likelihood of it being liver or heart. Although this approach was not implemented (as it would mask the resolution of a spectral approach) it would have increased the correct identification rate to about 92%.

The algorithm was also able to identify and eliminate much of the material that was not of interest (e.g. esophagus and blood splatter). However, the algorithm did not perform well in Image 8 where much of the esophagus and lung tissue are both associated with "red" in DataCube4, whereas in other images lung is more strongly associated with green and blue in DataCube4. Again, this is an impact of the "one criteria fits all" regime.

The software imports and processes the dataset for a tray in less than 1 second, including writing an image. Thus even in a very high speed chain, of say 15 animals per minute (or 1 animal per 4 seconds) the algorithms have sufficient spare cycle time for additional data processing to occur.

The time taken to manually handle the trays into the light boxes and manually take the images could take up to one minute per tray. Although this timeframe would not be needed for an on-line tunnel, it does provide some assurance that the impact of heat from the NIR lamps has not desiccated the offal surfaces, as water specular reflection and wet blood splatter is still apparent in the RGB images. Further, the impact of coagulation of blood (which appears similar to blood rich tissue like liver and kidneys) would be much less on an eviscera conveyor as the time from evisceration to grading is typically less than 60 seconds.

- **6.3.2 Condemned Offal Identification Algorithms**

Data sets ("images") of 71 trays of offal comprising mixed and single offal were processed and the outputs recorded in Appendix 10.2. The outputs were assessed against the recorded reason for being condemned and the assessment recorded in Table 2.

The software imports, processes and presents the dataset for a tray within a few seconds, including writing an image. Thus even in a very high speed chain, of say 15 animals per minute (or 1 animal per 4 seconds) the algorithms have sufficient spare cycle time for additional data processing to occur.

- **6.3.3 DEXA Images Assessment**

X-ray images were obtained from a Dual Energy X-ray Scanner (DEXA) baggage scanner. Such scanners have high spatial resolution but are optimised to differentiate biological and non-biological materials based on density (or more technically, the sum of the Z values of each element in the beam length). Thus tissues comprising similar organic materials (e.g. all offal tissues comprise "water" and "cells walls" but of varying thickness, or beam length) are not easily differentiated in DXA units. However, as shown in exemplar images in Appendix 10, the ability of x-ray technologies to examine internal structures and defects in offal is promising. X-ray images for Offal 18, 19, 39 and 44 where obtained through the offal and shows fine details of internal structures (such as arteries and veins, bronchi and bronchioles), external structures (such as surface fat on livers and hearts and gall bladders and ducts) and, with human interpretation, unhealthy material (such as liver fluke, abscesses and arguably cysts).

The X-ray unit uses dual energy X-ray absorptiometry (DEXA) optimised for baggage scanning. While the spatial resolution is excellent, the low-high energy split does not discriminate well for organic materials (which preferentially absorb X-rays in the low energy range). Therefore, for this Milestone, human interpretation was required and was able to discriminate some defects (external and internal) through the tissue. The images also showed very detailed internal structures.

7.0 CONCLUSIONS/RECOMMENDATIONS

Based on the searches conducted in MLA and AMPC publications, journal databases, patent databases and internet search engines, AMPC appears to have the Freedom to Operate (FTO) a multi-sensor tunnel comprising DXA imaging, Hyperspectral (NIR) imaging, and RGB & UV imaging for offal inspection. While the use of THESE sensors in THIS application appears to have FTO, this position would need to be reassessed should:

- Other sensors be introduced, as there may be a patent protecting the use of the new sensor (technology) in scanning offal.
- The scope of the application is extended, as there may be a patent covering a technology used in this project in the new application.

- The tunnel be sold outside Australia, NZ, USA or EU.

It is recommended that a watching brief be established to identify new patent publications and/or grants that may cause a new infringement.

The offal identification algorithm demonstrated the ability of spectral devices to accurately classify tissue speedily even when tissue was partly obscured by other tissue. The condemned offal algorithms demonstrated the ability of spectral devices to differentiate healthy tissue from condemnable tissue. Creating interfaces for the webcam and HSI imager that control the light sensitivity should further improve the accuracy of the algorithms. This recommendation as already been acted upon.

The cameras have the disadvantage of only being able to "see" the upper surfaces (i.e. facing the camera). While this is satisfactory for classifying offal, consideration will need to be given to turning the offal to enable the RGB and HSI imagers to see thin surface defects that DEXA technologies cannot detect. Improving the X-ray detectors may also allow the surface defects to be seen without touching the offal.

The X-ray unit uses dual energy X-ray absorptiometry (DEXA) optimised for baggage scanning. The spatial resolution is excellent and allowed very detailed internal structures to be observed. However, the low-high energy split does not discriminate well for organic materials (which preferentially absorb X-rays in the low energy range). It is recommended that detectors with better discriminate in the low energy ("organic") region be used. It is also recommended that a bespoke X-ray tunnel be designed and built that minimises the parallax with the X-ray image and between the X-ray and other imagers.

While the algorithms worked well on the dataset available, they have only been tested on a limited range of diseases and age of animals. Future work needs to extend this dataset and incorporate machine learning techniques.

8.0 BIBLIOGRAPHY

1. Patents US8000440, NZ 548456; EU20141557 "Target composition determination method and apparatus".
2. Leath S, 2006, "Detecting Hollow Heart Disease in Potatoes" FRST Contract C06X0808
3. Challies MJ, Ross CM, Leath SR, Rapp D, 2017, "Rapid phenotyping of pathogenic and non-pathogenic E. coli O26 using Hyperspectral Imaging", NZMS Annual Conference 2017
4. Challies MJ, Taukiri K, Leath SR, King W, 2009, "Effect of sampling strategy for in-field pasture quality measurement", The 14th International Conference of Near Infrared Spectroscopy. November 2009
5. Patents US10539867, PCT/NZ2003/000279 "CL measurement Device
6. Patents US7626149B2, WO2006016824A1 "Non-invasive temperature and composition sensor for partially aqueous targets".

9.0 APPENDICES

This section should include any supporting documentation which has been referenced in the report. Each Appendix must be named and numbered.

9.1 Appendix 1 – Milestone 1 Images

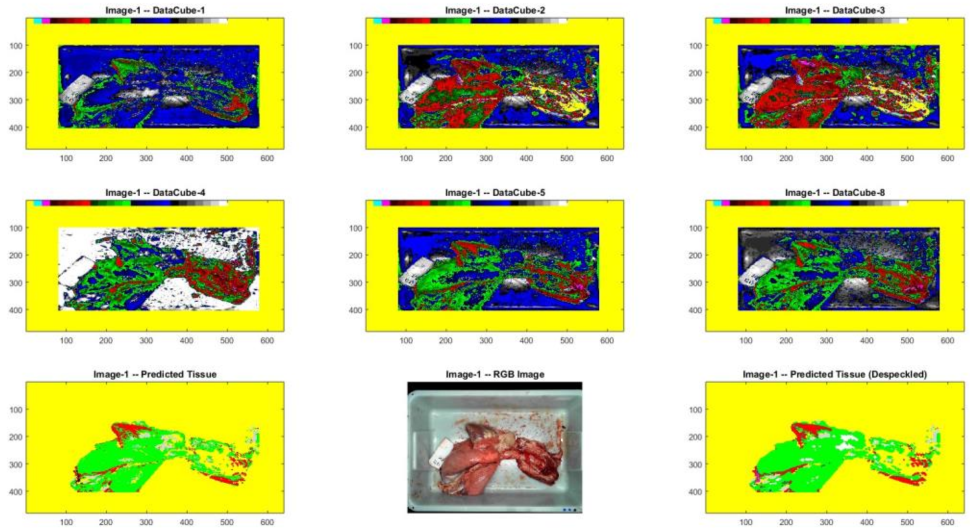

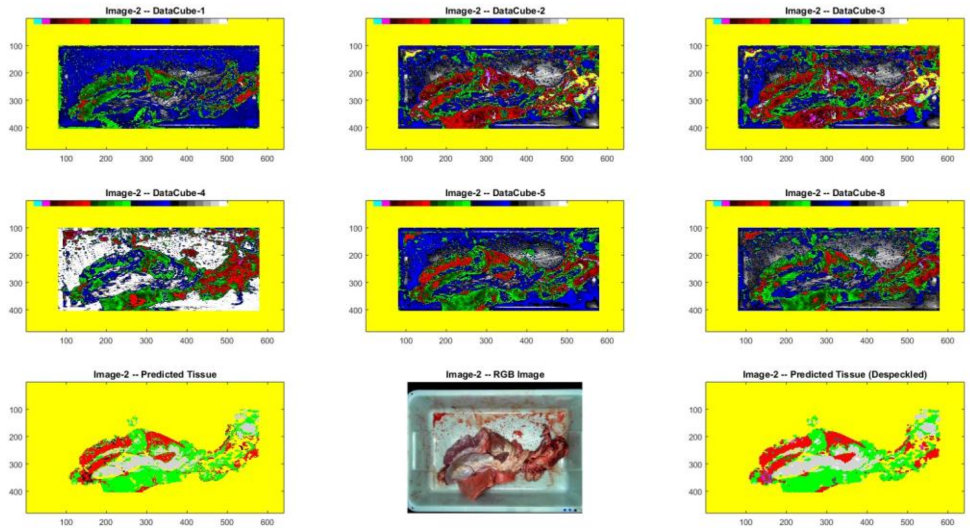

Code	
Red = Heart (or muscle)	Grey = Fat
Green = Lung	Magenta = Liver and Kidney

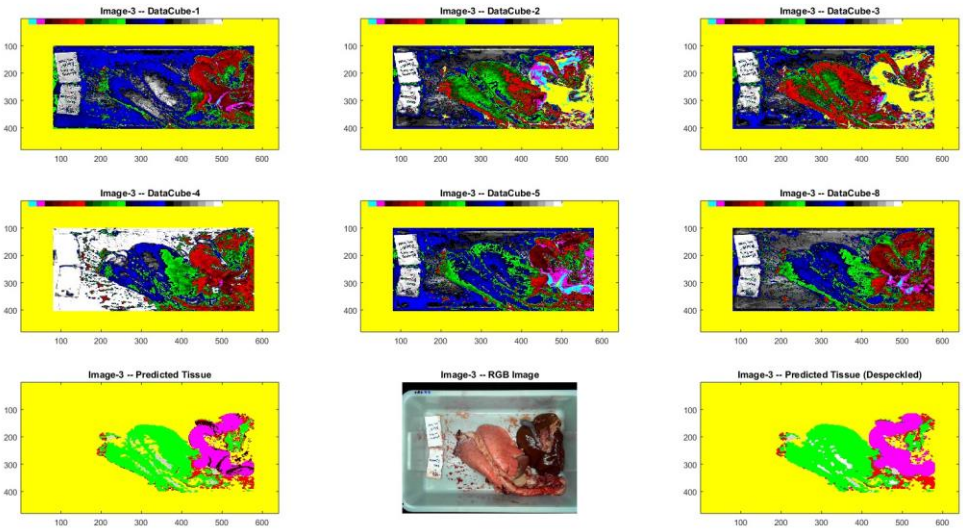

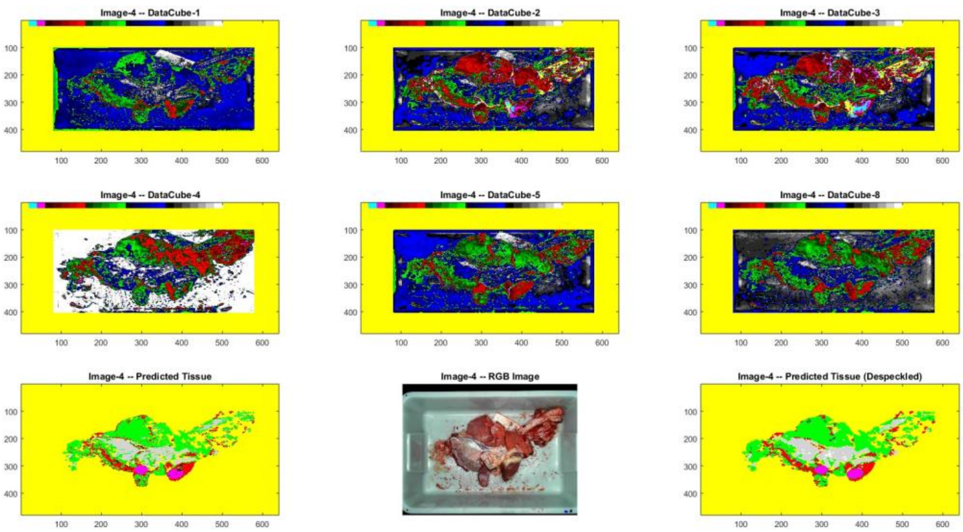

Code	
Red = Heart (or muscle)	Grey = Fat
Green = Lung	Magenta = Liver and Kidney

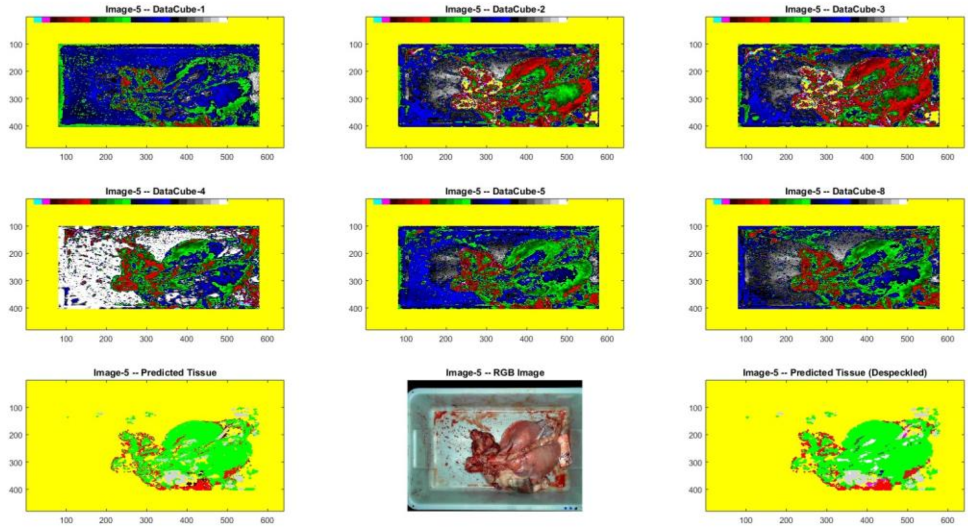

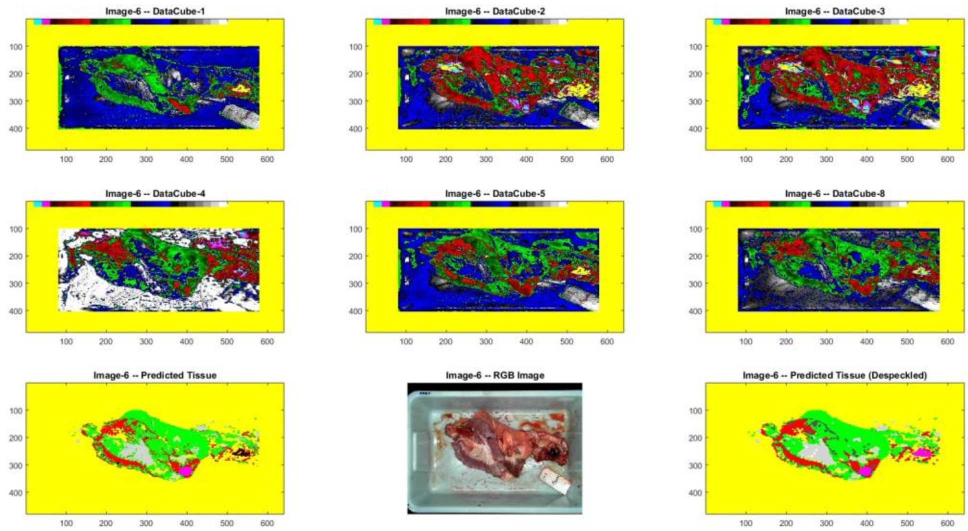

Code	
Red = Heart (or muscle)	Grey = Fat
Green = Lung	Magenta = Liver and Kidney

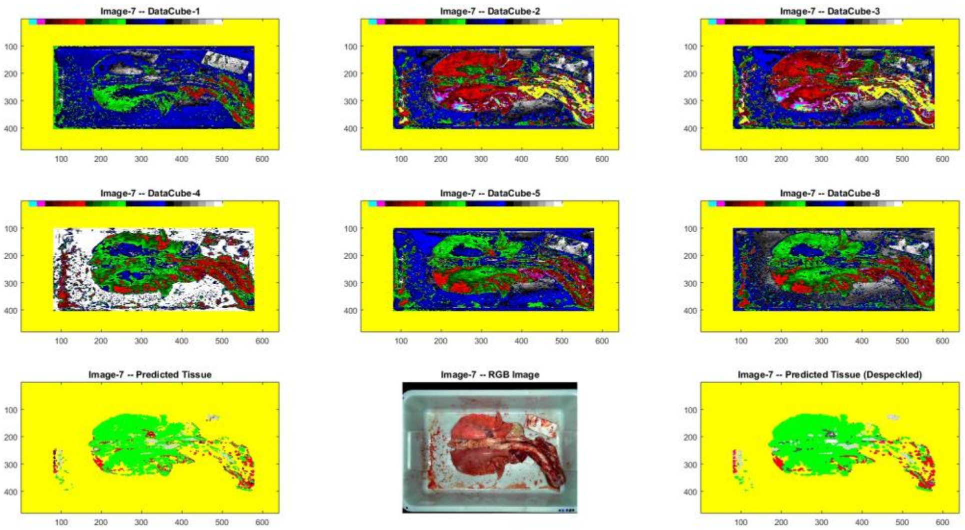

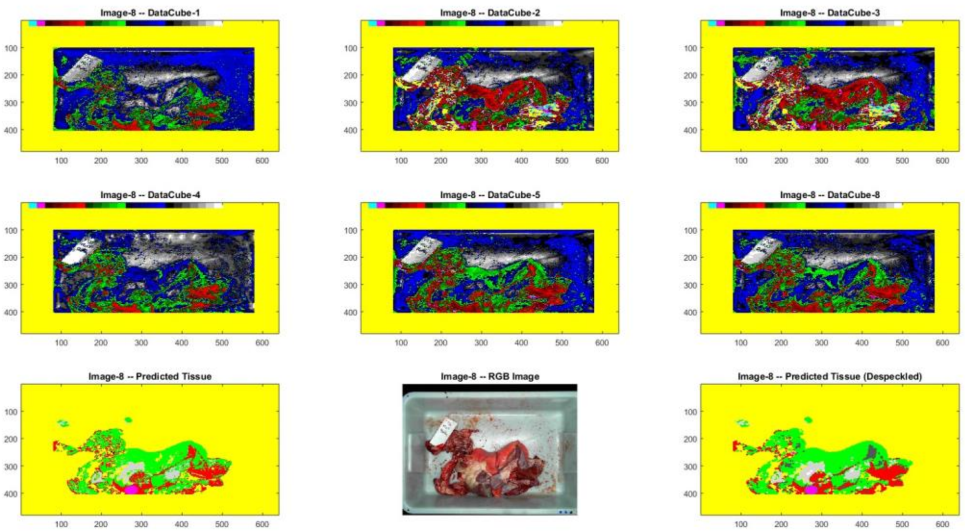

Code

Red = Heart (or muscle)

Grey = Fat

Green = Lung

Magenta = Liver and Kidney

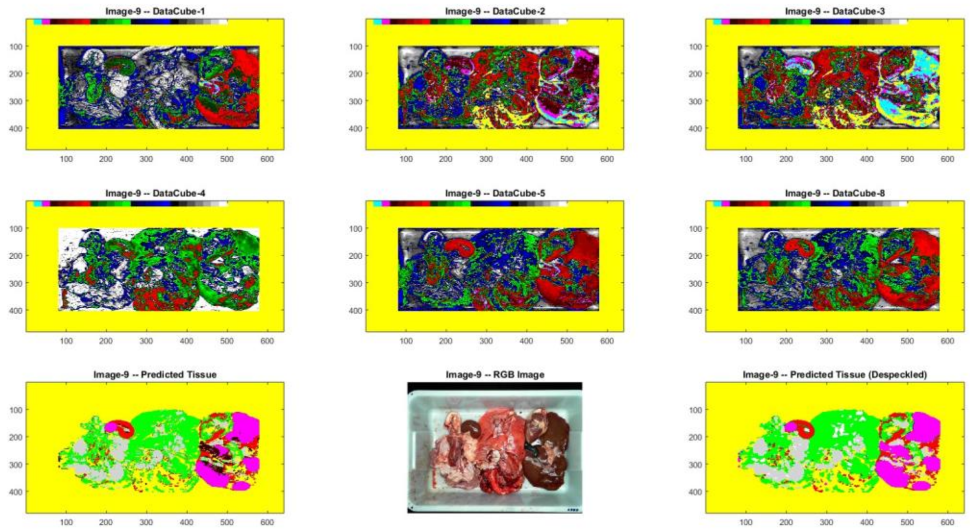

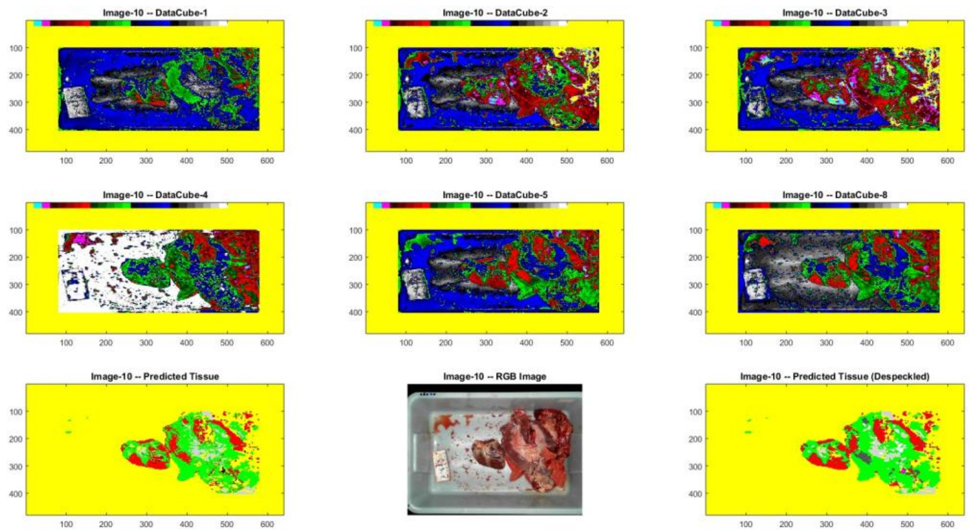

Code

Red = Heart (or muscle)	Grey = Fat
Green = Lung	Magenta = Liver and Kidney

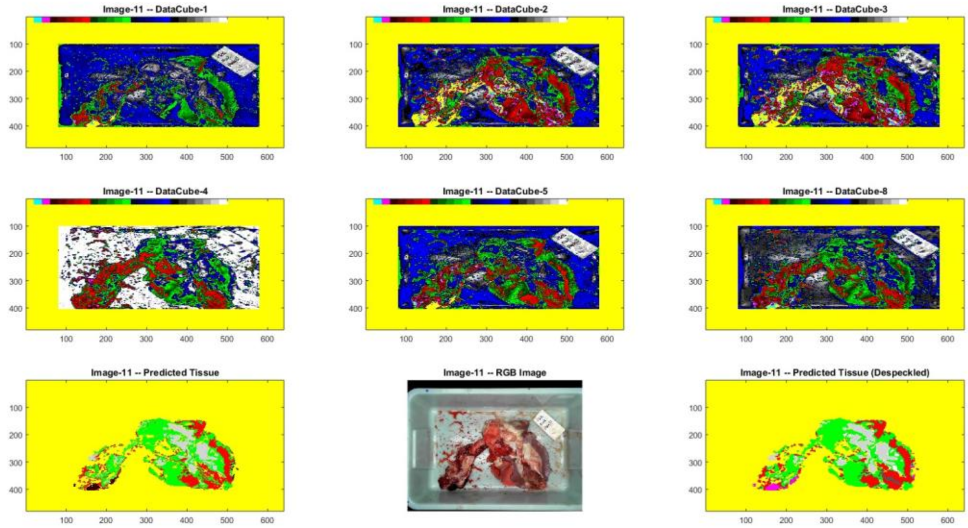

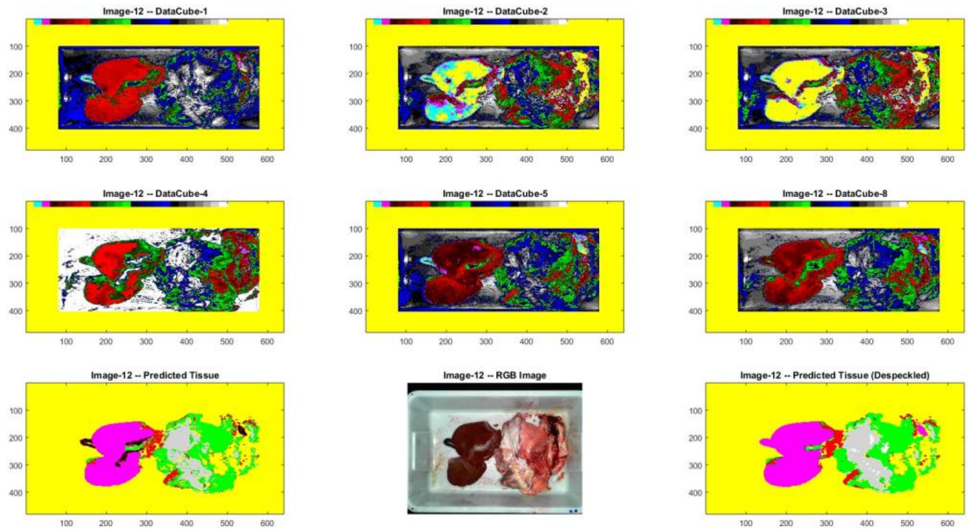

Code	
Red = Heart (or muscle)	Grey = Fat
Green = Lung	Magenta = Liver and Kidney

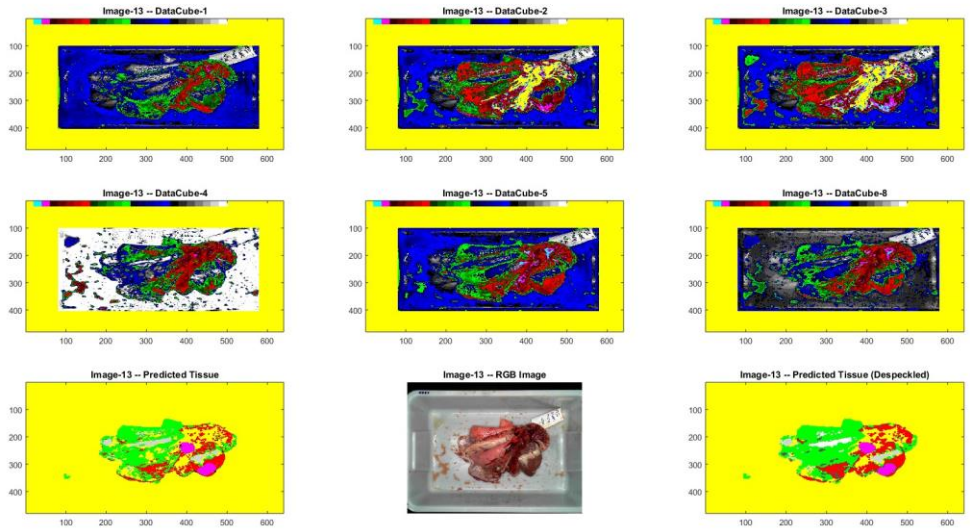

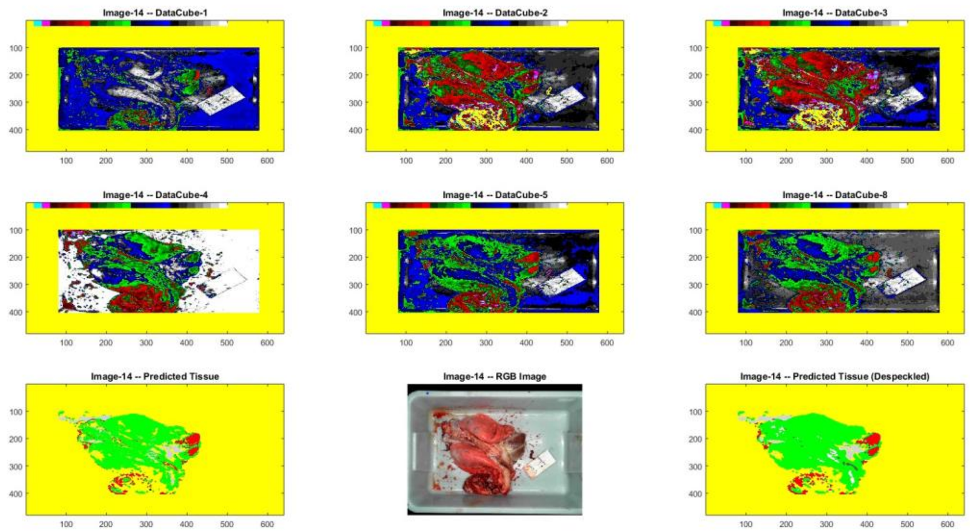

Code

Red = Heart (or muscle)	Grey = Fat
Green = Lung	Magenta = Liver and Kidney

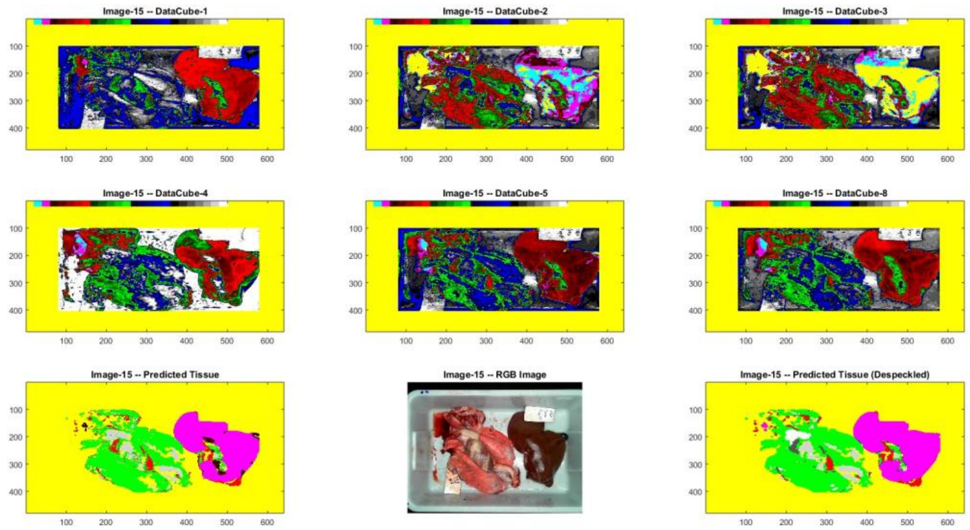

<u>Code</u>

Red = Heart (or muscle)	Grey = Fat
Green = Lung	Magenta = Liver and Kidney

9.2 Appendix 2 - Milestone 2 Images

Data by disease

Disease	Number of examples	Number Correct
For Offal ID development	5	3
Liver Cirrhosis	18	18
Liver Abscess	8	8
Liver cysts	3	3
Heart c. ovis	12	12
Lung	4	4
Kidney	6	6
Adhesion Diseases (e.g. pleurisy)	13	0
Liver Fluke	2	2
Peritonitis	4	0

Data by tray

(Green = Disease Identified, Orange = Marginal, Red = Not Identified)

Image ID	Tray ID	Offal type and disease	Correct?
1	2	Liver Cirrhosis	Y
2	1	Heart c.ovis	Y
3	3	Liver, Cirrhosis	Y
4	4	Liver Cirrhosis	Y
5	5	Diaphragm ,Peritonitis	N
6	1	Heart, c.ovis, cisternae	Y
7	2	Heart c.ovis	Y
8	3	Liver Cirrhosis	Y
9	4	Diaphragm, peritonitis	N
10	5	Liver Cirrhosis	Y
11	1	Liver Cirrhosis	Y
12	2	Kidney necrosis	Y
13	4	Liver Cirrhosis	Y
14	3	Liver Cirrhosis	Y
15	1	Liver Cirrhosis	Y
16	2	Liver Cirrhosis	Y
17	3	Liver Cirrhosis	Y
18	4	Liver fluke and cirrhosis	Y
19	5	Liver fluke	Y
20	1	Heart, tip under fat	For ID work
21	2	Heart c.ovis	Y
22	3	Heart c.ovis	Y
23	4	Lung pleurisy	N
24	5	Lung pleurisy	N
25	1	Heart, lung abscess and pleurisy	Y

Image ID	Tray ID	Offal type and disease	Correct?
26	2	Heart c.ovis	Y
27	3	Liver cyst	Y
28	4	Liver pericarditis	Y
29	5	Heart pericarditis	N
30	1	Deep c.ovis	Y
31	2	Diaphragm slight sarcoidosis (white cyst)	N
32	3	Heart c.ovis	Y
33	4	Heart C.ovis	Y
34	5	Liver Cirrhosis and fluke	Y
35	1	Liver eczema	Y
36	2	Kidney nephritis	Y
37	3	Lung pleurisy	N
38	4	Liver abscess	Y
39	5	Liver abscess	Y
40	1	Liver cirrhosis	Y
41	2	Kidney nephritis	Y
42	3	Lung Pleurisy and heart	N
43	4	Liver abscess	Y
44	5	Lung pleurisy, abscess on liver	N
45	1	Liver abscess in Glogi	Y
46	2	Lung and heart pleurisy	N
47	3	Lung abnormal spot	Y
48	4	lung pleurisy	N
49	5	liver abscess inside and surface	Y
50	1	Liver abscess by gallbladder	Y
51	2	Liver with holes	Y
52	3	Liver nodules abscess	Y
53	4	Heart c.ovis	Y
54	5	Kidney nephritis	Y
55	1	Liver umbilicus is stuck	N
56	2	Diaphragm, pleurisy	N
57	3	Kidney nephritis	Y
58	4	Liver cirrhosis	Y
59	5	Heart c.ovis	Y
60	1	Liver cirrhosis	Y
61	2	Diaphragm pleurisy	N
62	3	Liver cirrhosis	Y
63	4	Diaphragm pleurisy	N
64	5	Lung, abscess and biomass adhesion	Y
65	1	Kidney lesia	Y
66	2	Heart c.ovis	Y
67	3	Heart (okay) lung, pluck, pleurisy	N
68	4	combination of several offal	For ID work
69	5	Heart c.ovis and peritoneum	For ID work

Image ID	Tray ID	Offal type and disease	Correct?
70	1	Pluck, pleurisy diaphragm and heart	N
71	2	Above pluck with an added liver	For ID work
72	3	Liver cyst up to 5 okay	Y
73	4	lung abscesses	Y
74	5	Liver cysts	Y
75	1	Heart c.ovis, lung Abscess	For ID work
76	2	Heart and liver	For ID work

Images of Output Data and Interpretation

===

<u>Offal 1</u>

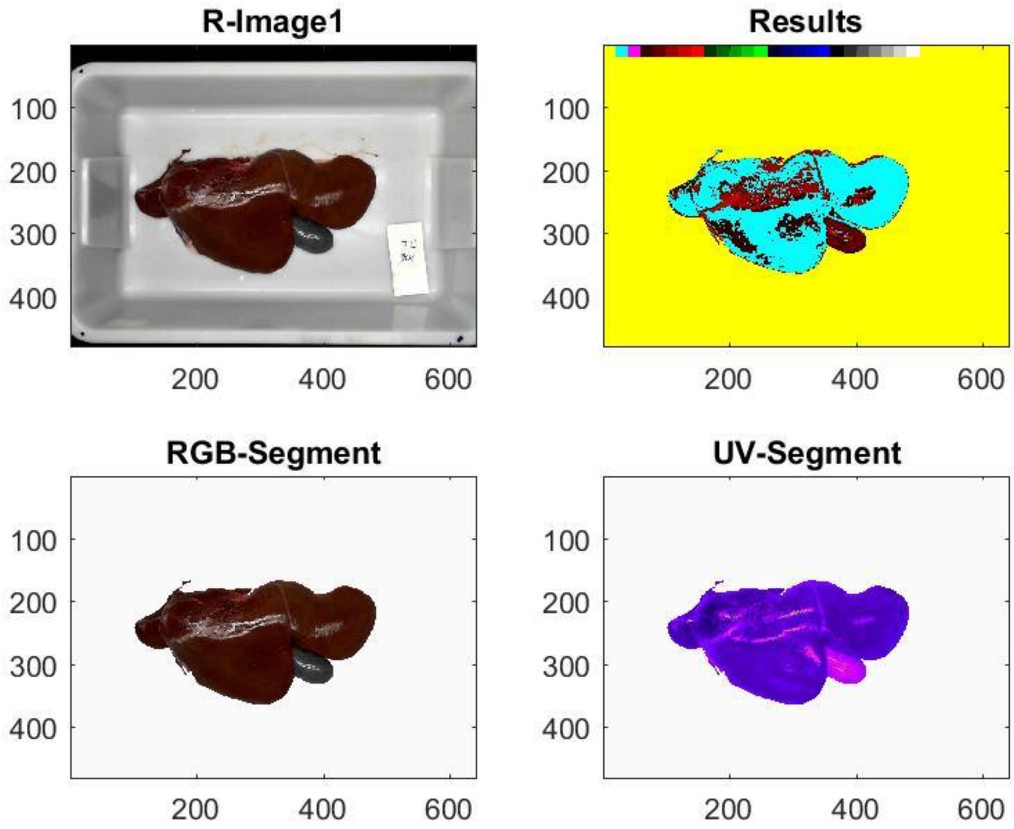

Interpretation:

Brown (least severe) and black (most severe) show regions of cirrhosis

Aqua shows regions of healthy tissue

Comments:

This liver was condemned for cirrhosis

The gall bladder has been incorrectly highlighted and this effect will be removed in future work.

<u>Offal 2</u>

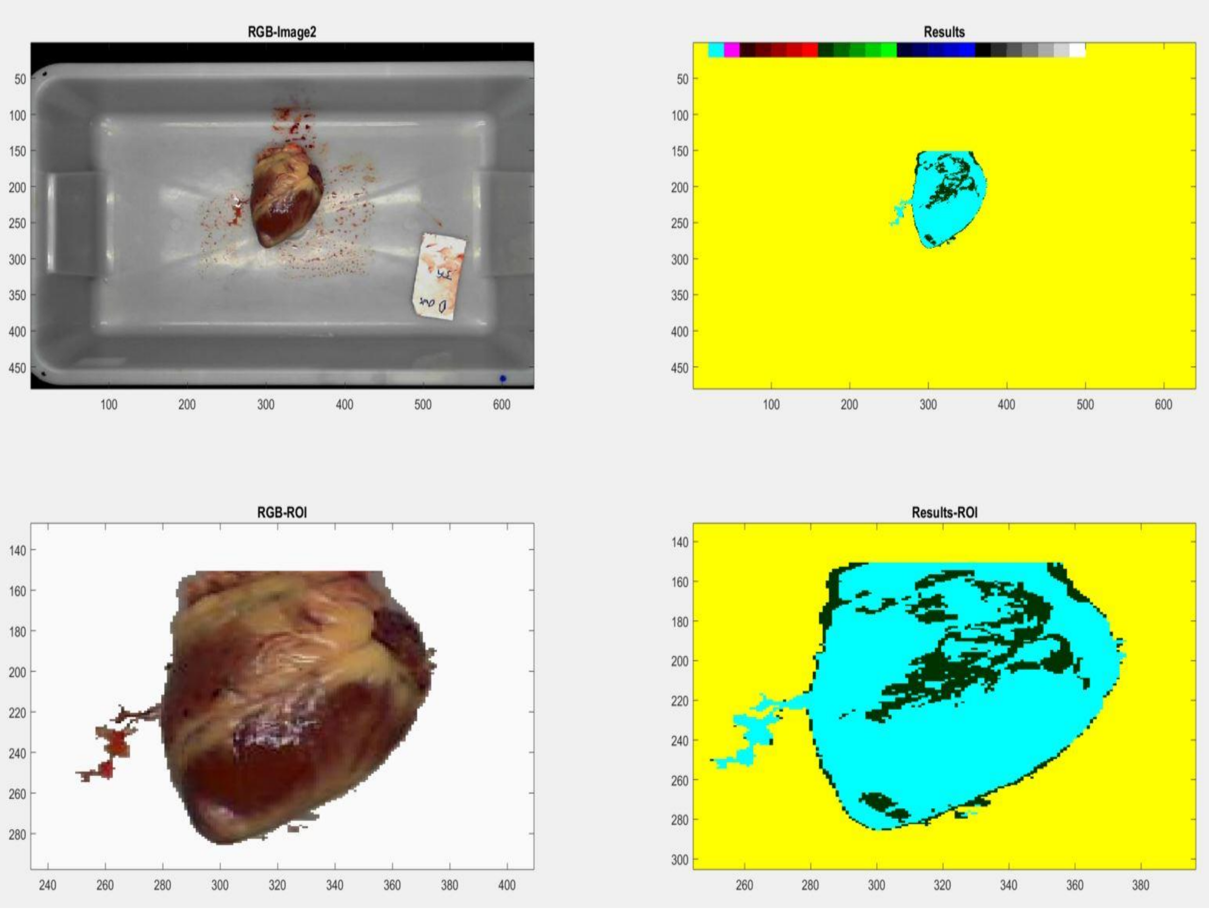

Interpretation:

Olive shows regions of c. ovis cysts

Aqua shows regions of healthy tissue

Comments:

This heart was condemned for c. ovis

The cyst is correctly identified at the apex of the heart. There is a region of epicardial adipose tissue that also is highlighted and within this region lies an additional cyst.

<u>Offal 3</u>

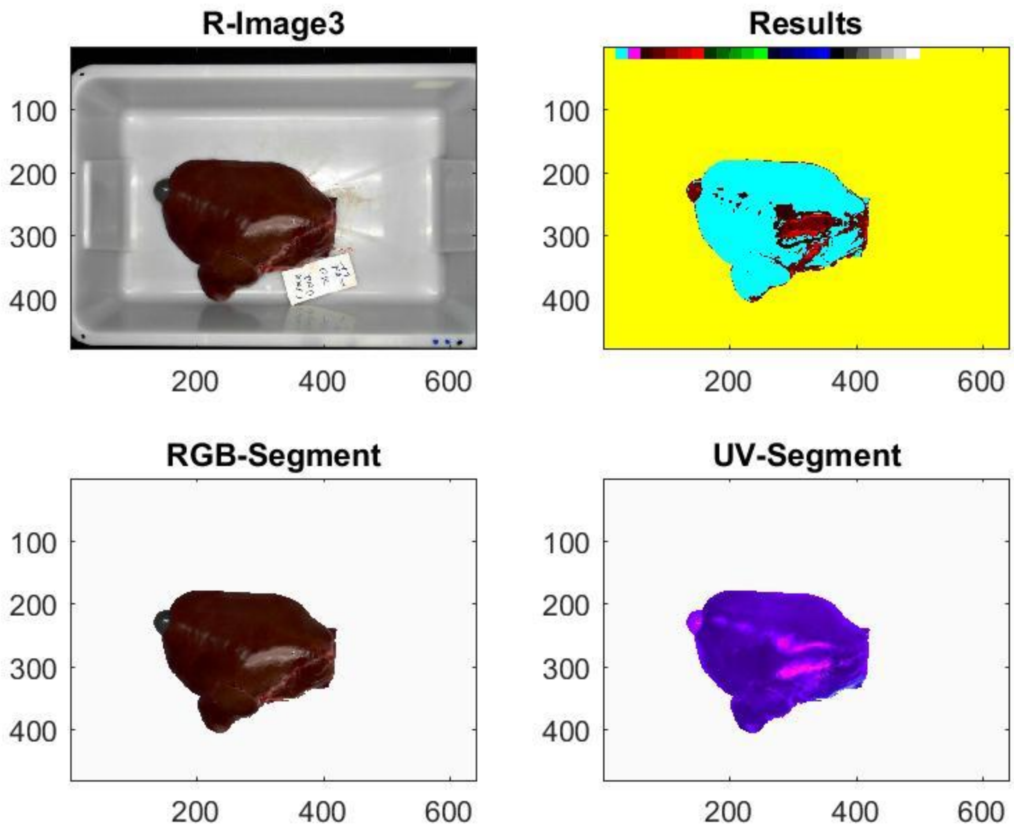

Interpretation:

Brown (least severe) and black (most severe) show regions of cirrhosis

Aqua shows regions of healthy tissue

Comments:

This liver was condemned for cirrhosis.

The gall bladder has been incorrectly highlighted and this effect will be removed in future work.

Offal 4

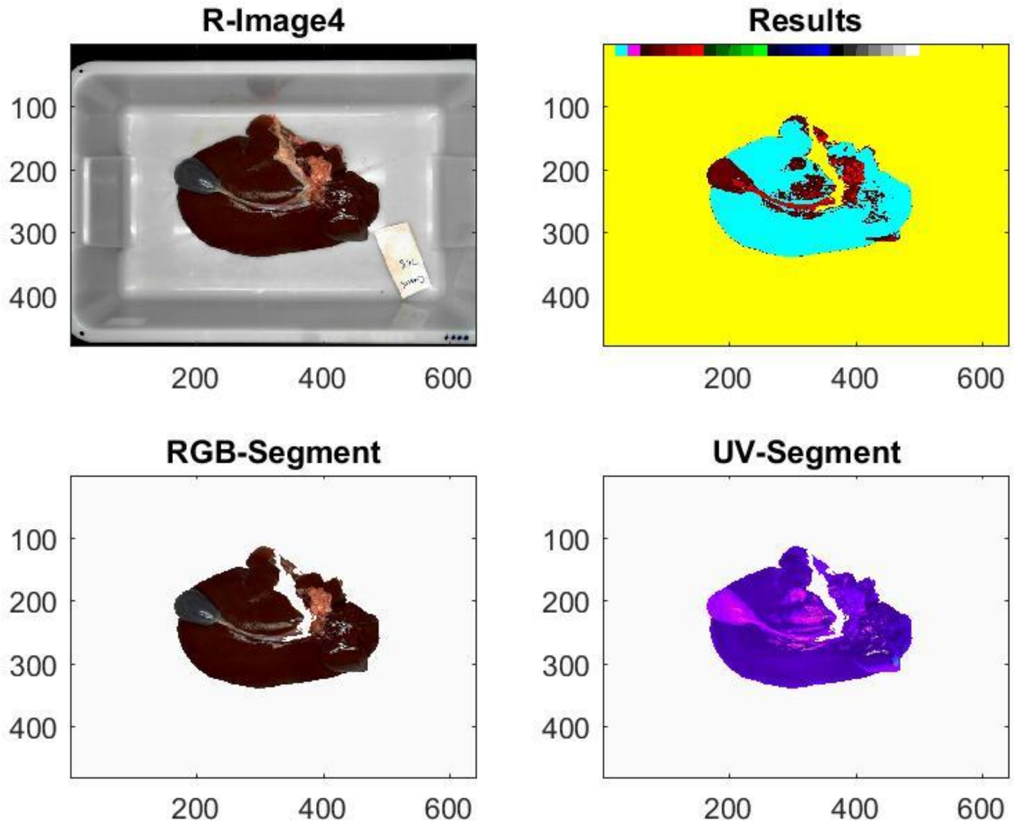

Interpretation:

Brown (least) and black (most) show regions of cirrhosis

Aqua shows regions of healthy tissue

Comments:

This liver was condemned for cirrhosis.

The gall bladder and some fat tissue has been incorrectly highlighted and this effect will be removed in future work.

Offal 5

Interpretation:

Not analysed

Comments:

This diaphragm was condemned for peritonitis, an inflammation of the peritoneum, the thin layer of tissue covering the inside of the abdomen and most of its organs.

A better understanding of how the inflammation is determined would be helpful in developing an algorithm.

Offal 6

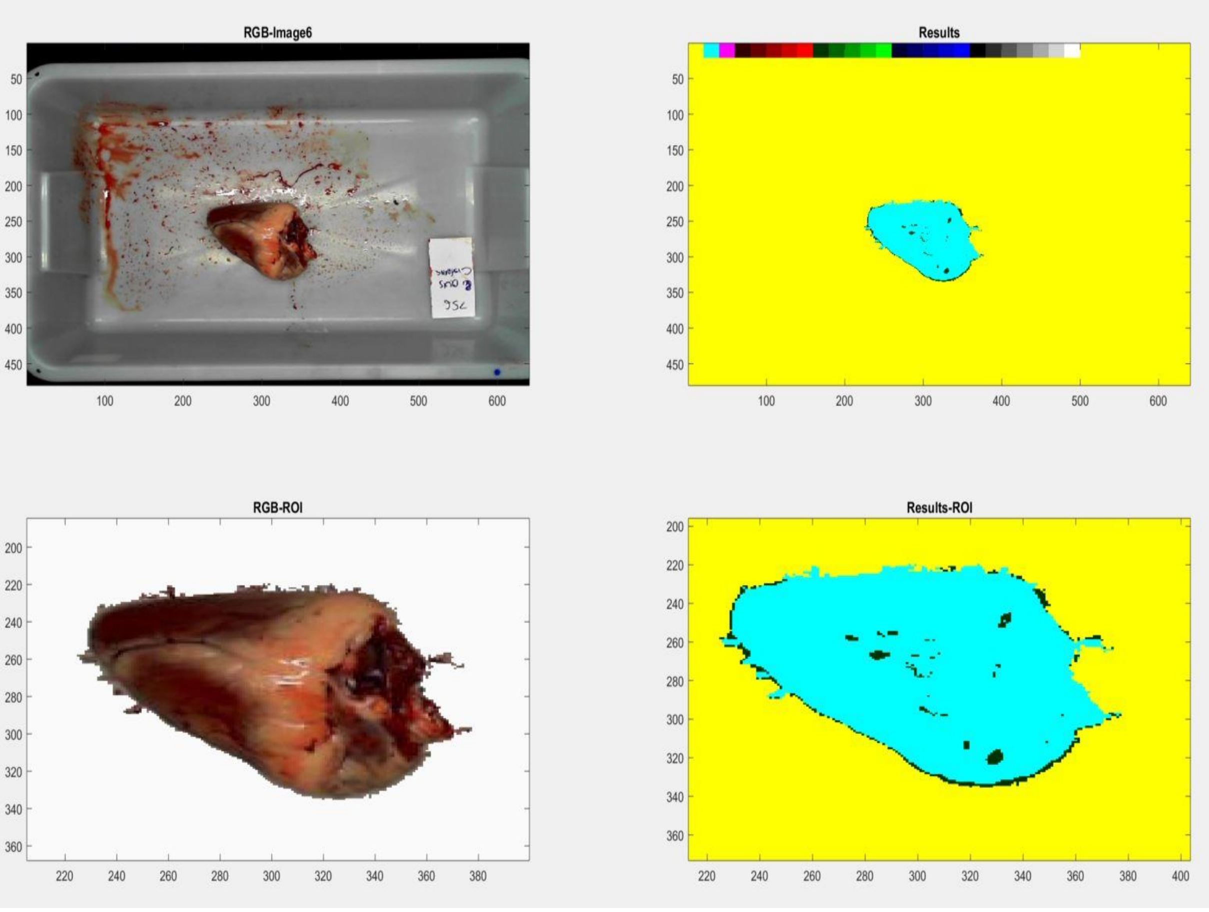

Interpretation:

Olive shows regions of c. ovis cysts

Aqua shows regions of healthy tissue

Comments:

This heart was condemned for c.ovis cisternae. The cysts appear as whiter spots in the epicardial adipose tissue.

Offal 7

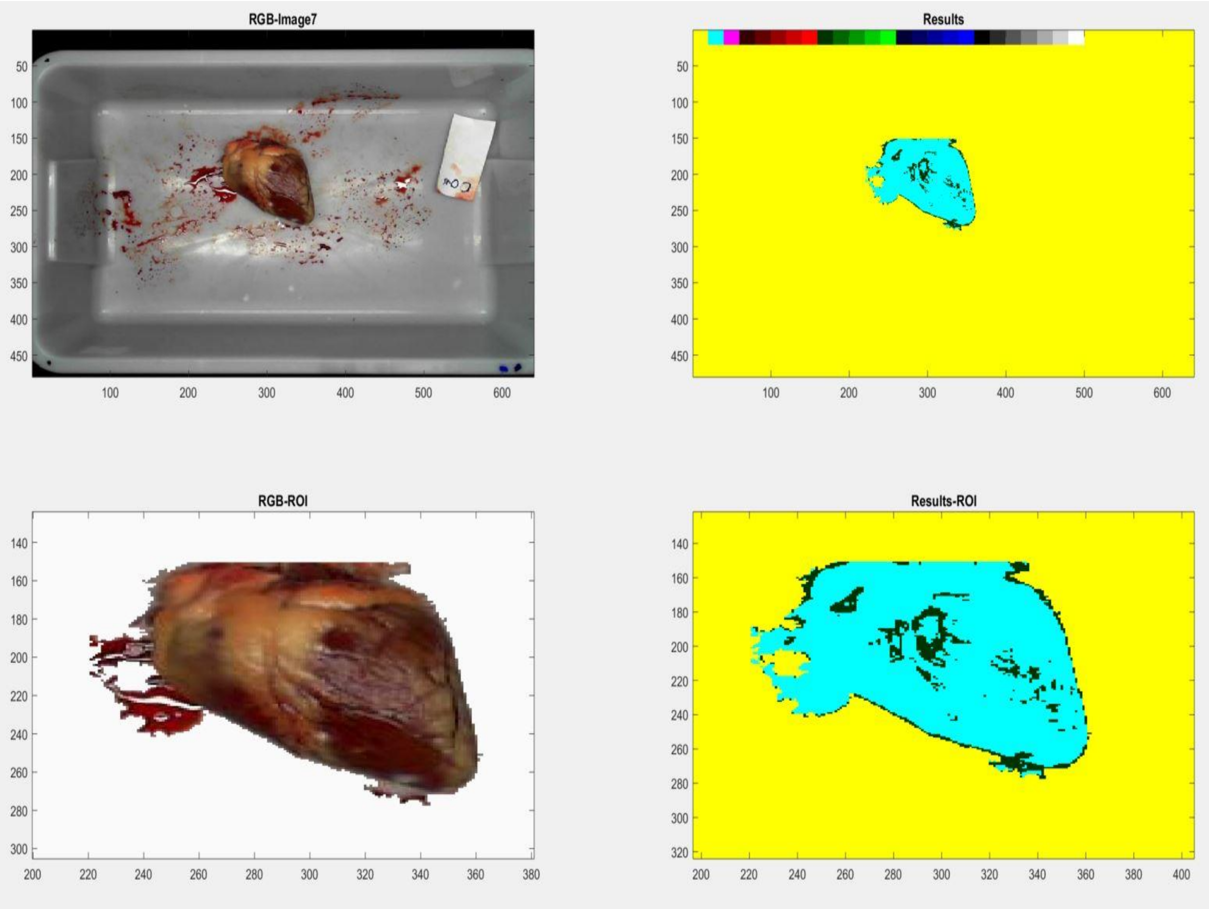

Interpretation:

Olive shows regions of c. ovis cysts

Aqua shows regions of healthy tissue

Comments:

This heart was condemned for c. ovis near the apex of the heart. There are false positive pixels in the epicardial adipose tissue.

Offal 8

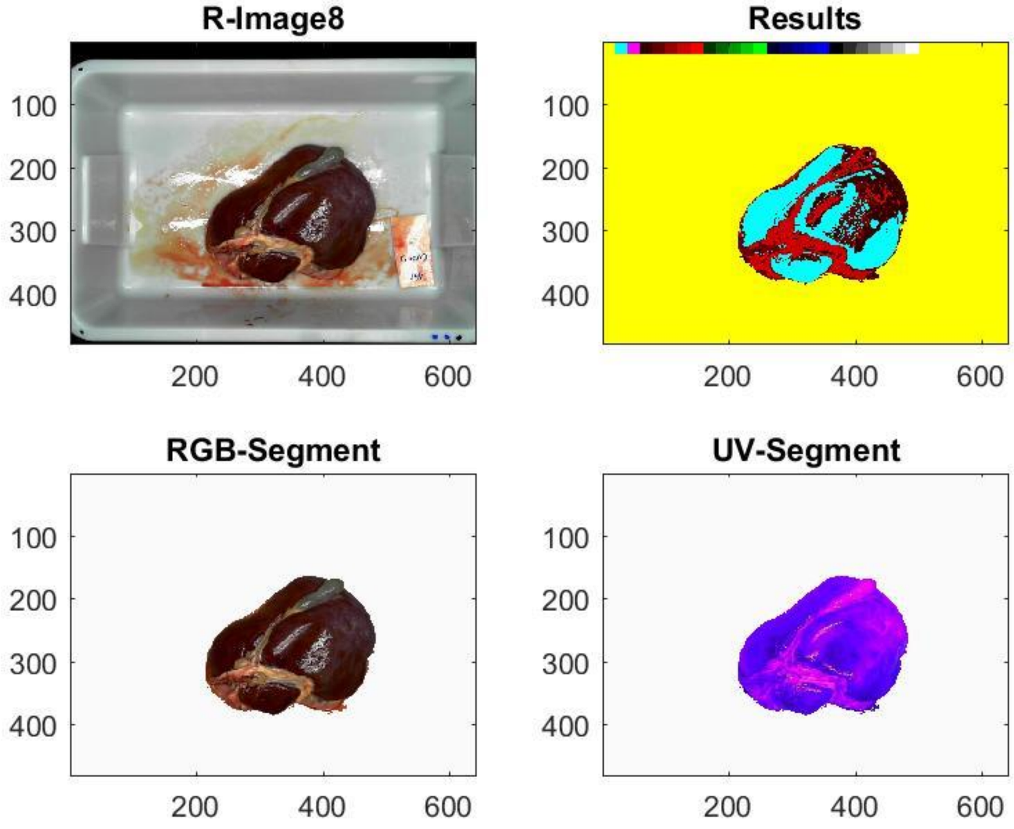

Interpretation:

Brown (least) and black (most) show regions of cirrhosis

Aqua shows regions of healthy tissue

Comments:

This liver was condemned for cirrhosis.

The gall bladder and some fat tissue has been incorrectly highlighted and this effect will be removed in future work.

<u>Offal 9</u>

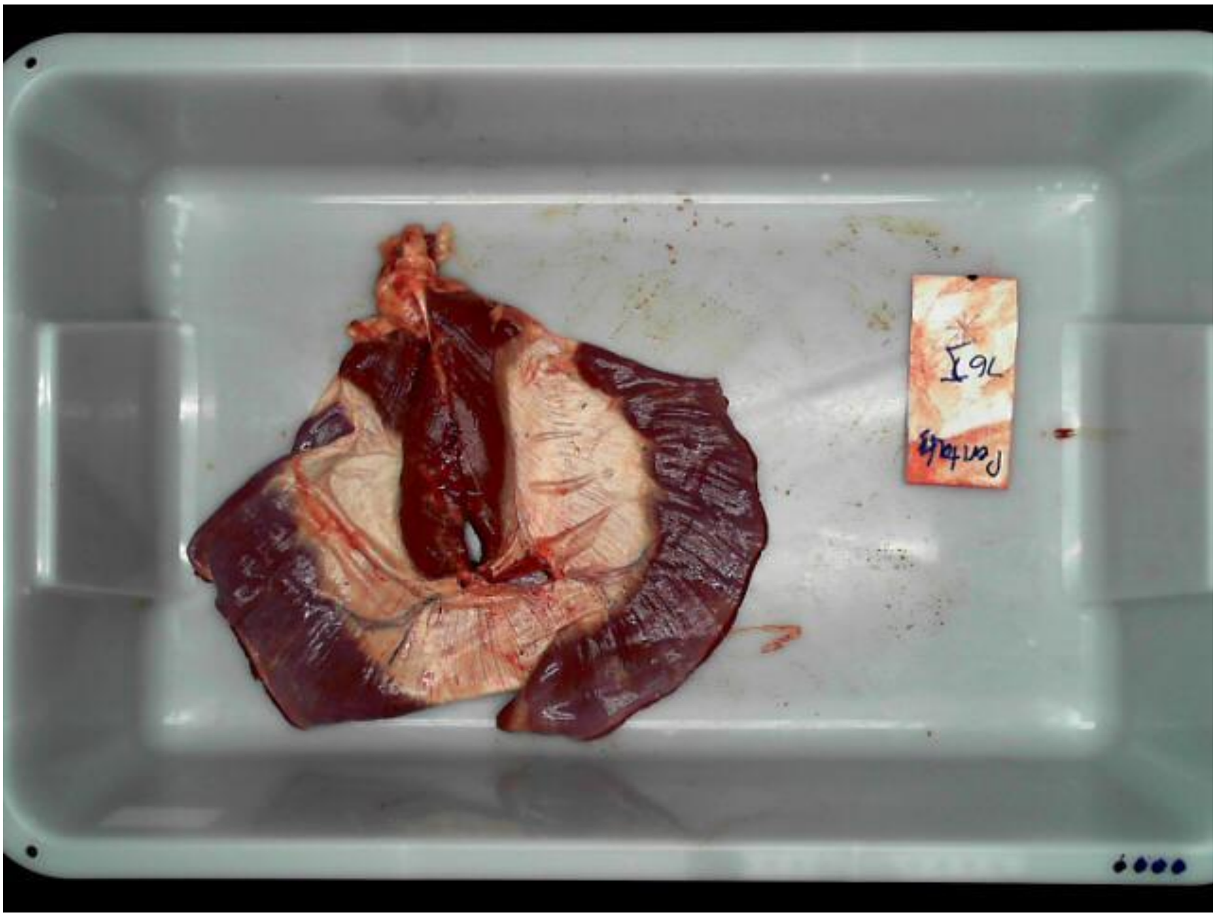

Interpretation:

Not analysed

Comments:

This diaphragm was condemned for peritonitis, an inflammation of the peritoneum, the thin layer of tissue covering the inside of the abdomen and most of its organs.

A better understanding of how the inflammation is determined would be helpful in developing an algorithm.

Offal 10

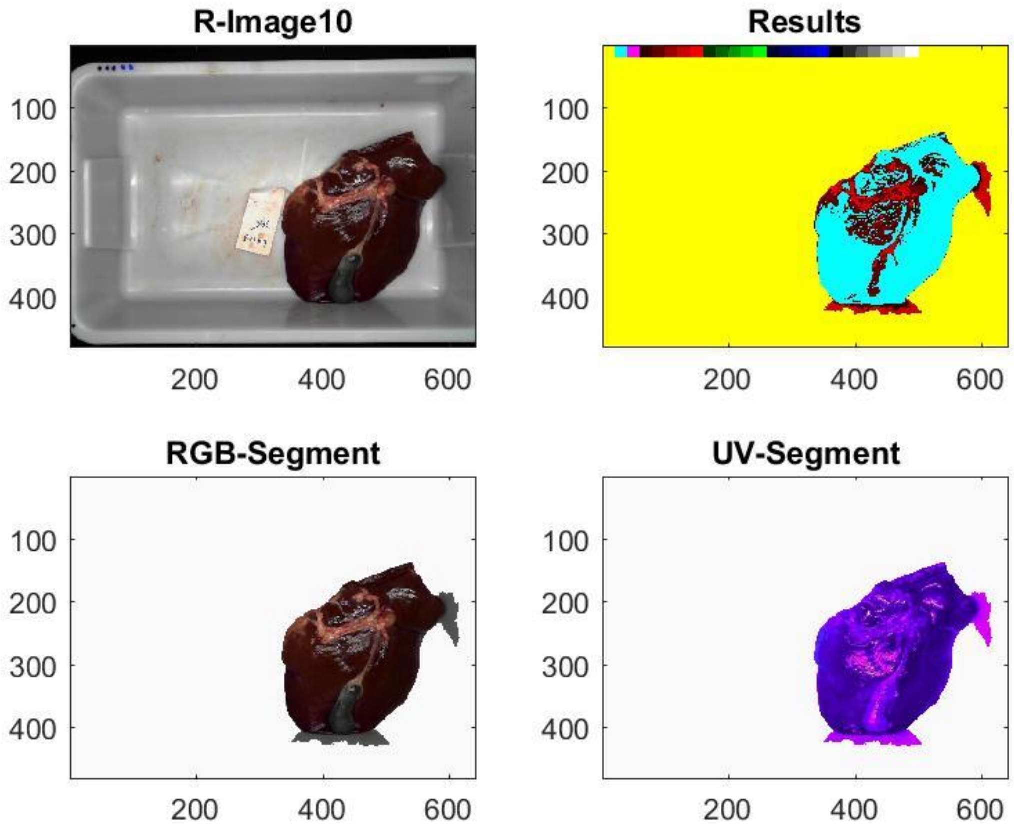

Interpretation:

Brown (least) and black (most) show regions of cirrhosis

Aqua shows regions of healthy tissue

Comments:

This liver was condemned for cirrhosis.

Some fat tissue has been incorrectly highlighted and this effect will be removed in future work.

Offal 11

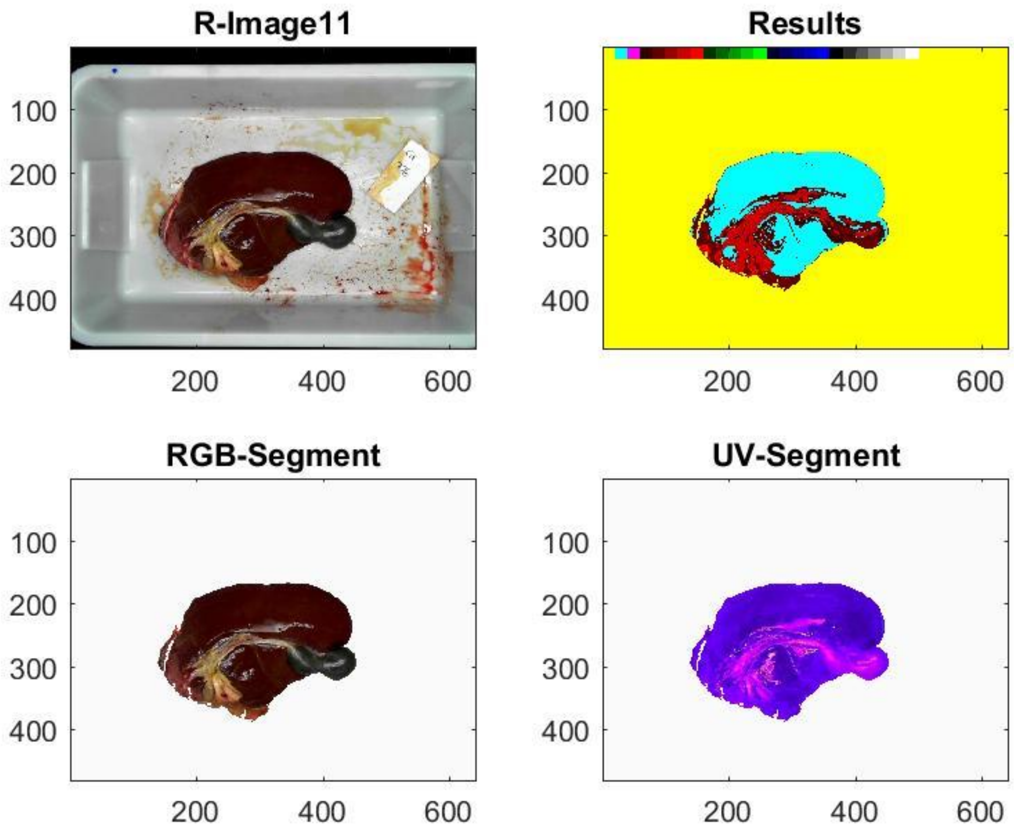

Interpretation:

Brown (least) and black (most) show regions of cirrhosis

Aqua shows regions of healthy tissue

Comments:

This liver was condemned for cirrhosis.

The gall bladder and some fat tissue has been incorrectly highlighted and this effect will be removed in future work.

Offal 12

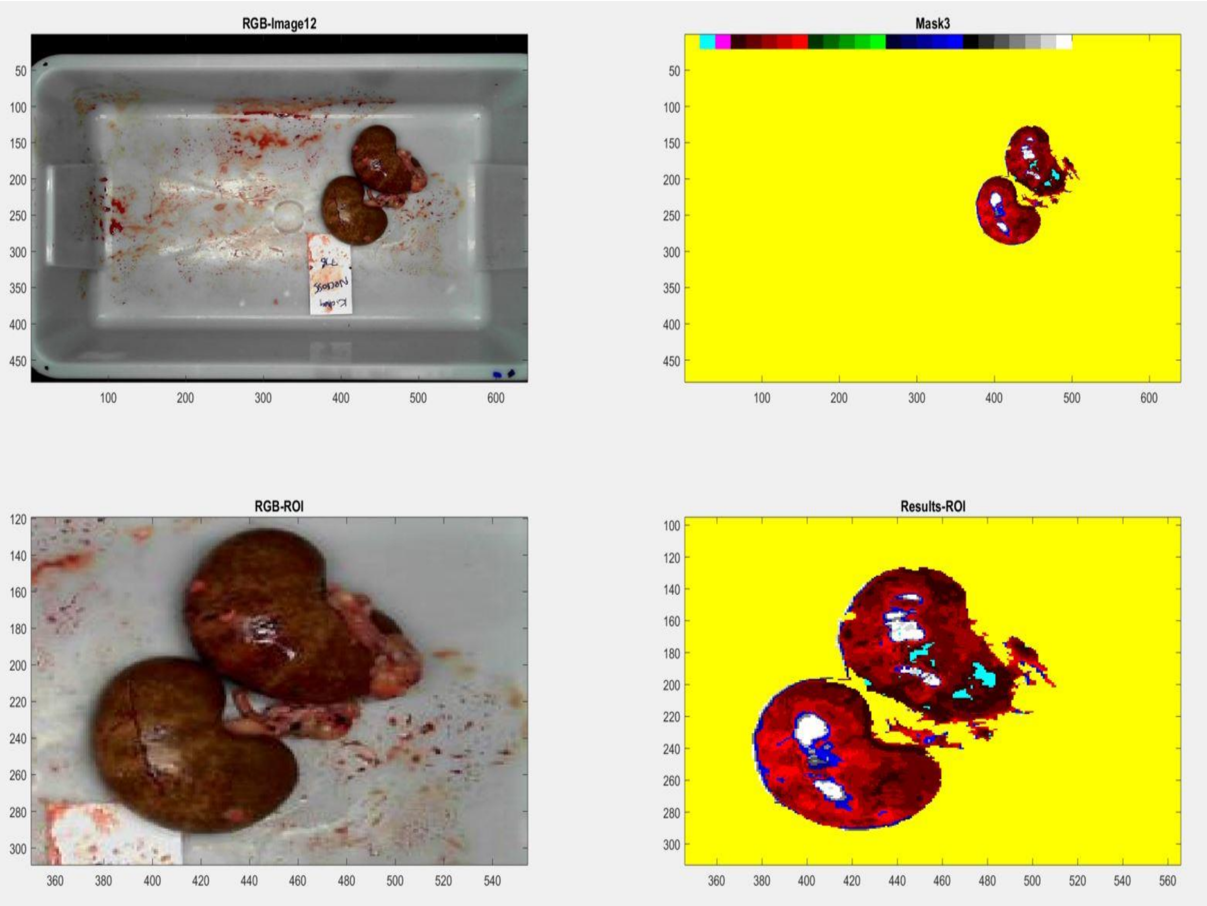

Interpretation:

Red (least), light brown, dark brown and blue (most) show regions of nephritis

White are reflective light

Aqua shows regions of healthy tissue

Comments:

This kidney was condemned for necrosis

Offal 13

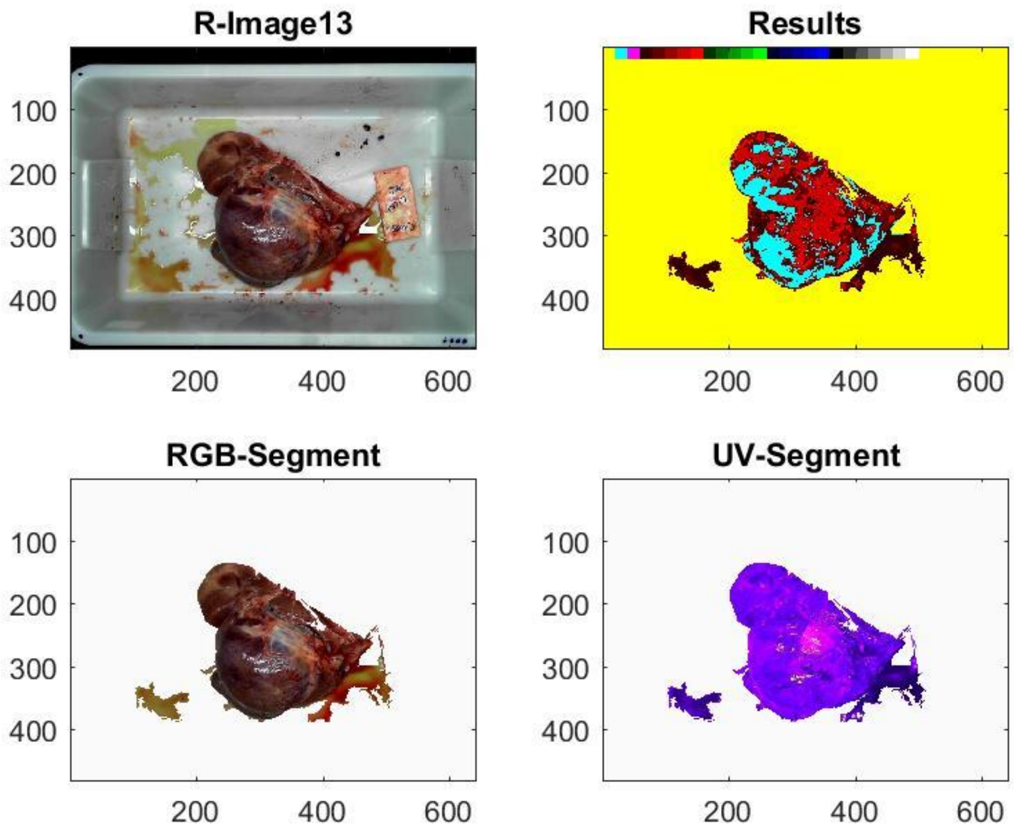

Interpretation:

Brown (least) and black (most) show regions of cirrhosis

Aqua shows regions of healthy tissue

Comments:

This liver was condemned for severe cirrhosis.

Offal 14

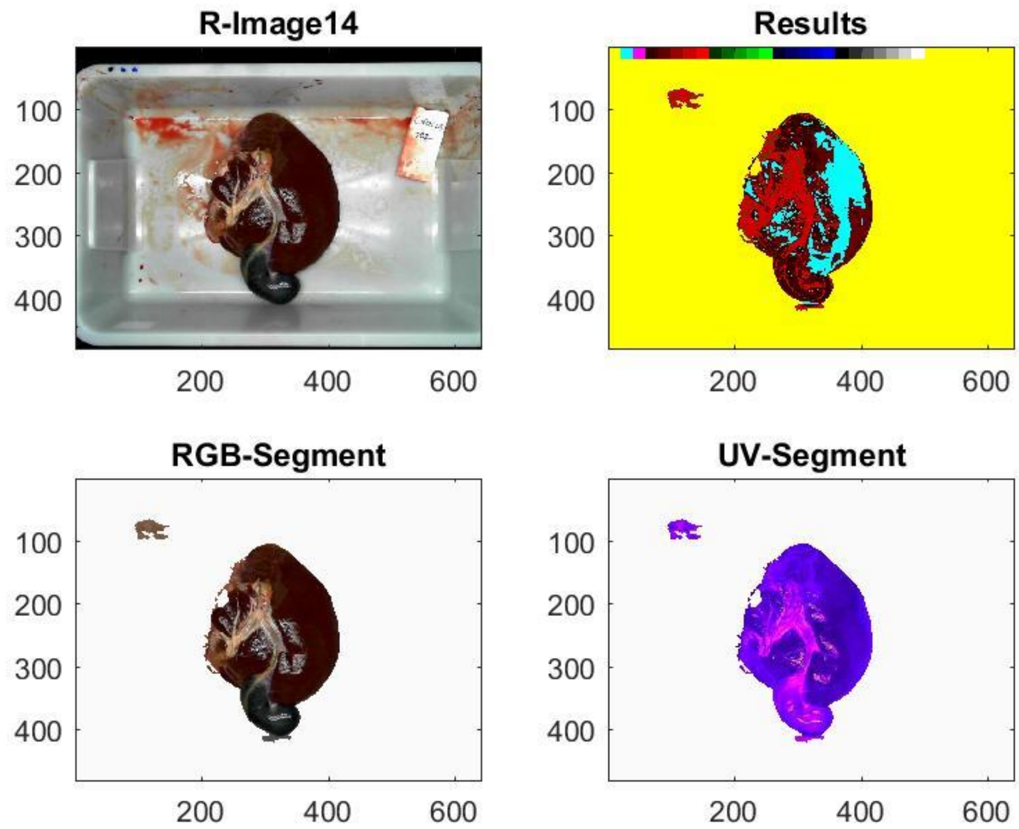

Interpretation:

Brown (least) and black (most) show regions of cirrhosis

Aqua shows regions of healthy tissue

Comments:

This liver was condemned for cirrhosis.

The gall bladder and some fat tissue has been incorrectly highlighted and this effect will be removed in future work.

Offal 15

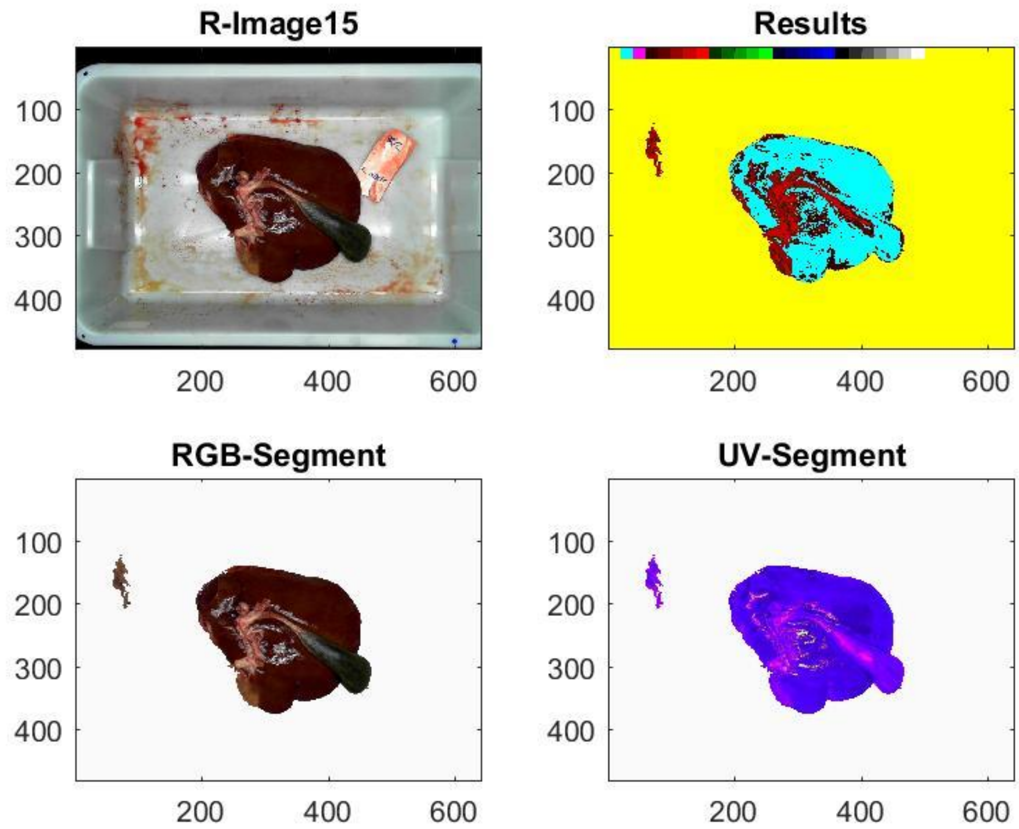

Interpretation:

Brown (least) and black (most) show regions of cirrhosis

Aqua shows regions of healthy tissue

Comments:

This liver was condemned for cirrhosis.

The gall bladder and some fat tissue has been incorrectly highlighted and this effect will be removed in future work.

Offal 16

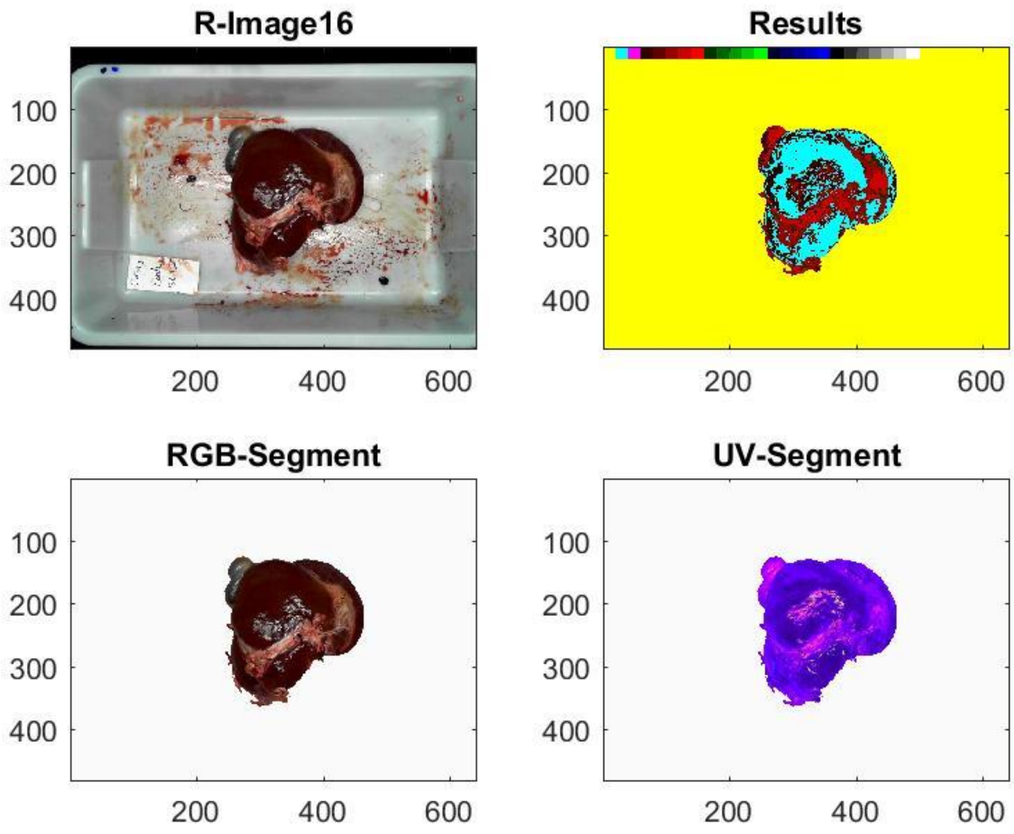

Interpretation:

Brown (least) and black (most) show regions of cirrhosis

Aqua shows regions of healthy tissue

Comments:

This liver was condemned for cirrhosis.

The gall bladder and some fat tissue has been incorrectly highlighted and this effect will be removed in future work.

Offal 17

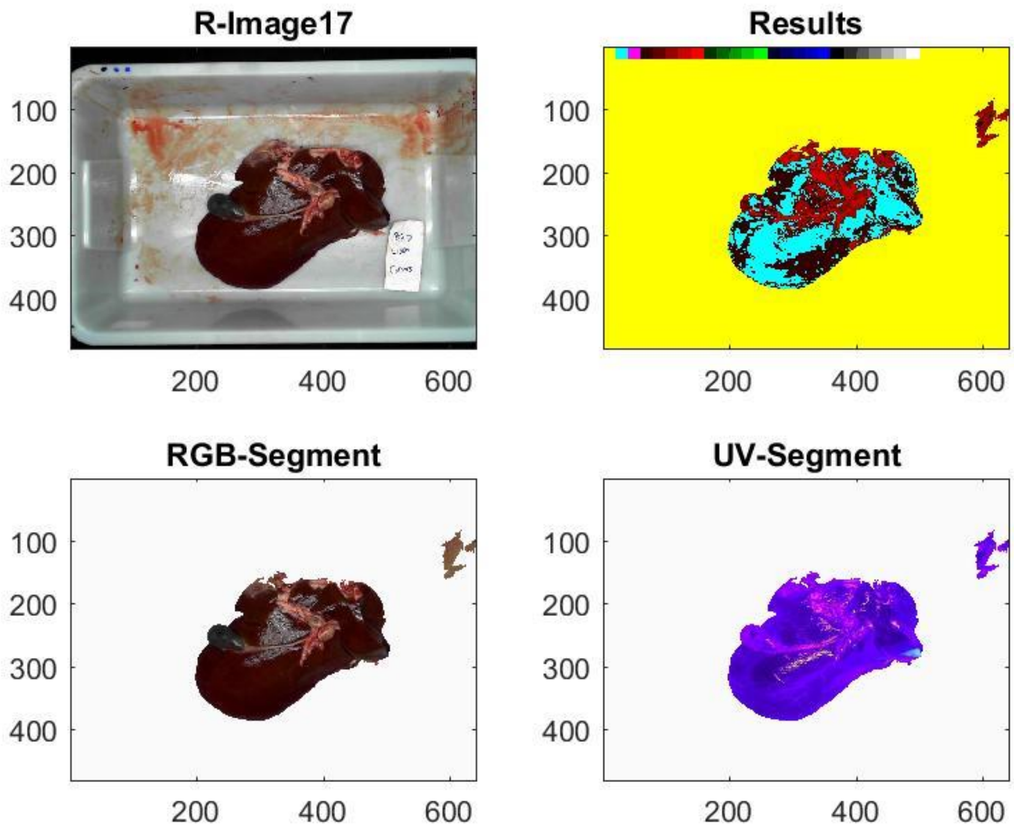

Interpretation:

Brown (least) and black (most) show regions of cirrhosis

Aqua shows regions of healthy tissue

Comments:

This liver was condemned for cirrhosis.

The gall bladder and some fat tissue has been incorrectly highlighted and this effect will be removed in future work.

Offal 18

Offal Set 18

Interpretation:

The region enclosed by the ellipse shows the liver fluke observable in the colour image.

Comments:

The liver fluke nematode in this liver is small and the tissue surrounding it has a very similar appearance to the “silver-skin” around the adipose tissue.

The presence of liver fluke is marginal in this X-ray. However, the liver fluke, gall bladder and duct have been imaged from the underside (i.e. through the bottom of the tray and liver). The X-ray also shows the internal structure of the liver in detail.

Offal 19

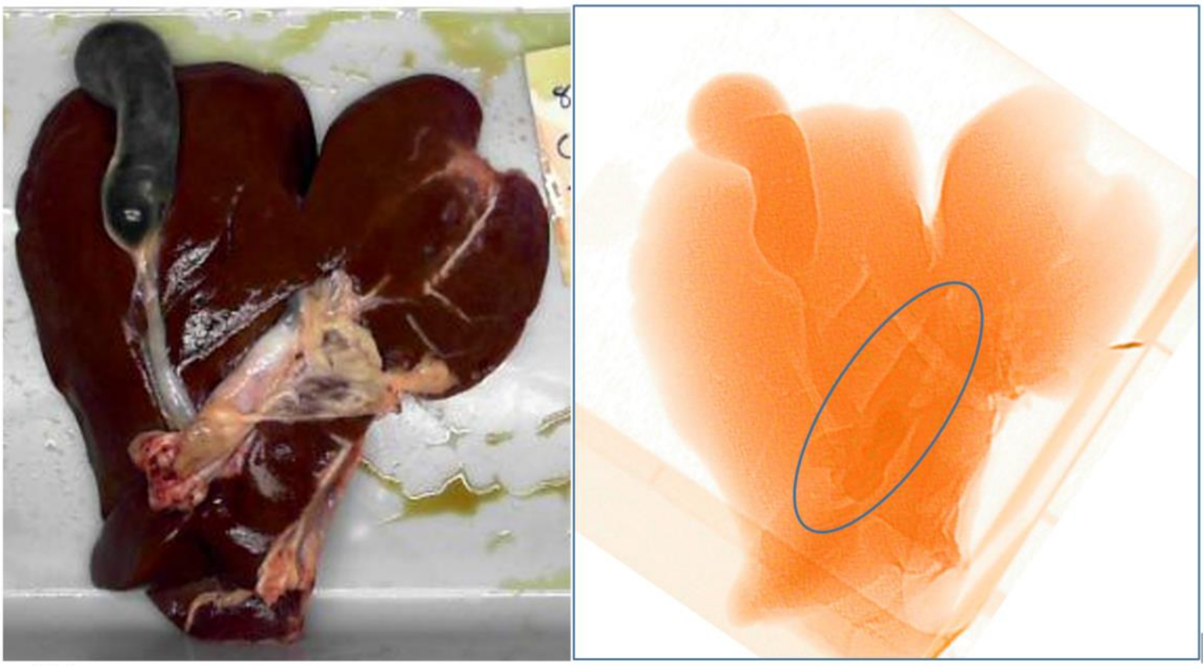

Offal Set 19

Interpretation:

The region enclosed by the ellipse shows the liver fluke observable in the colour image.

Comments:

The liver fluke nematode in this liver is large and the tissue surrounding it has a very similar appearance to the "silver-skin" around the adipose tissue and gall duct.

The presence of liver fluke is marginal in this X-ray. However, the liver fluke, gall bladder and duct have been imaged from the underside (i.e. through the bottom of the tray and liver). The X-ray also shows the internal structure of the liver in detail.

Offal 20

This heart was condemned for c.ovis, however the cyst was obscured by fat during imaging. It has therefore not been processed

Offal 21

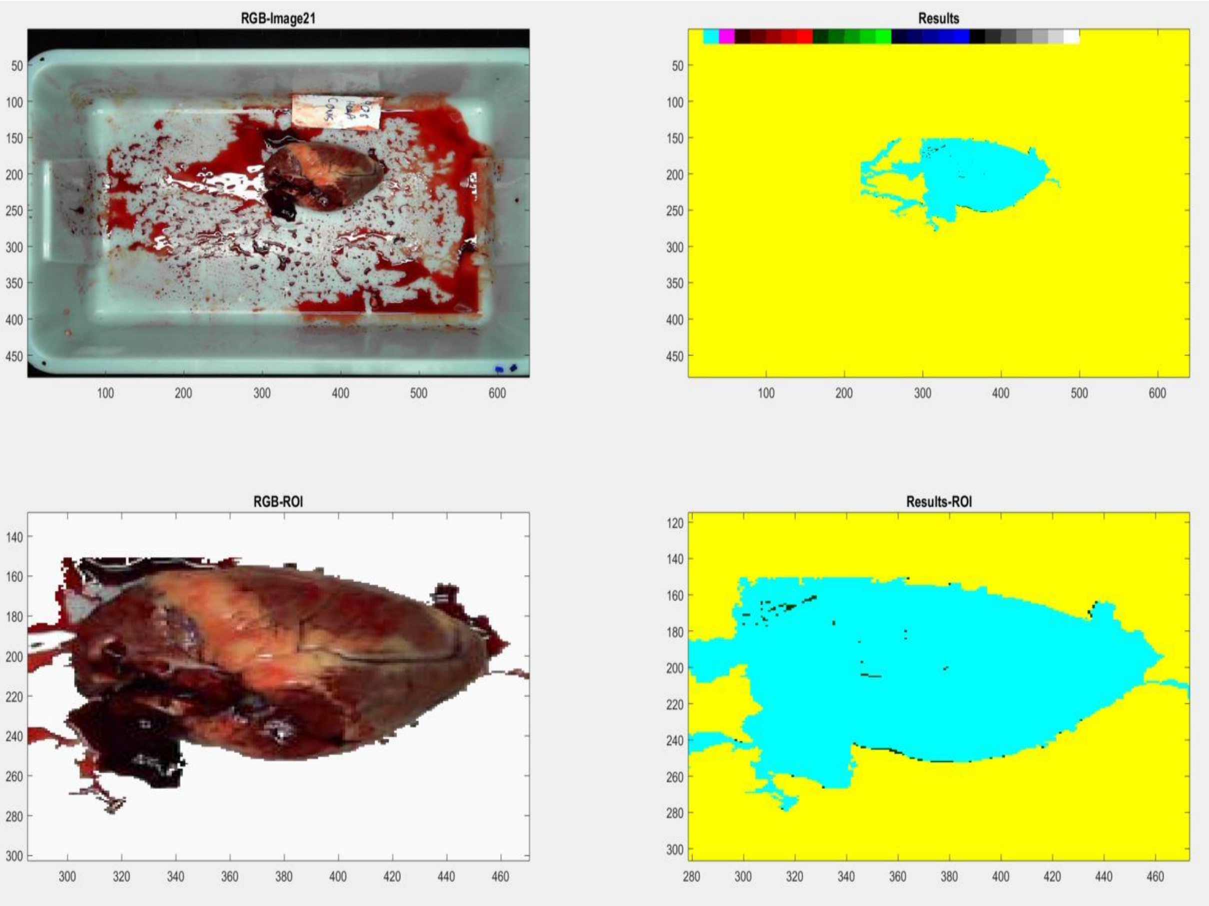

Interpretation:

Olive shows regions of c. ovis cysts

Aqua shows regions of healthy tissue

Comments:

This heart was condemned for c. ovis, however the cysts seem to be obscured.

Offal 22

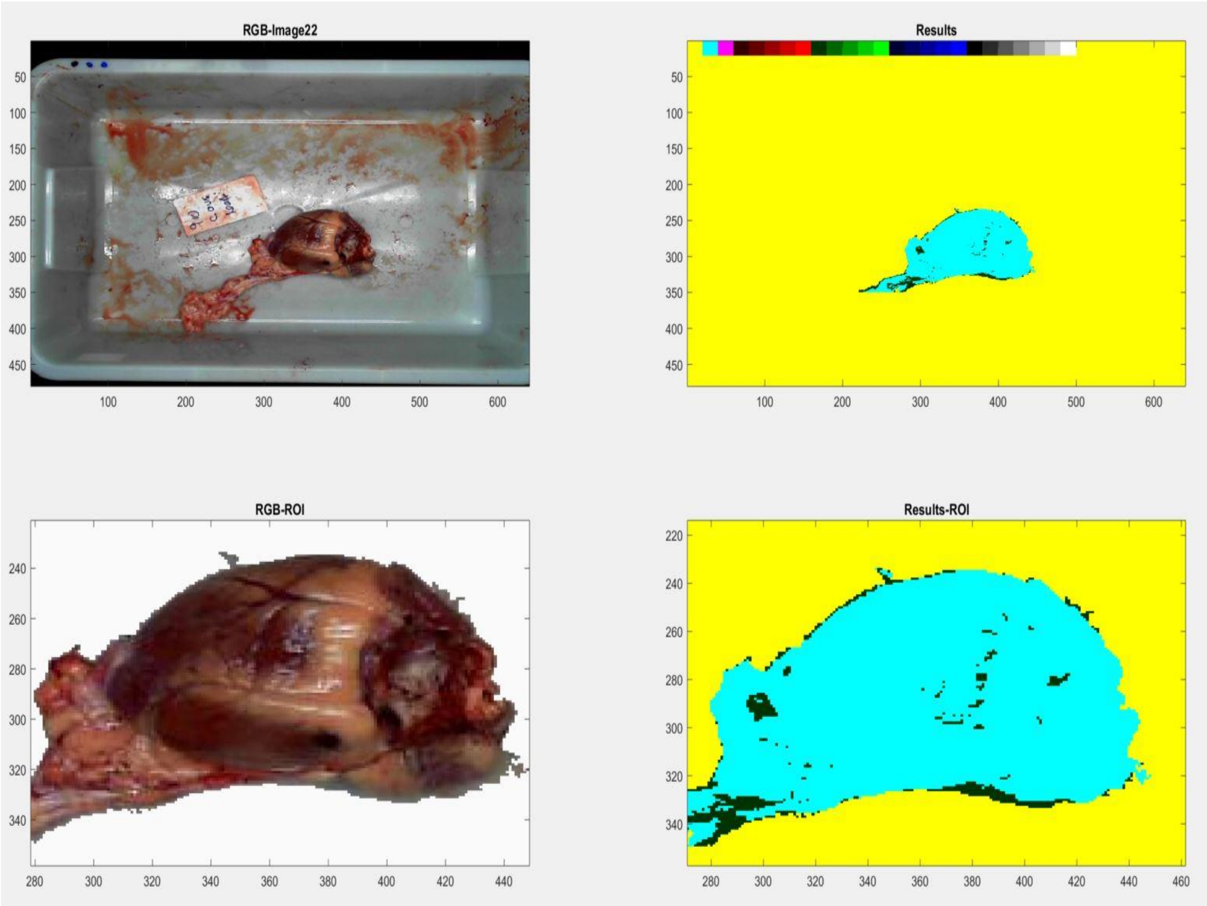

Interpretation:

Olive shows regions of c. ovis cysts

Aqua shows regions of healthy tissue

Comments:

This heart was condemned for c. ovis at [310,280]

AMPC

Offal 23

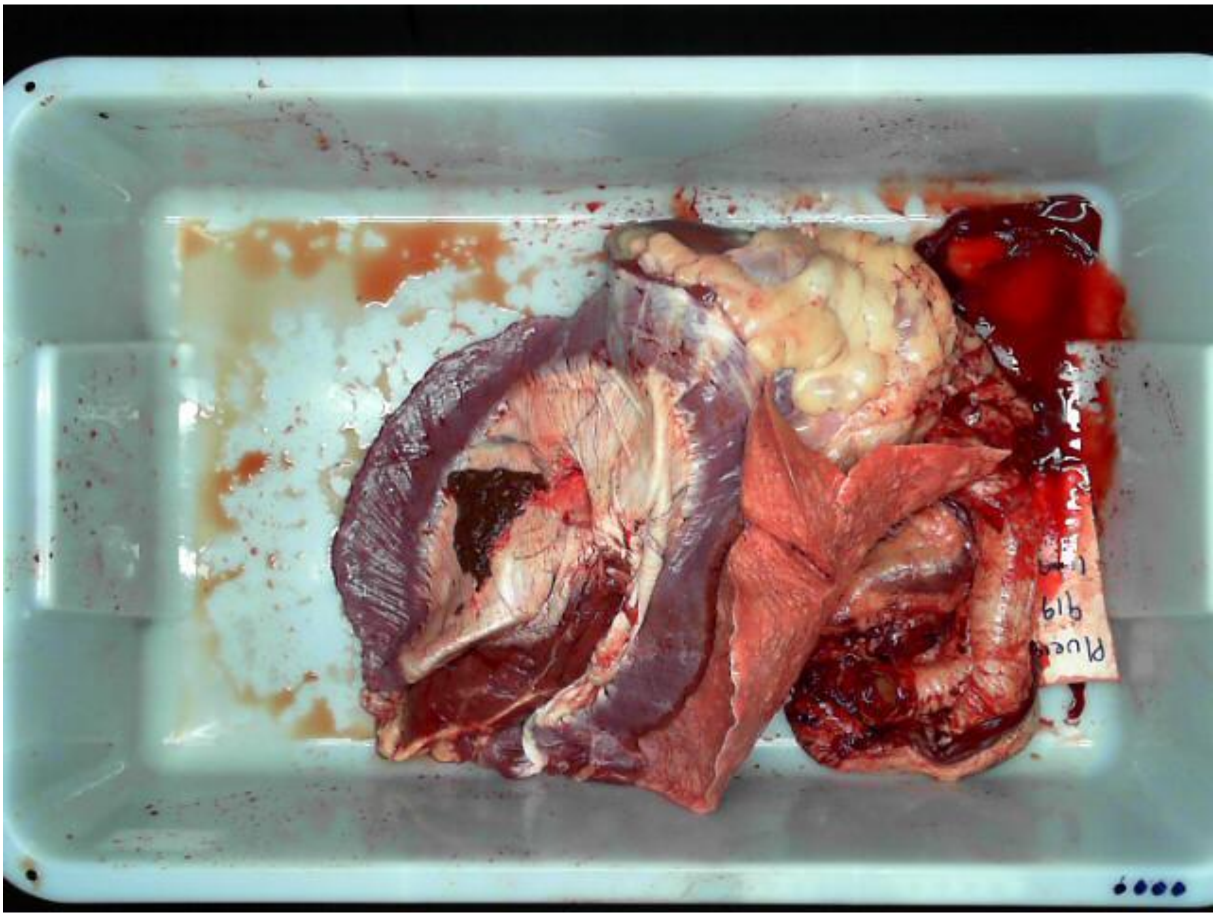

Interpretation:

Not analysed

Comments:

This pluck was condemned for pleurisy.

Pleurisy is the adhesion of lung material to the diaphragm, therefore the material that needs to be detected is a thin layer of “glue” between two tissues. Thus the thin layer is not easily seen by non-penetrative imaging (i.e. cameras and hyperspectral imaging) and also does not create a strong density difference detectible by DXA X-ray imagers.

Offal 24

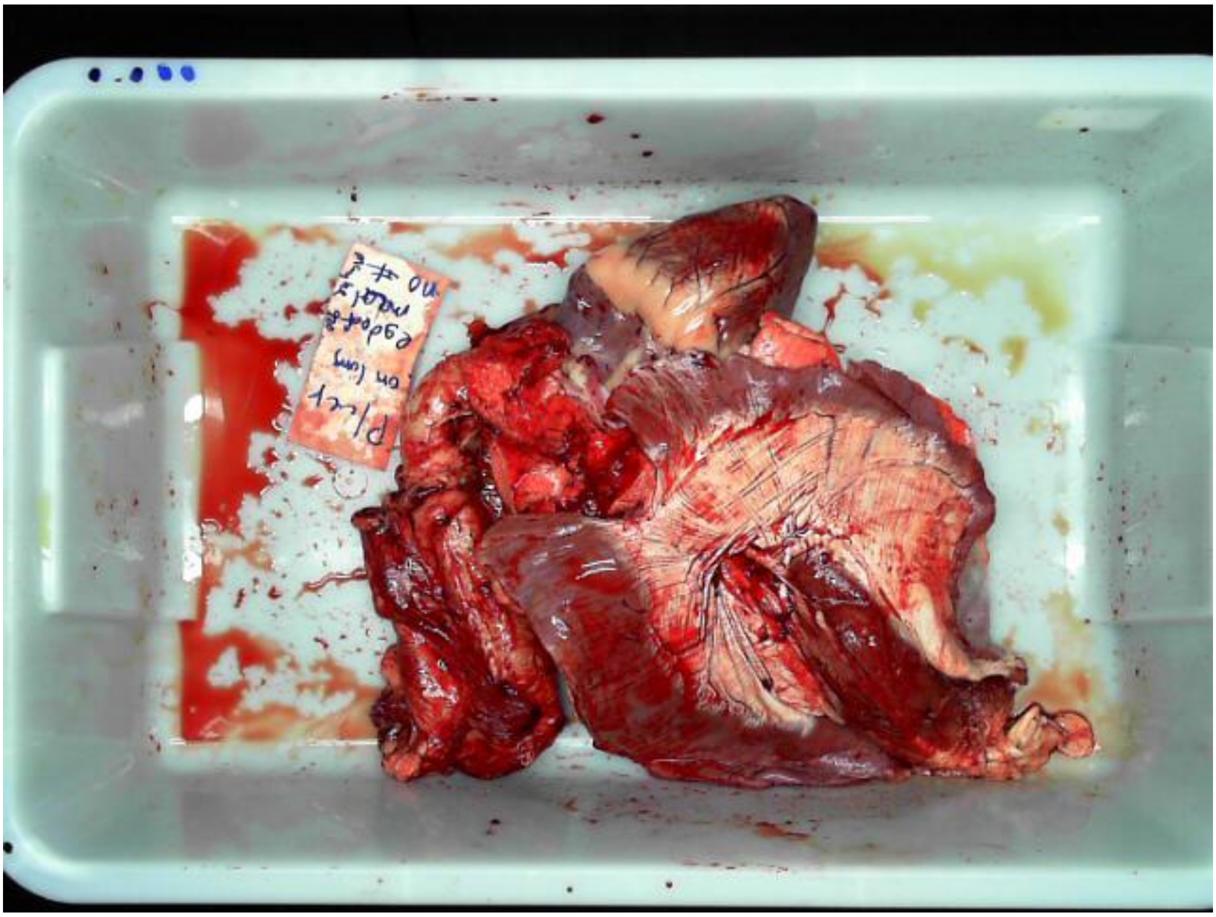

Interpretation:

Not analysed

Comments:

This pluck was condemned for pleurisy. Pleurisy is the adhesion of lung material to the diaphragm, therefore the material that needs to be detected is a thin layer of "glue" between two tissues. Thus the thin layer is not easily seen by non-penetrative imaging (i.e. cameras and hyperspectral imaging) and also does not create a strong density difference detectible by DXA X-ray imagers.

<u>Offal 25</u>

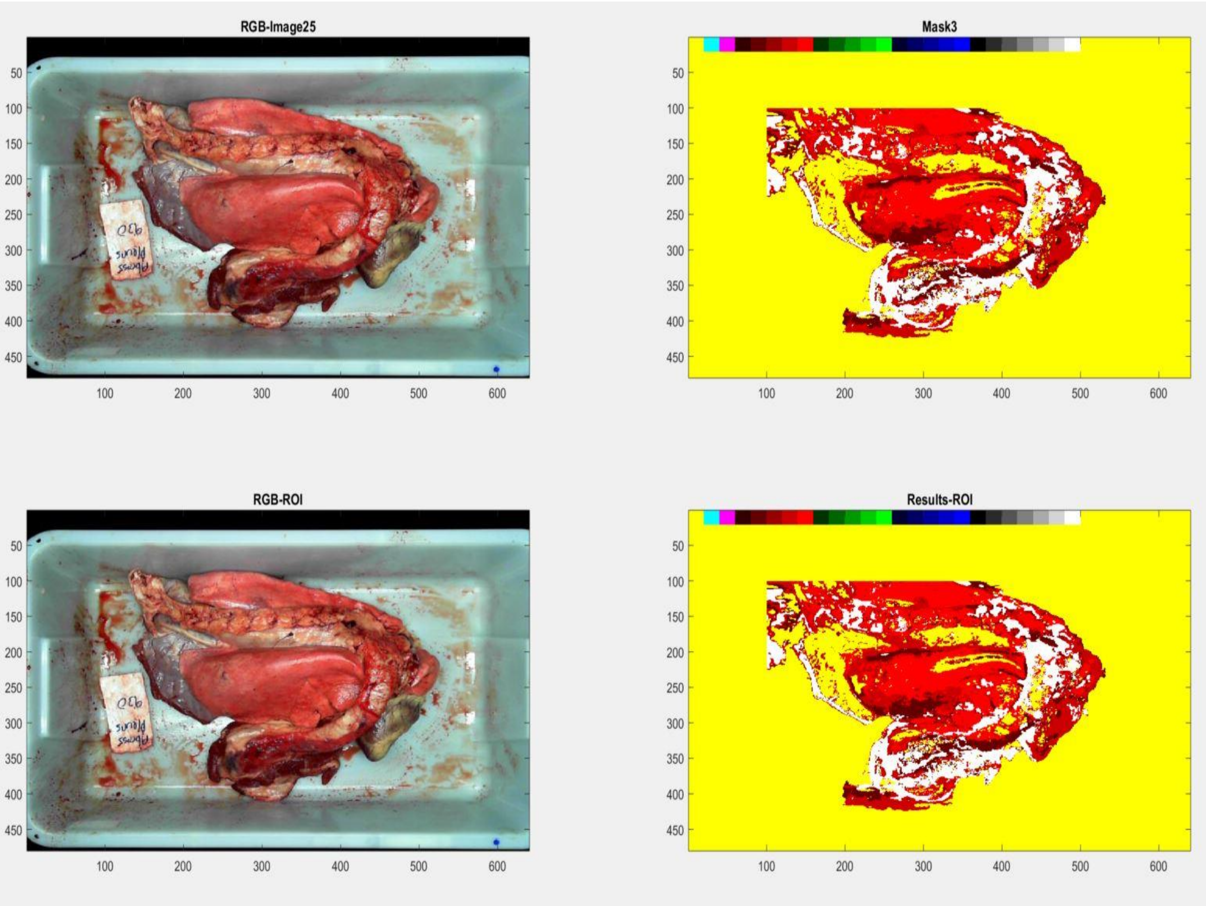

Interpretation:

Red (healthy) to light brown to dark brown (most unhealthy) lung tissue

White show tissue not of interest.

Comments:

This lung was condemned for the presence of abscesses in the lower lung and pleurisy. The abscess has been indicated but with only a slight intensity due to the impact of the dark tissue around the trachea causing an automatic adjustment in colour intensity in the cameras.

Offal 26

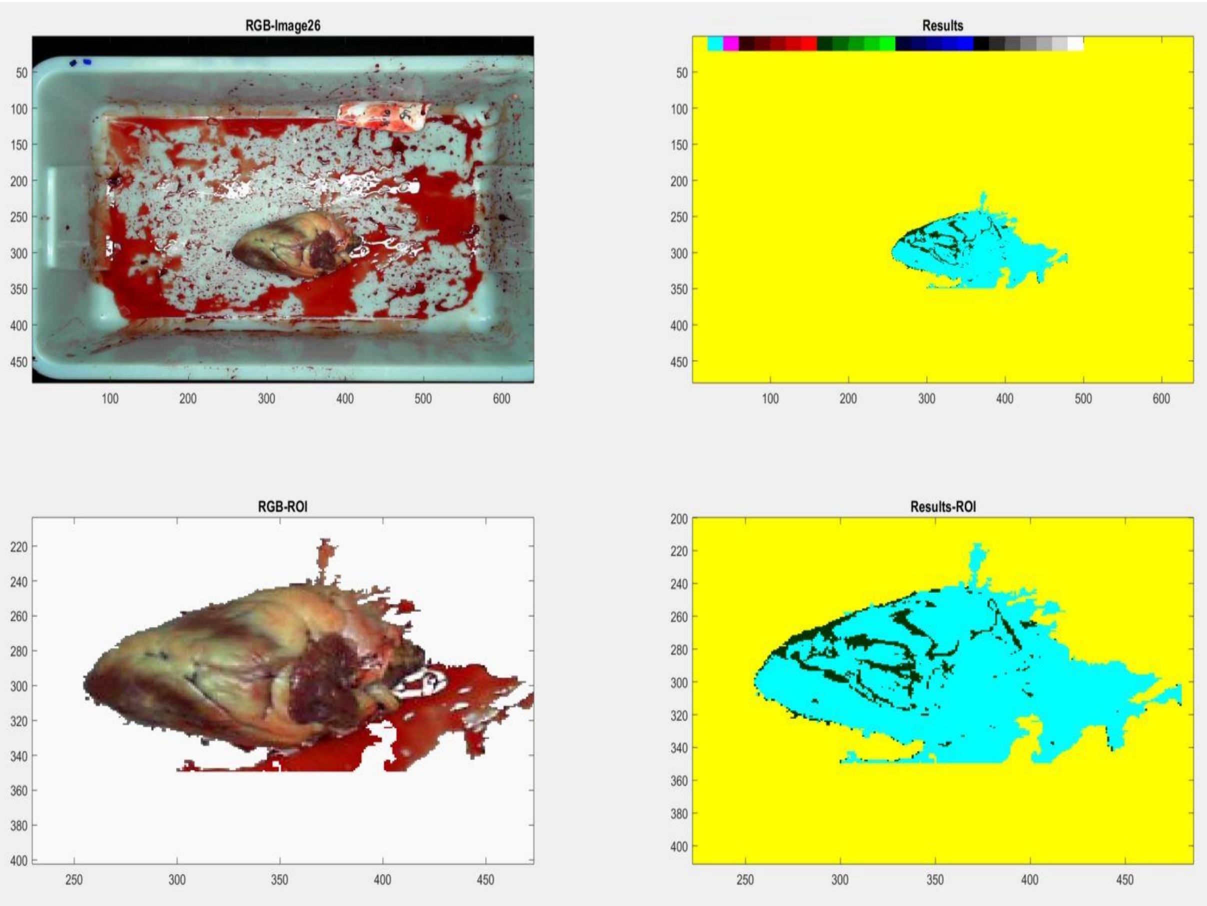

Interpretation:

Olive shows regions of c. ovis cysts

Aqua shows regions of healthy tissue

Comments:

This heart was condemned for the presence of c. ovis at [280,310]

<u>Offal 27</u>

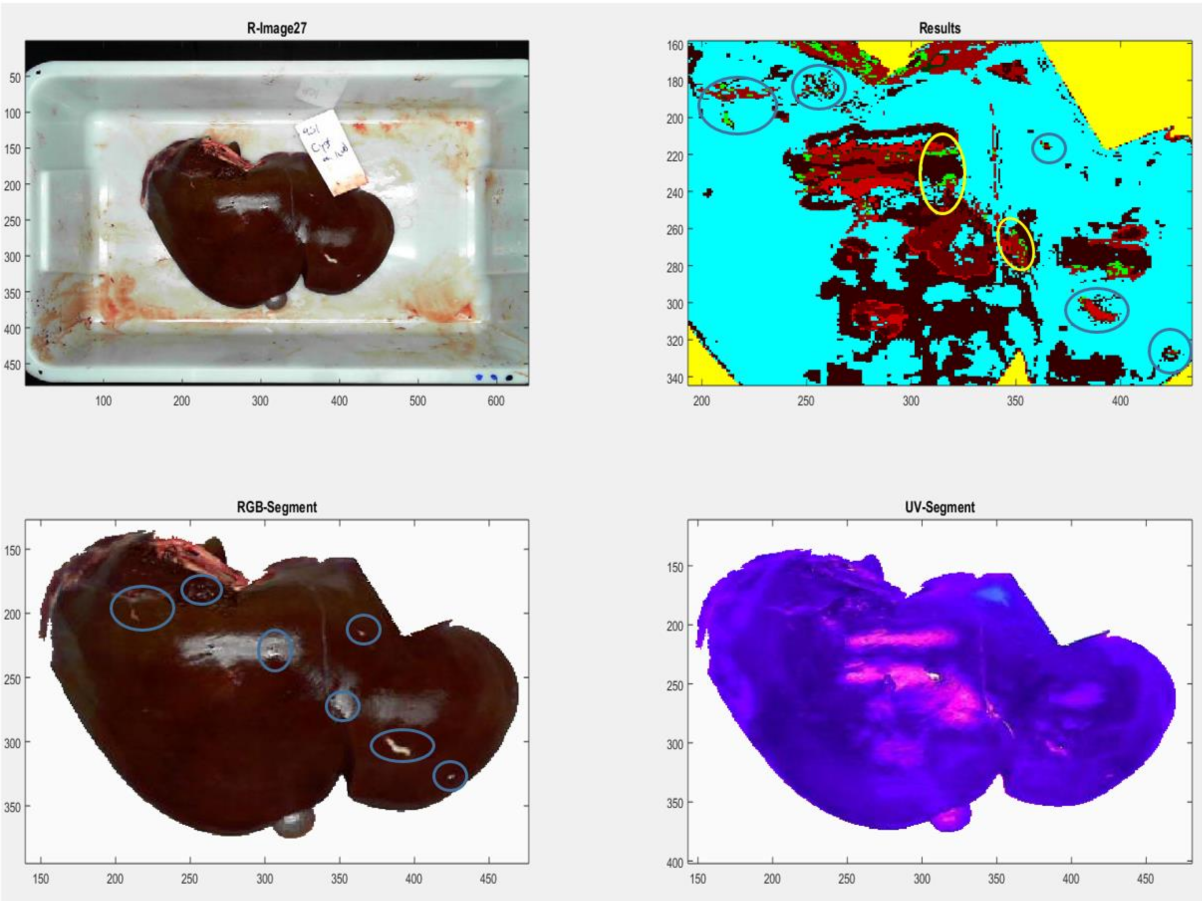

Interpretation:

Brown (least) and black (most) show regions of cirrhosis

Green shows “abnormal biomass”

Aqua shows regions of healthy tissue

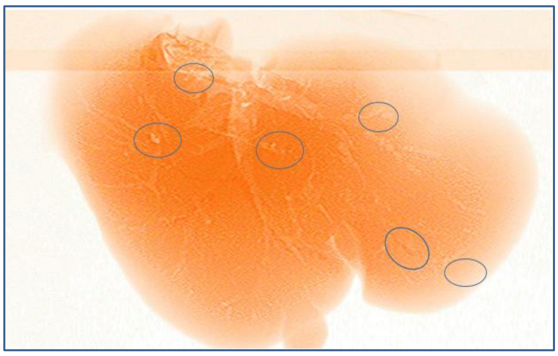

Comments:

This liver was condemned for having more than 5 cysts.

This cysts are identified by green/brown within the ellipses.

The DXA image was manually assessed with a prior knowledge, but demonstrates that cysts are visible to a “trained” eye. White spots in the lower middle suggest that internal cysts may also have been present.

<u>Offal 28</u>

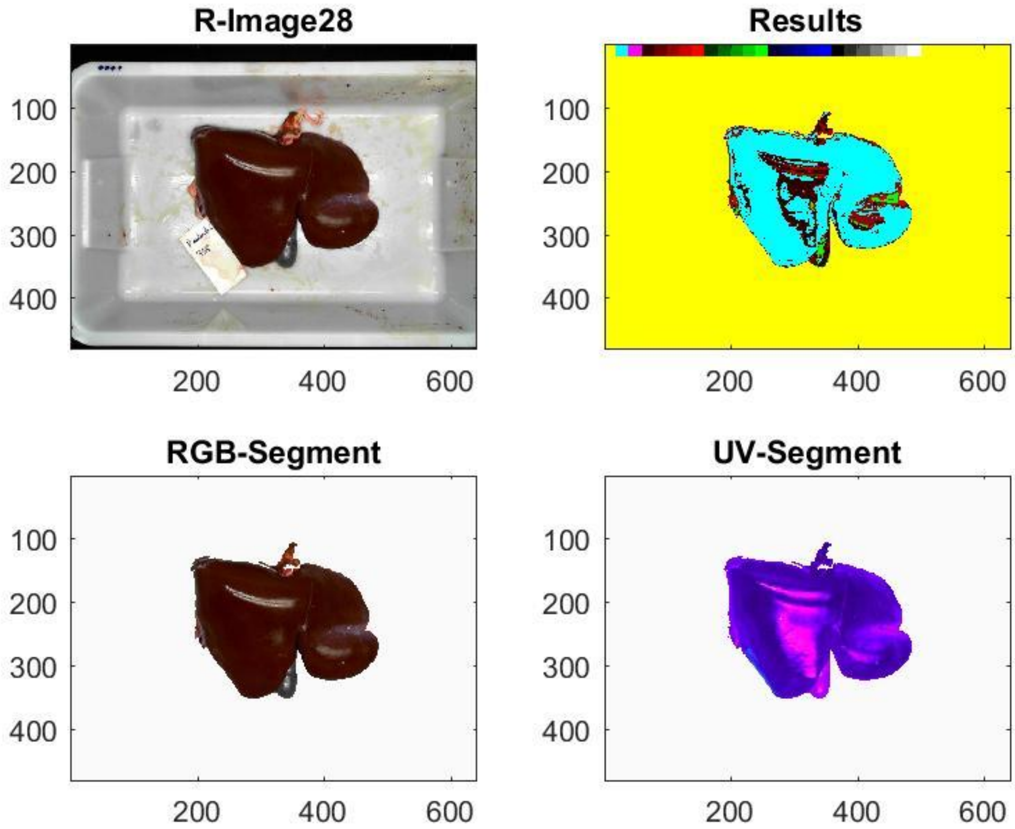

Interpretation:

Brown (least) and black (most) show regions of cirrhosis

Green shows “abnormal biomass”

Aqua shows regions of healthy tissue

Comments:

This liver was condemned for cirrhosis.

This liver was condemned for having liver pericarditis, which is seen as “green” in the top right image.

Offal 29

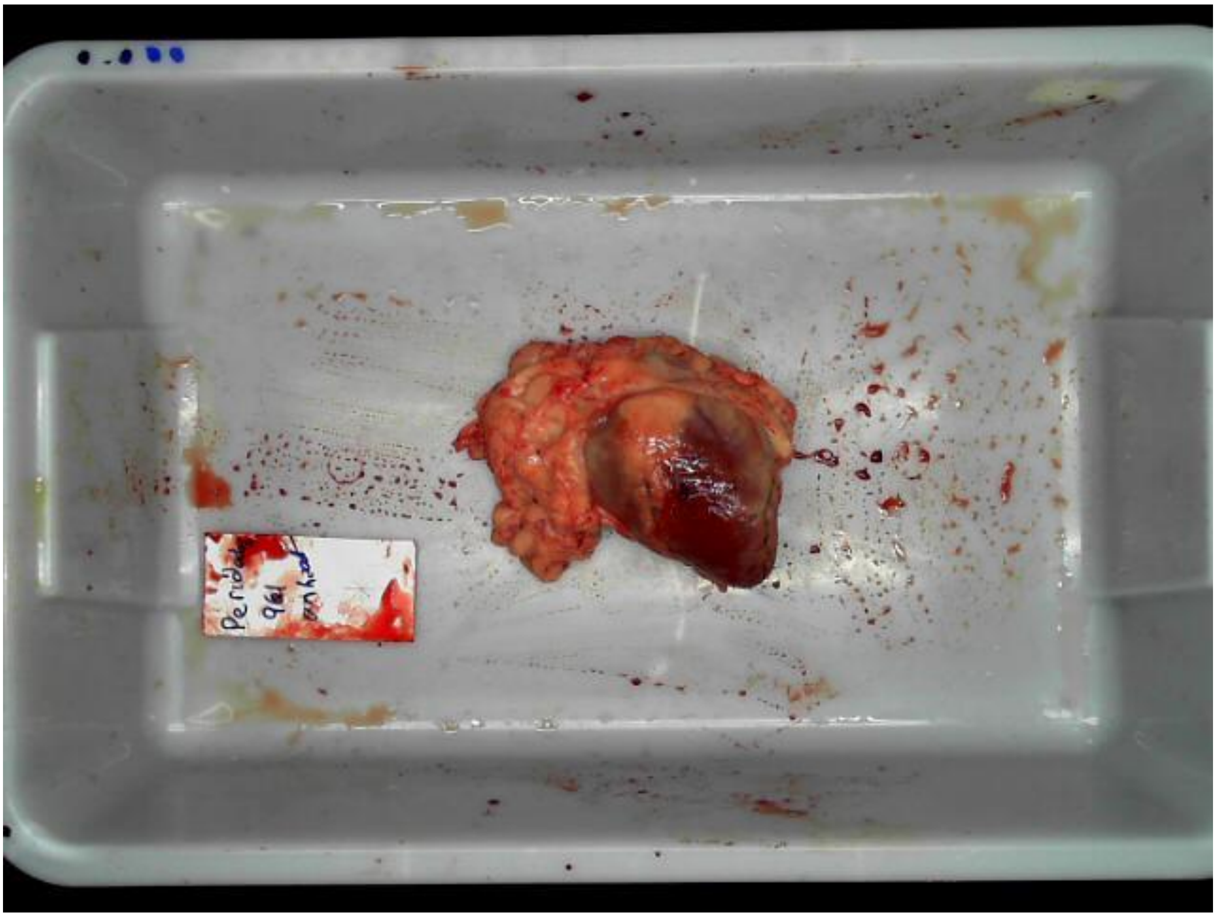

Interpretation:

Not analysed

Comments:

This heart was condemned for the presence of pericarditis, a thin layer of fluid in the pericardial sac

Offal 30

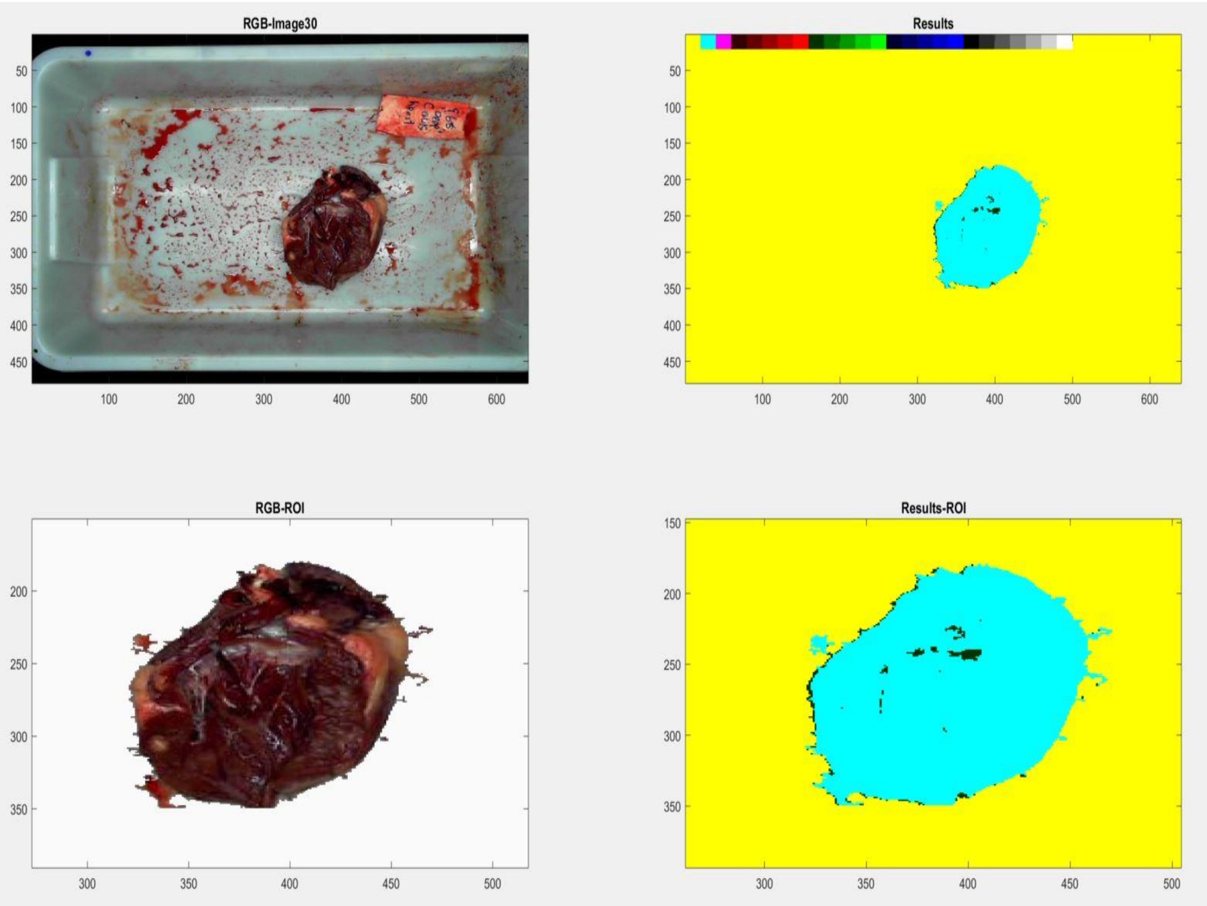

Interpretation:

Olive shows regions of c. ovis cysts

Aqua shows regions of healthy tissue

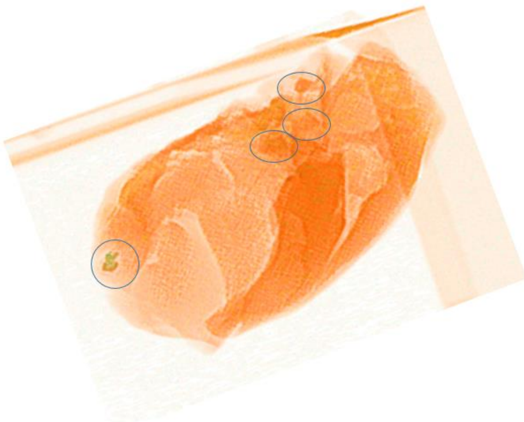

Comments:

This heart was condemned for the presence of deep c. ovis

The DXA image was manually assessed with a prior knowledge, but demonstrates that cysts are visible to a "trained" eye. The left-most cyst has a [false-colour] tinge of green and indicates that this cyst is more dense and pronounced than the other cysts..

Offal 31

Interpretation:

Not analysed

Comments:

This diaphragm was condemned for the presence of slight sarcoidosis (white cyst) on the top edge of the diaphragm (1 o'clock)

<u>Offal 32</u>

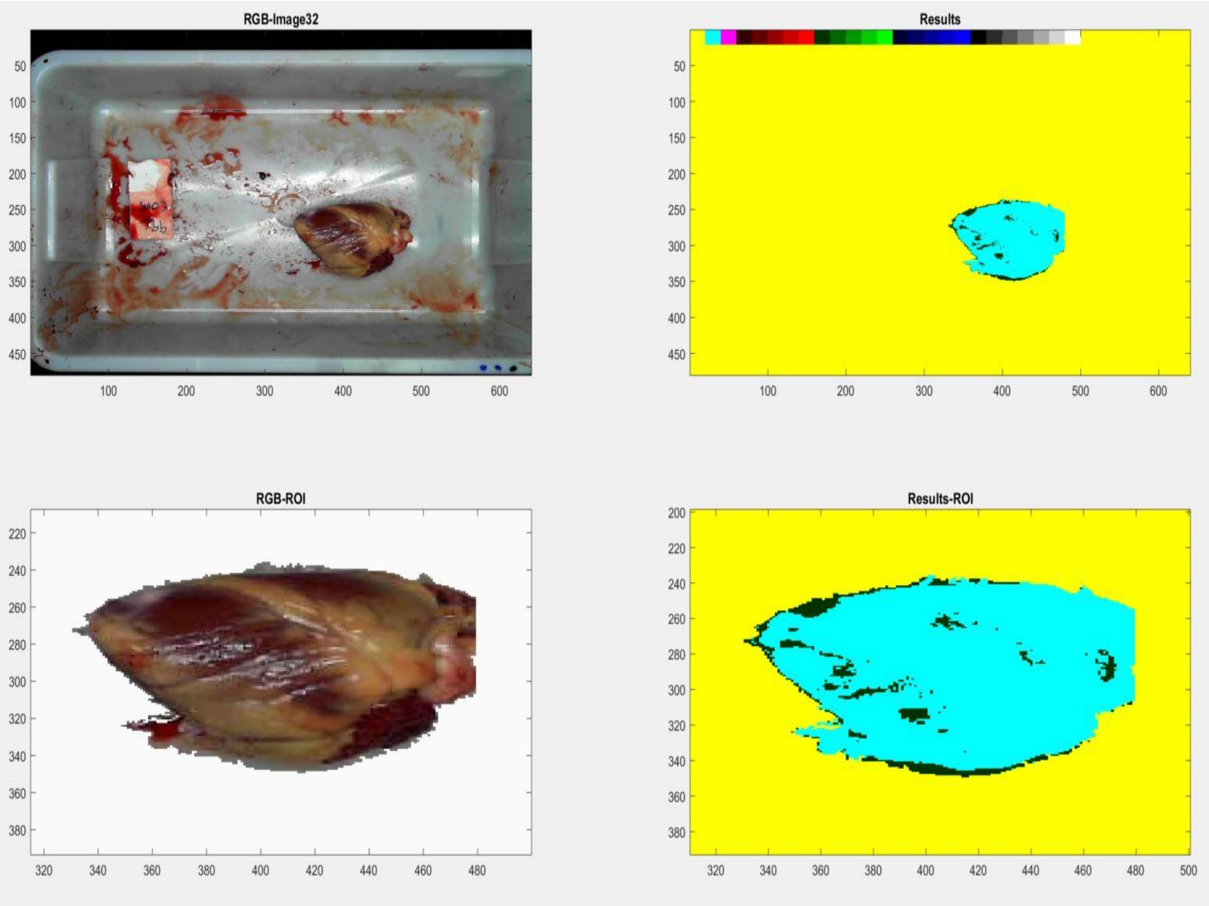

Interpretation:

Olive shows regions of c. ovis cysts

Aqua shows regions of healthy tissue

Comments:

This heart was condemned for the presence of c. ovis

Offal 33

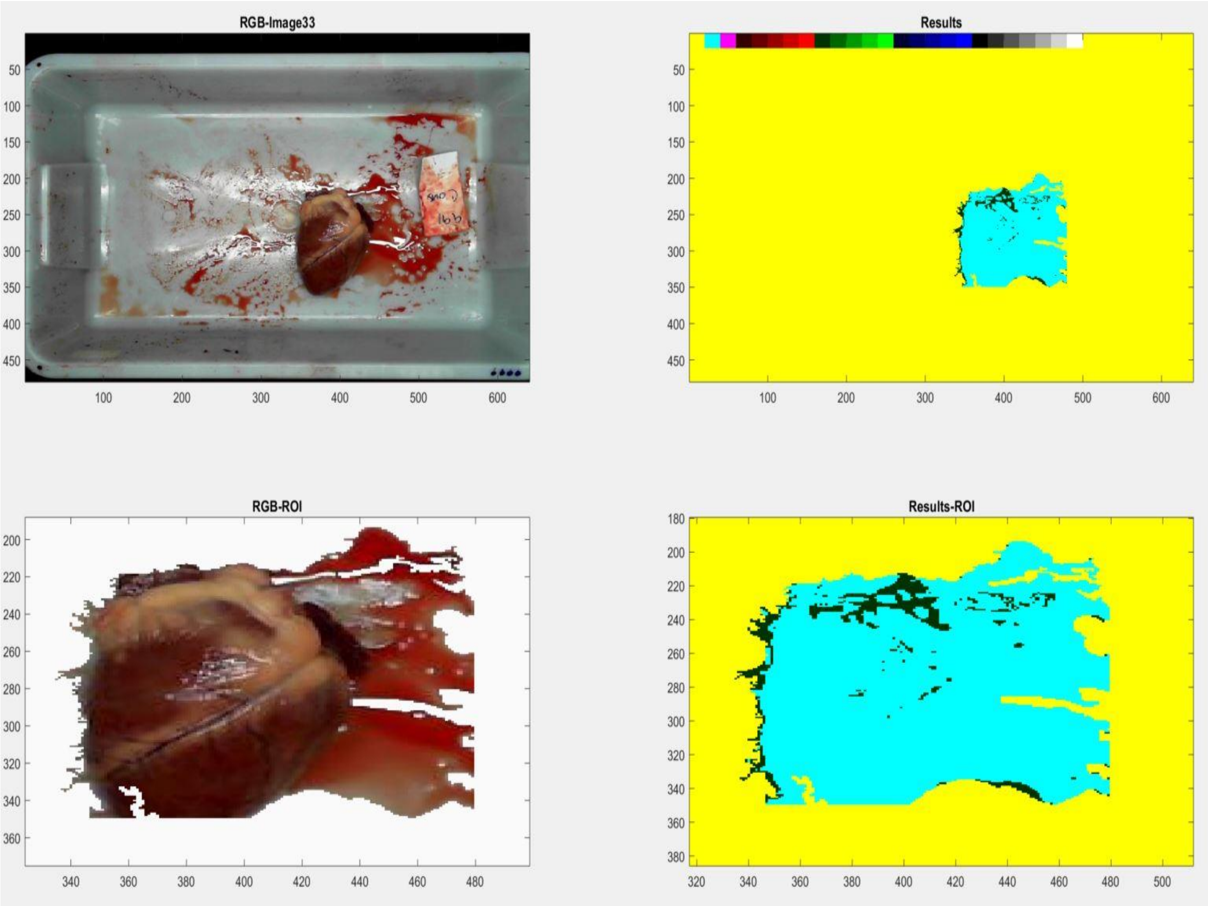

Interpretation:

Olive shows regions of c. ovis cysts

Aqua shows regions of healthy tissue

Comments:

This heart was condemned for the presence of c. ovis

Offal 34

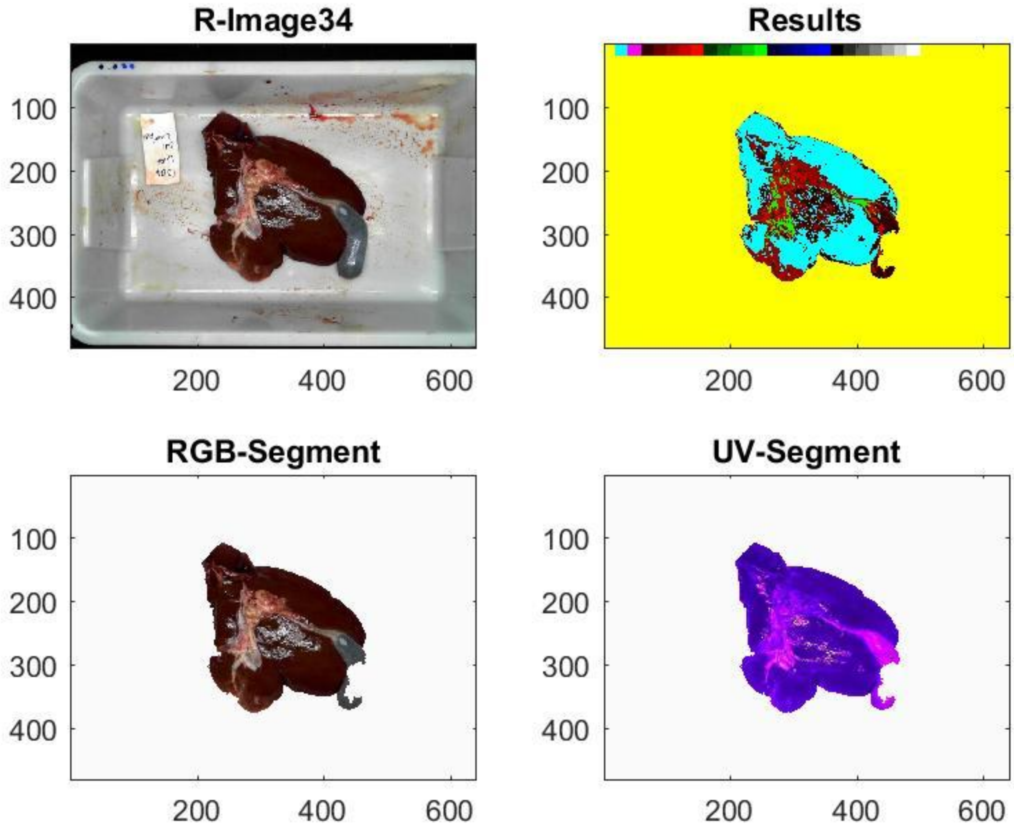

Interpretation:

Brown (least) and black (most) show regions of cirrhosis

Green is “abnormal biomass”

Aqua shows regions of healthy tissue

Comments:

This liver was condemned for the presence of cirrhosis and liver fluke

<u>Offal 35</u>

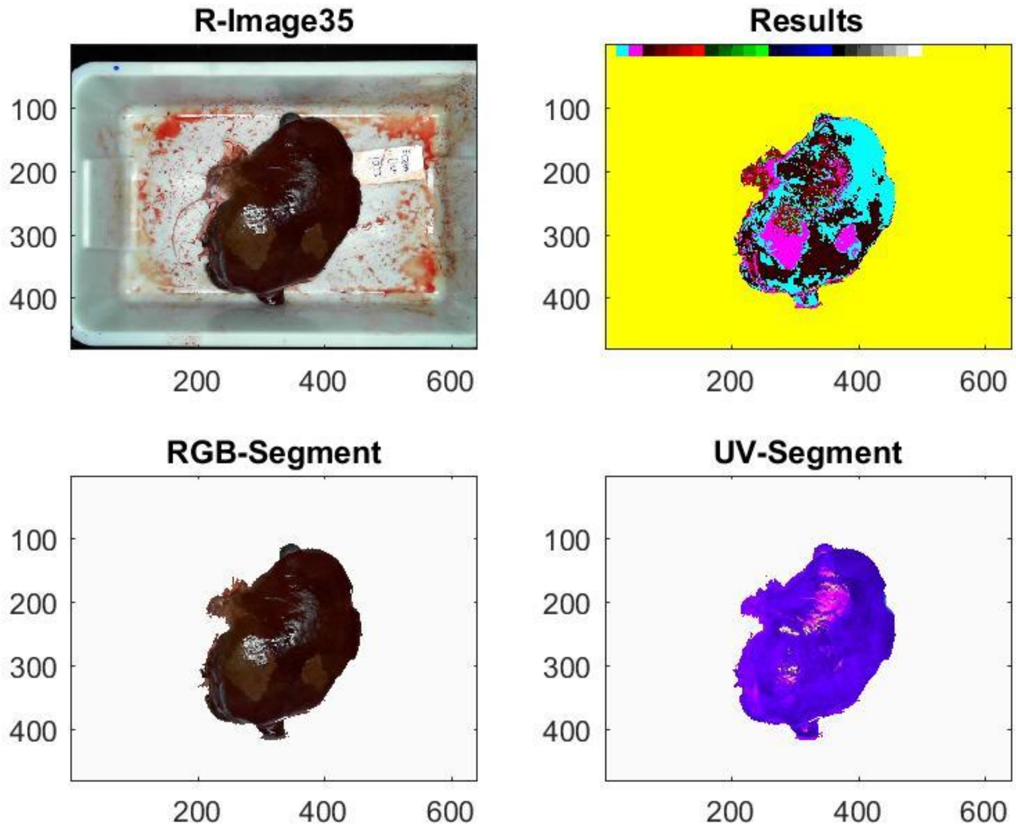

Interpretation:

Brown (least) and black (most) show regions of cirrhosis

Magenta shows facial eczema

Aqua shows regions of healthy tissue

Comments:

This liver was condemned for facial eczema. Facial Eczema and cirrhosis both cause scarring on the liver surface. The algorithm correctly identified the more obvious regions of FE but associated the more subtle regions with cirrhosis.

Offal 36

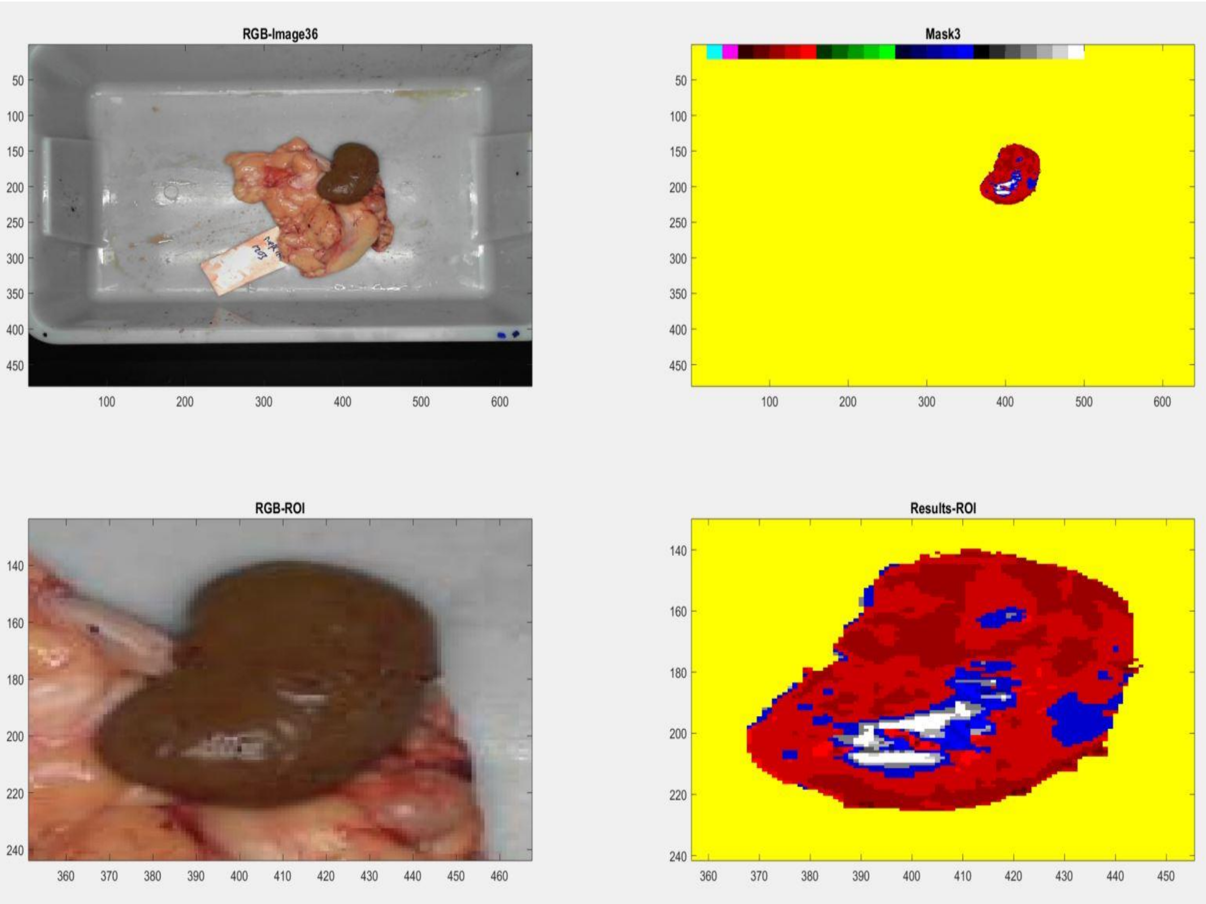

Interpretation:

Red (least), light brown, dark brown and blue (most) show regions of nephritis

White are reflective light

Aqua shows regions of healthy tissue

Comments:

This kidney was condemned for nephritis

<u>Offal 37</u>

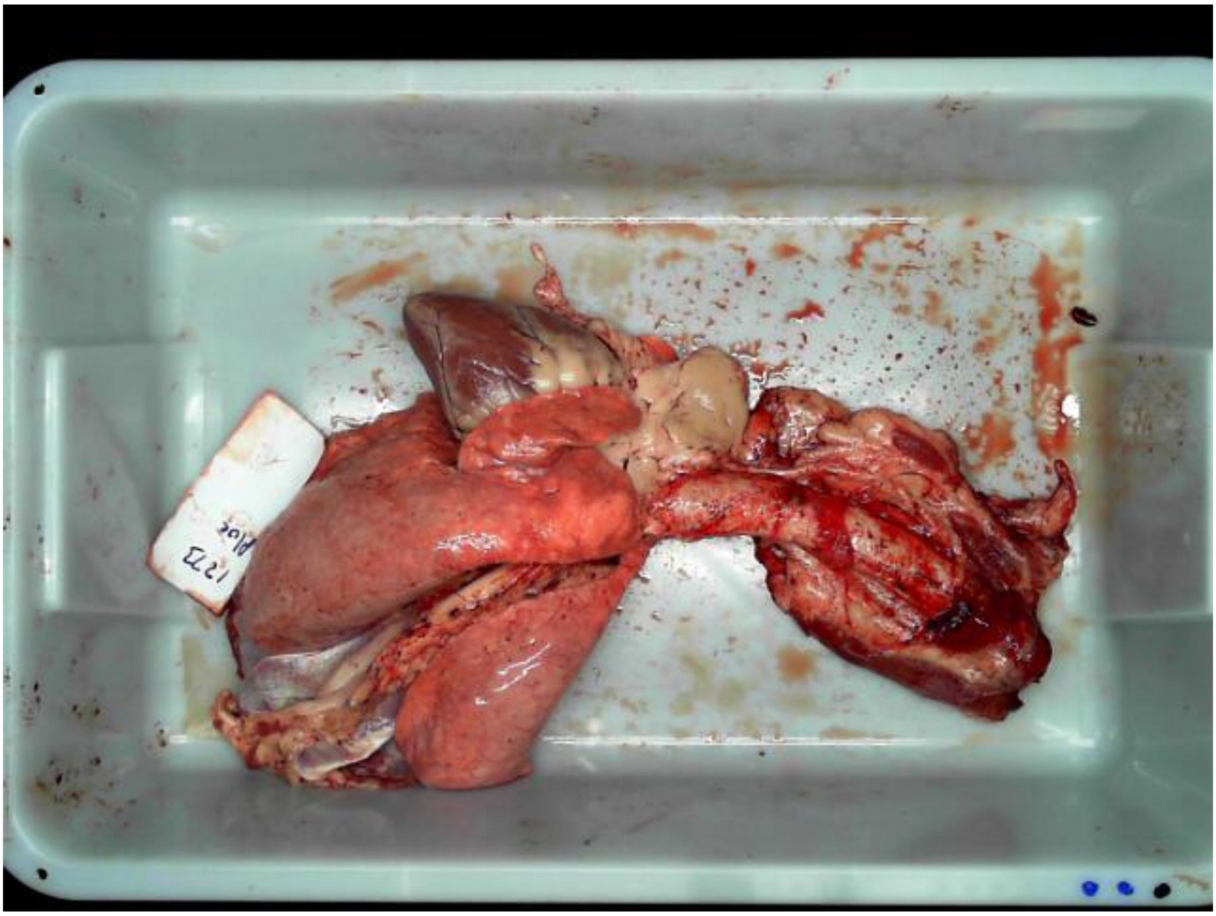

Interpretation:

Not analysed

Comments:

This pluck was condemned for pleurisy. Pleurisy is the adhesion of lung material to the diaphragm, therefore the material that needs to be detected is a thin layer of “glue” between two tissues. Thus the thin layer is not easily seen by non-penetrative imaging (i.e. cameras and hyperspectral imaging) and also does not create a strong density difference detectible by DXA X-ray imagers.

Offal 38

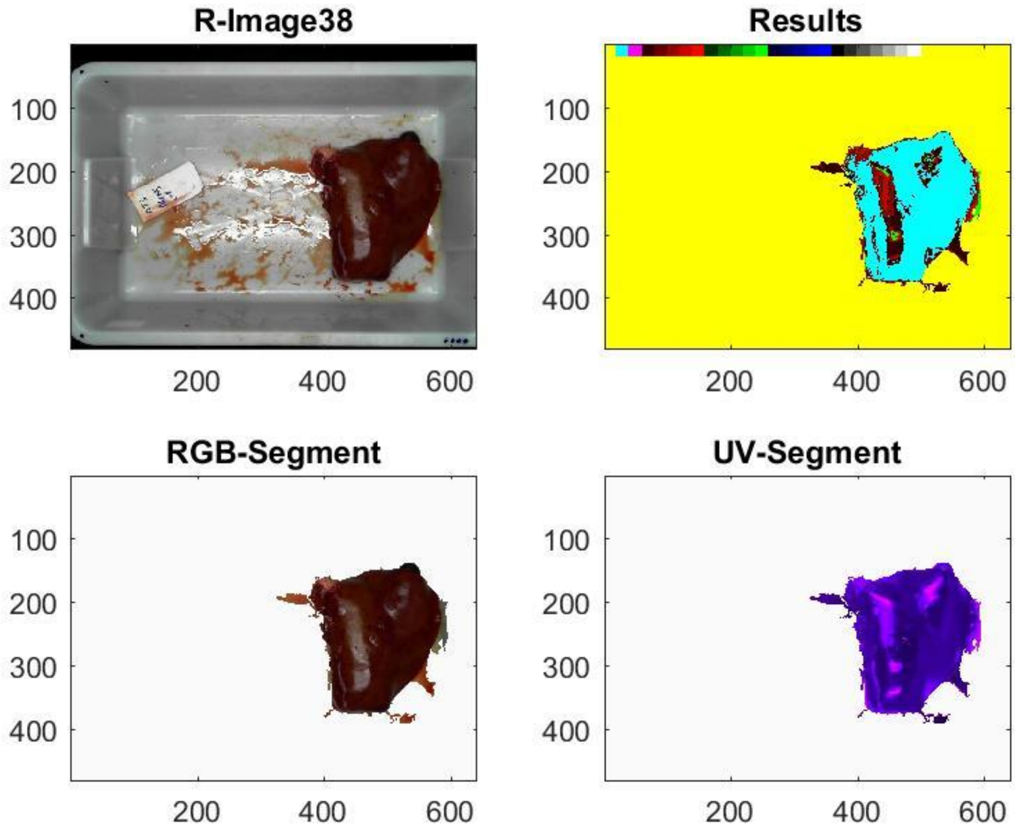

Interpretation:

Brown (least) and black (most) show regions of cirrhosis

Green shows “abnormal biomass”

Aqua shows regions of healthy tissue

Comments:

This liver was condemned for having abscesses. The presence of cirrhosis (confirmed visually) may indicate that the abscesses are complications of the cirrhosis.

Offal 39

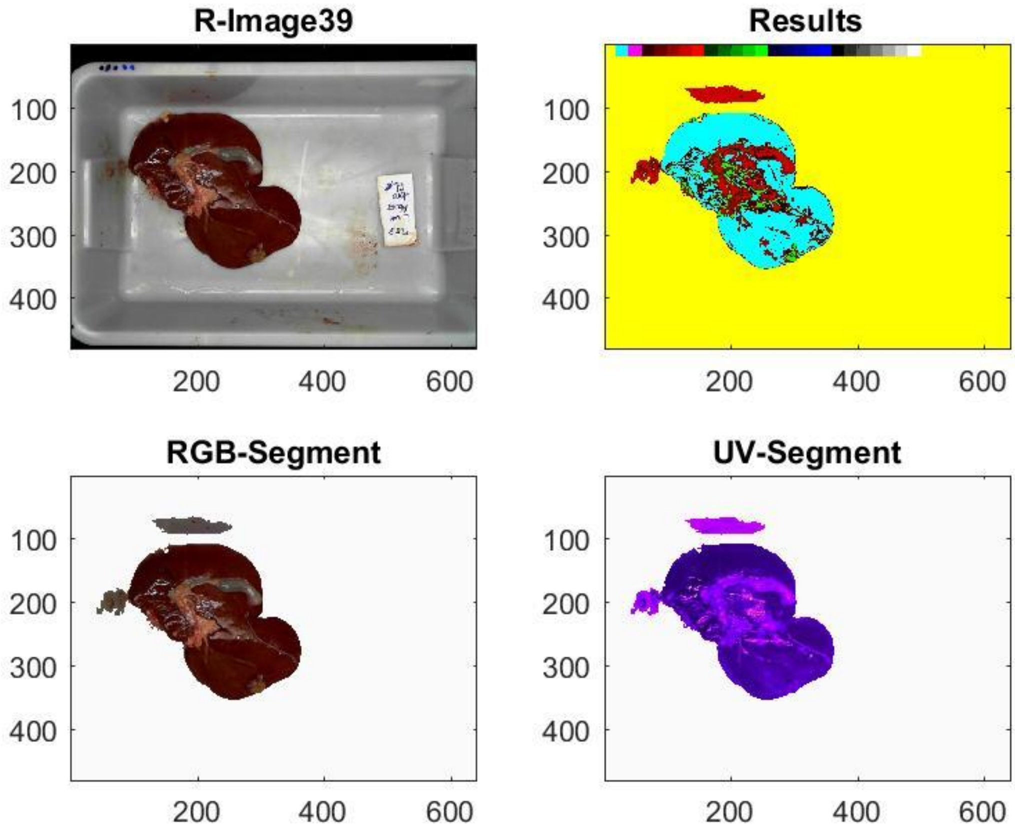

Interpretation:

Brown (least) and black (most) show regions of cirrhosis

Green is “abnormal biomass”

Aqua shows regions of healthy tissue

Comments:

This liver was condemned for abscesses (near the adipose tissue and also at the lower right edge of the liver)

Offal 39

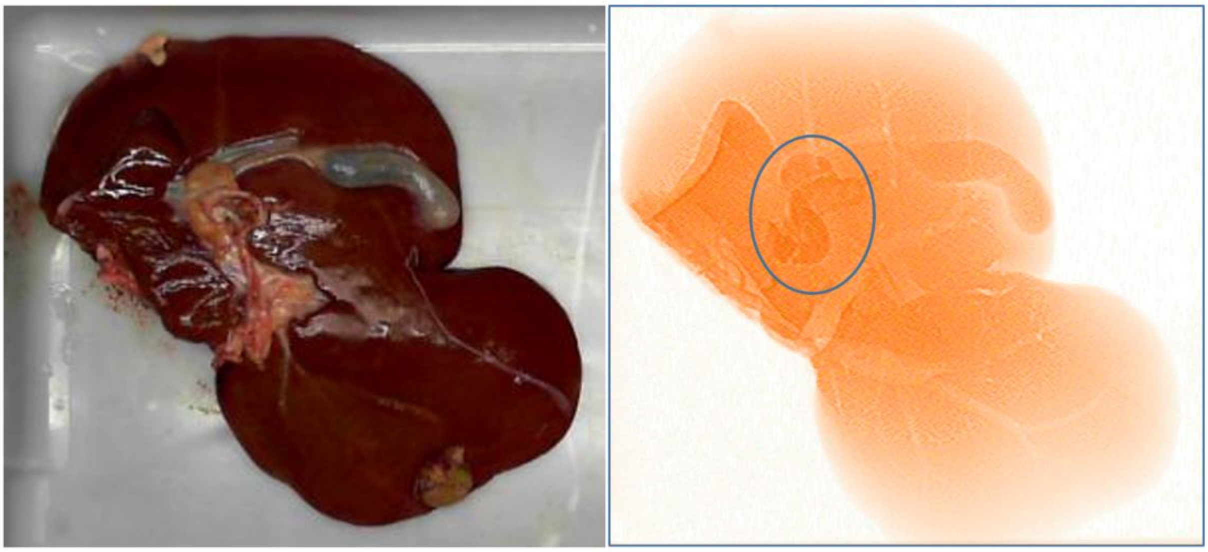

Offal 39

Interpretation:

The region enclosed by the ellipse shows the abscess observable in the colour image.

Comments:

The abscess in this liver is small and the tissue surrounding it has a very similar visual appearance to the “silver-skin” around the adipose tissue. However in the X-ray image the density difference (darker orange) is observable to human interpretation.

Had this abscess been internal it would also have been “observable”. The X-ray also shows the internal structure of the liver in detail, but not the surface disease at the bottom of the liver.

Offal 40

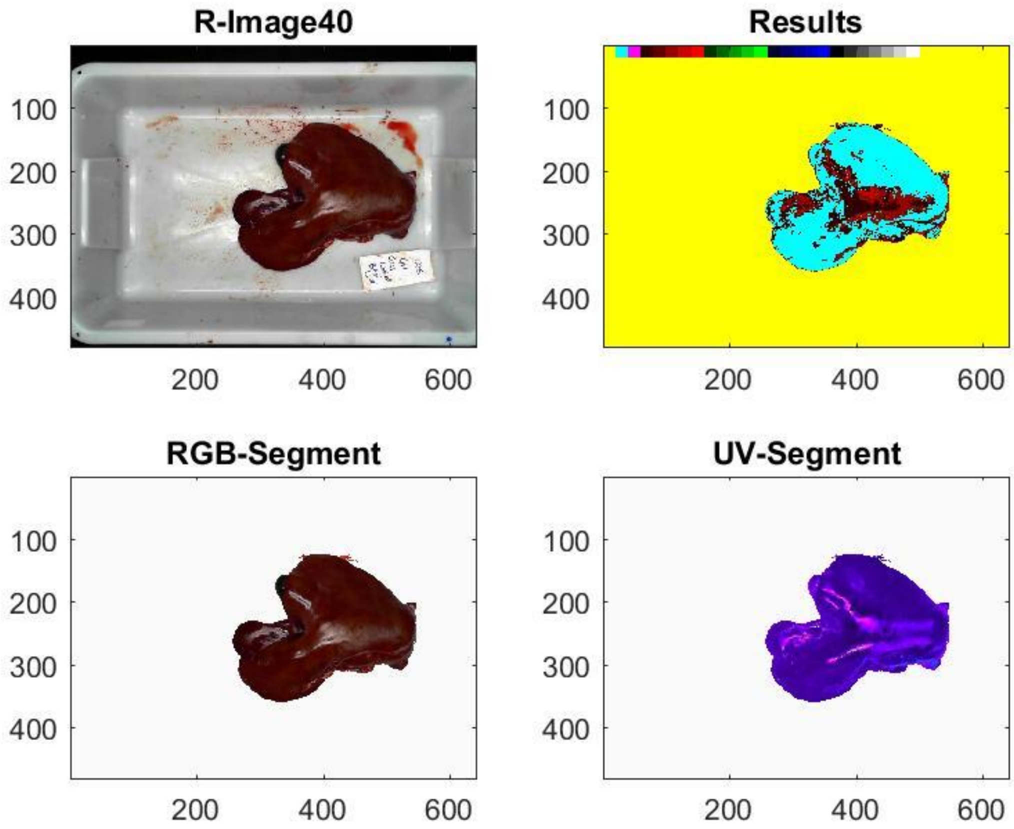

Interpretation:

Brown (least) and black (most) show regions of cirrhosis

Aqua shows regions of healthy tissue

Comments:

This liver was condemned for cirrhosis.

The gall bladder was correctly NOT highlighted.

Offal 41

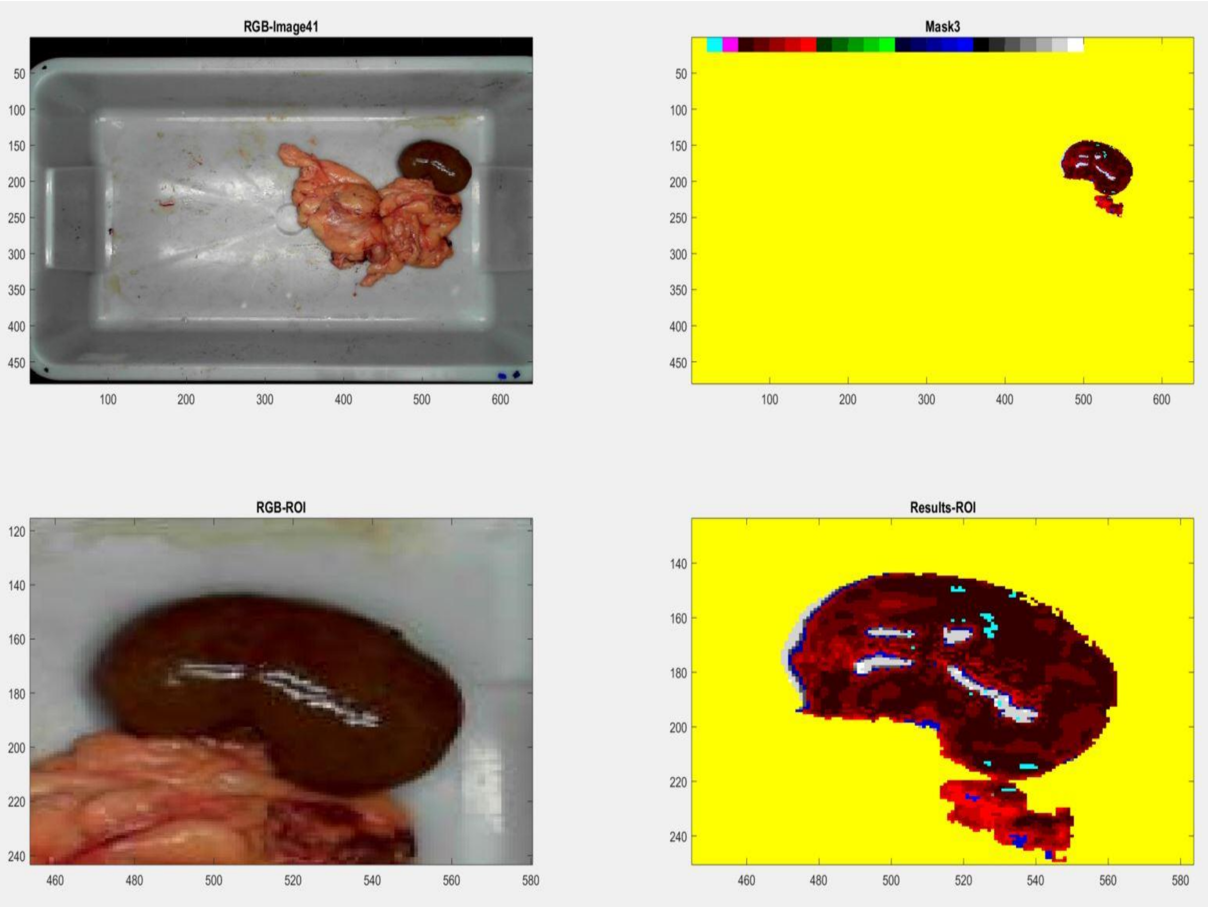

Interpretation:

Red (least), light brown, dark brown and blue (most) show regions of nephritis

White are reflective light

Aqua shows regions of healthy tissue

Comments:

This kidney was condemned for nephritis

Offal 42

Interpretation:

Not analysed

Comments:

This pluck was condemned for pleurisy. Pleurisy is the adhesion of lung material to the diaphragm, therefore the material that needs to be detected is a thin layer of “glue” between two tissues. Thus the thin layer is not easily seen by non-penetrative imaging (i.e. cameras and hyperspectral imaging) and also does not create a strong density difference detectible by DXA X-ray imagers.

Offal 43

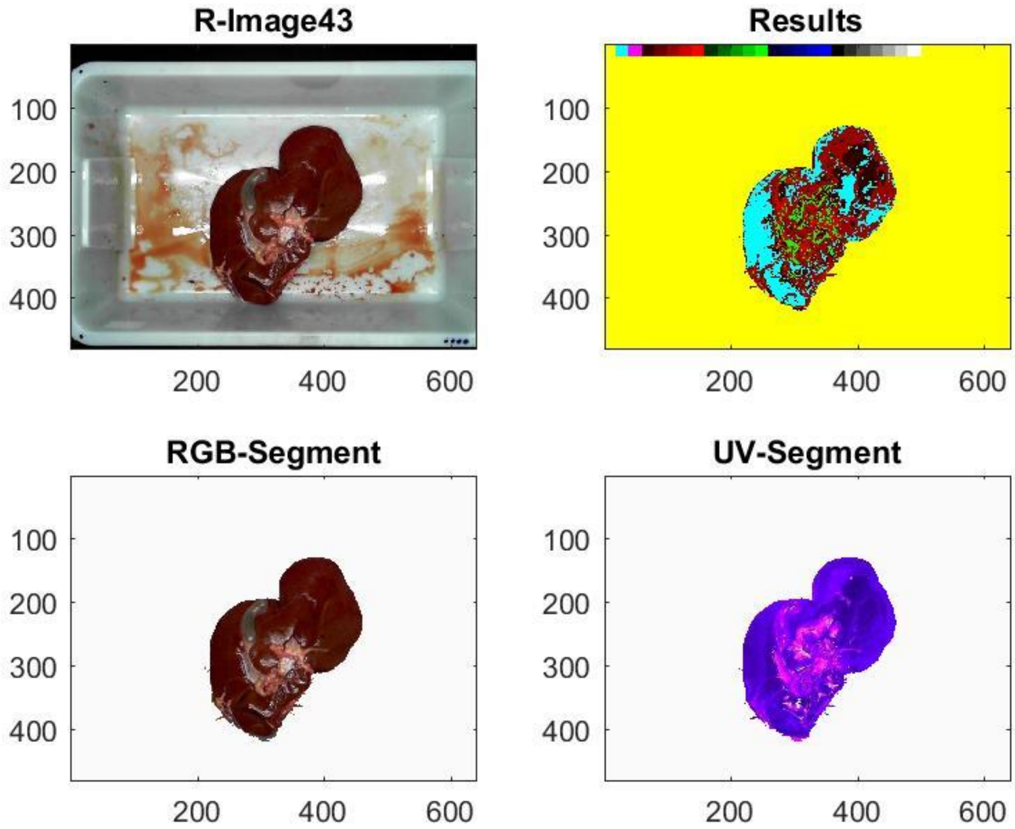

Interpretation:

Brown (least) and black (most) show regions of cirrhosis

Green shows "abnormal biomass"

Aqua shows regions of healthy tissue

Comments:

This liver was condemned for the presence of abscesses.

The gall bladder and some fat tissue has been incorrectly highlighted and this effect will be removed in future work.

Offal 44

Offal 44

Interpretation:

The region enclosed by the ellipse shows the abscess observable in the colour image.

Comments:

The abscess in this liver is small and the tissue surrounding it has a very similar visual appearance to the “silver-skin” around the adipose tissue. However in the X-ray image the density difference (darker orange) is observable to human interpretation.

Had this abscess been internal it would still have been “observable”. The X-ray also shows the internal structure of the liver in detail and, more strikingly, the internal structure of the lungs.

Offal 45

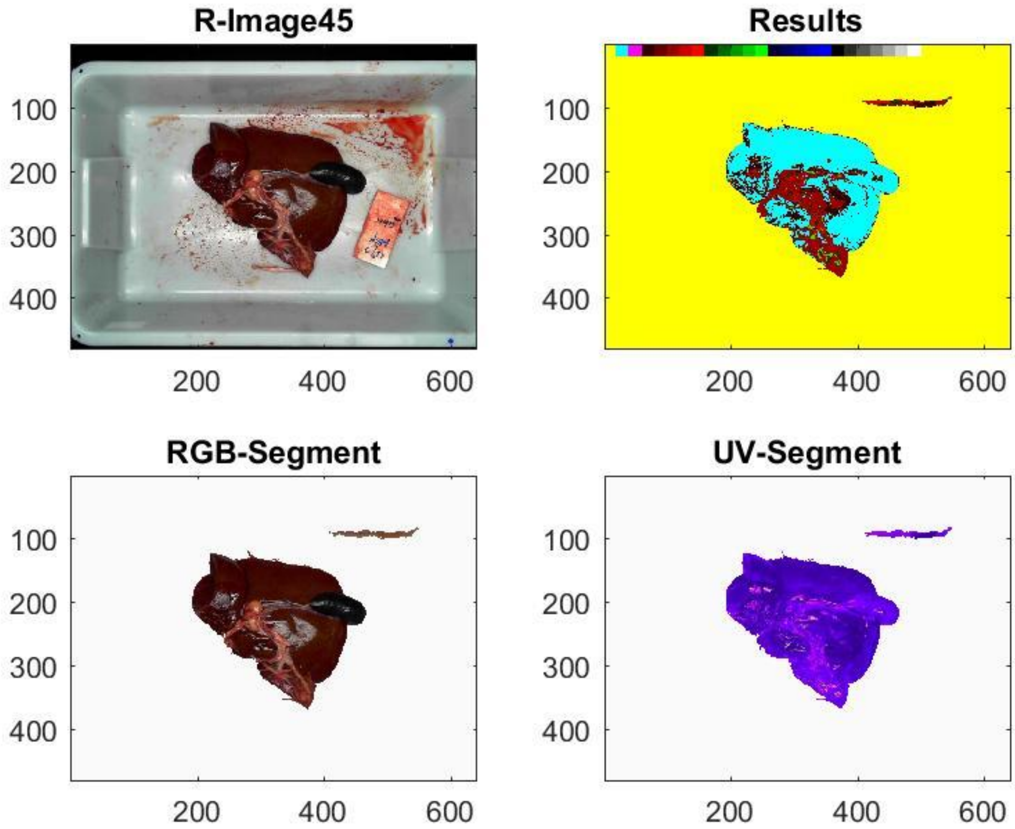

Interpretation:

Brown (least) and black (most) show regions of cirrhosis

Green shows abscesses

Aqua shows regions of healthy tissue

Comments:

The adipose tissue at the bottom of the liver is returned as abscess. This liver was condemned for “abscesses in the Glogi”

Offal 46

Interpretation:

Not analysed

Comments:

This pluck was condemned for pleurisy. Pleurisy is the adhesion of lung material to the diaphragm, therefore the material that needs to be detected is a thin layer of “glue” between two tissues. Thus the thin layer is not easily seen by non-penetrative imaging (i.e. cameras and hyperspectral imaging) and also does not create a strong density difference detectible by DXA X-ray imagers.

Offal 47

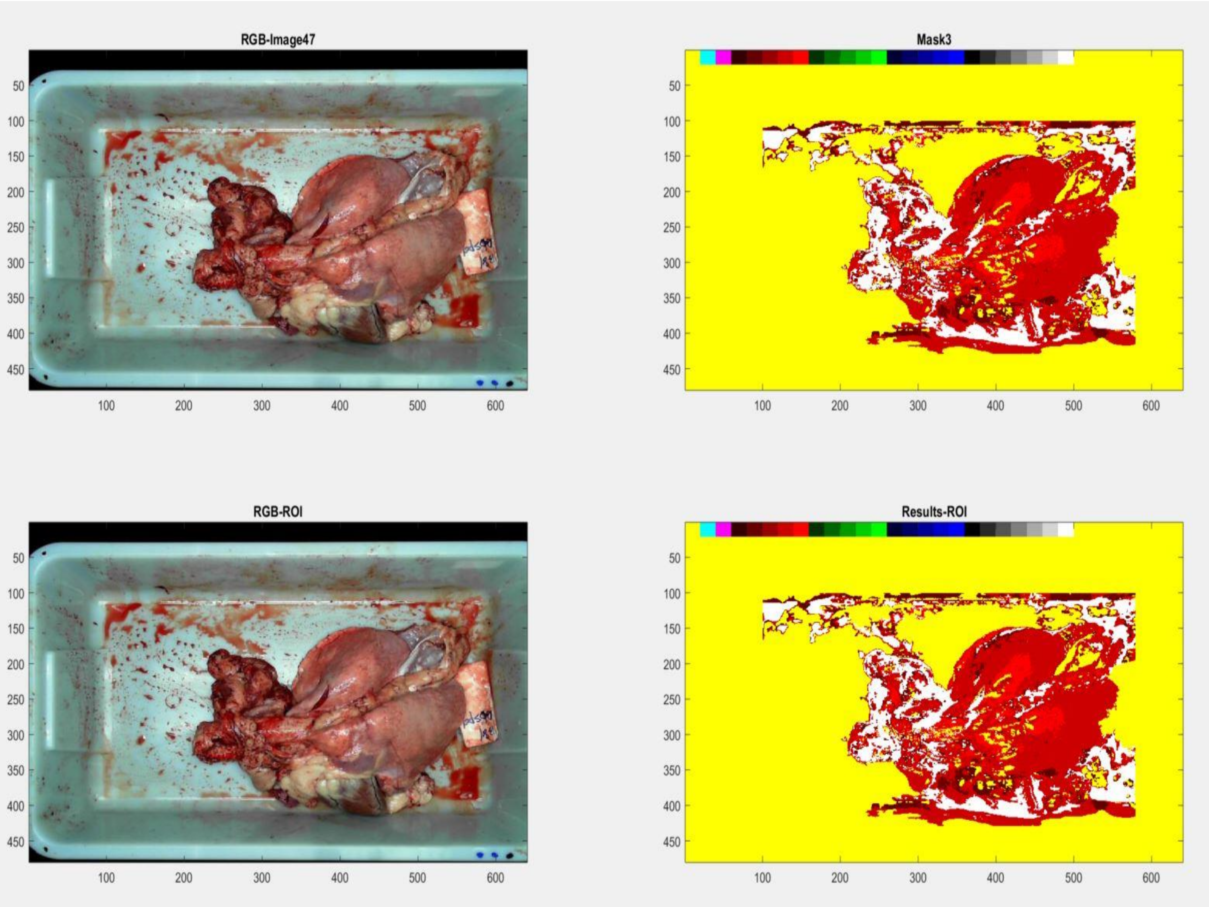

Interpretation:

Red (healthy) to light brown to dark brown (most unhealthy) lug tissue

White shows tissue not of interest.

Comments:

This lung was condemned for the presence of “abnormal spots” on the both lungs (associated with dark brown in the images).

Additional spots on the pluck are artifacts of the cameras automatically adjusting intensities whereas the processor assumes a constant light intensity.

Offal 48

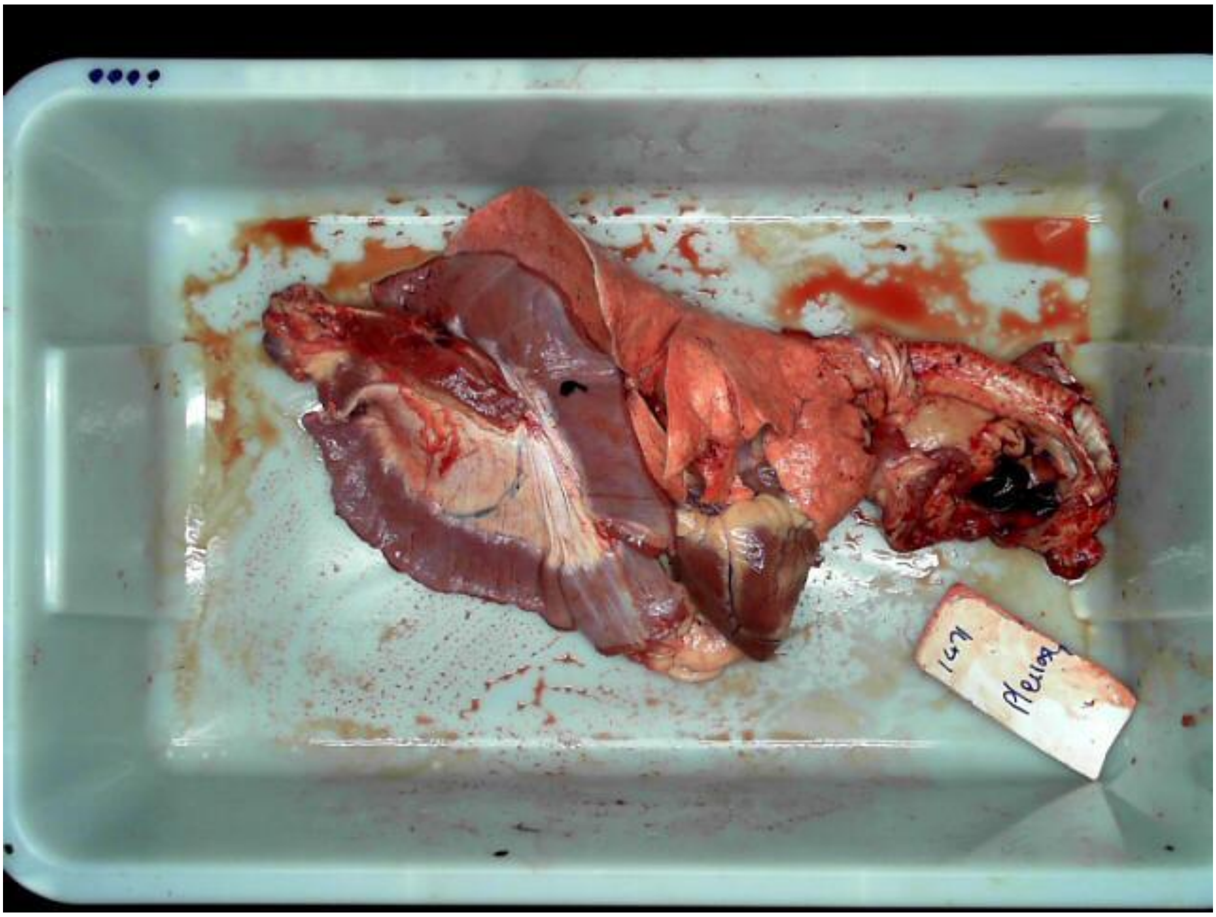

Interpretation:

Not analysed

Comments:

This pluck was condemned for pleurisy. Pleurisy is the adhesion of lung material to the diaphragm, therefore the material that needs to be detected is a thin layer of "glue" between two tissues. Thus the thin layer is not easily seen by non-penetrative imaging (i.e. cameras and hyperspectral imaging) and also does not create a strong density difference detectible by DXA X-ray imagers.

Offal 49

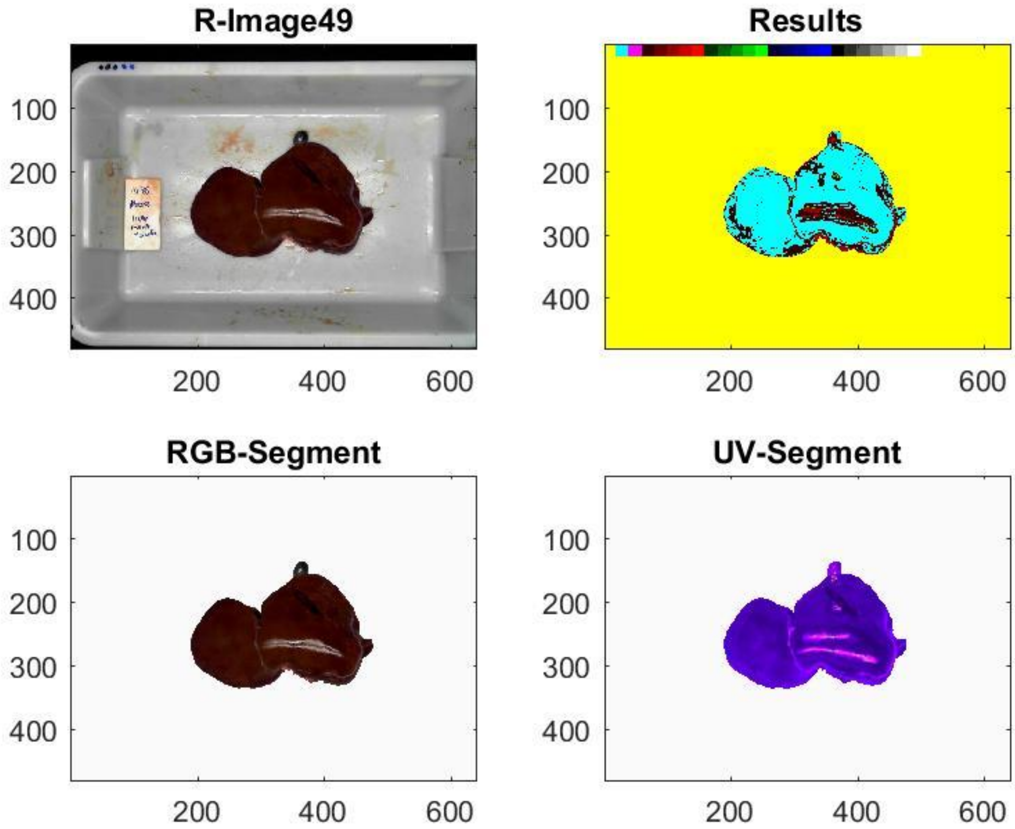

Interpretation:

Brown (least) and black (most) show regions of cirrhosis

Aqua shows regions of healthy tissue

Comments:

This liver was condemned for the presence of abscesses. Cirrhosis was confirmed visually on images.

Offal 50

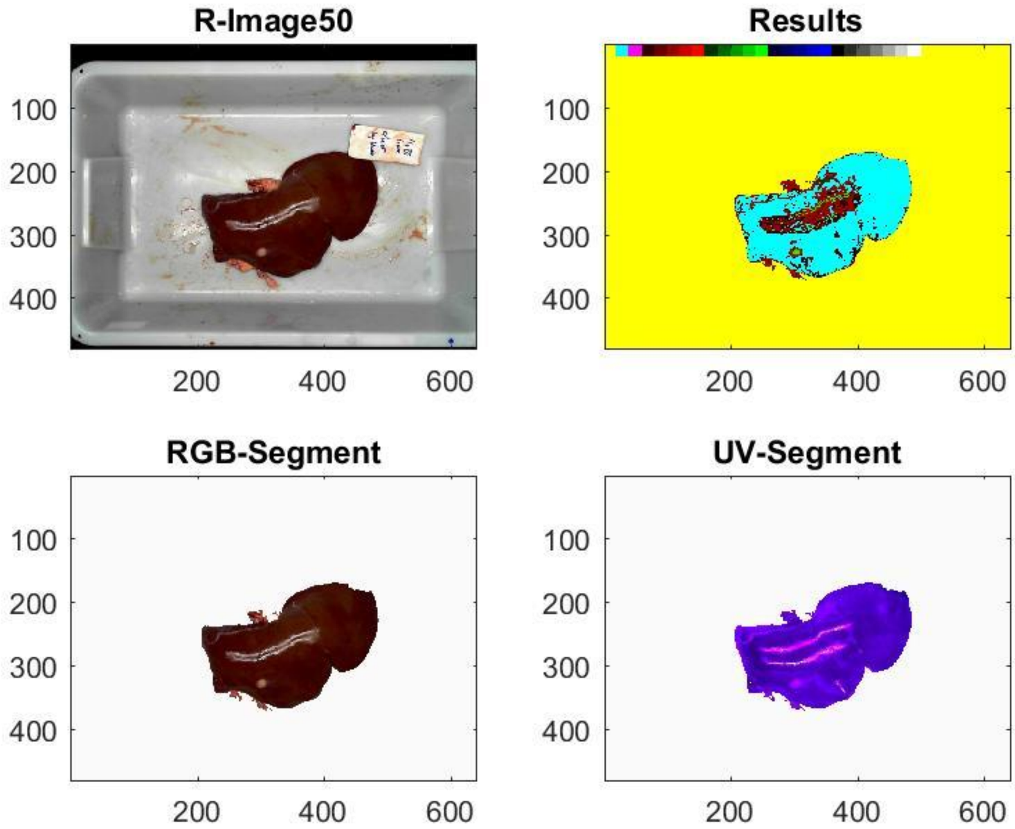

Interpretation:

Brown (least) and black (most) show regions of cirrhosis

Green shows abscesses

Aqua shows regions of healthy tissue

Comments:

This liver was condemned due to the presence of the large abscess.

Offal 51

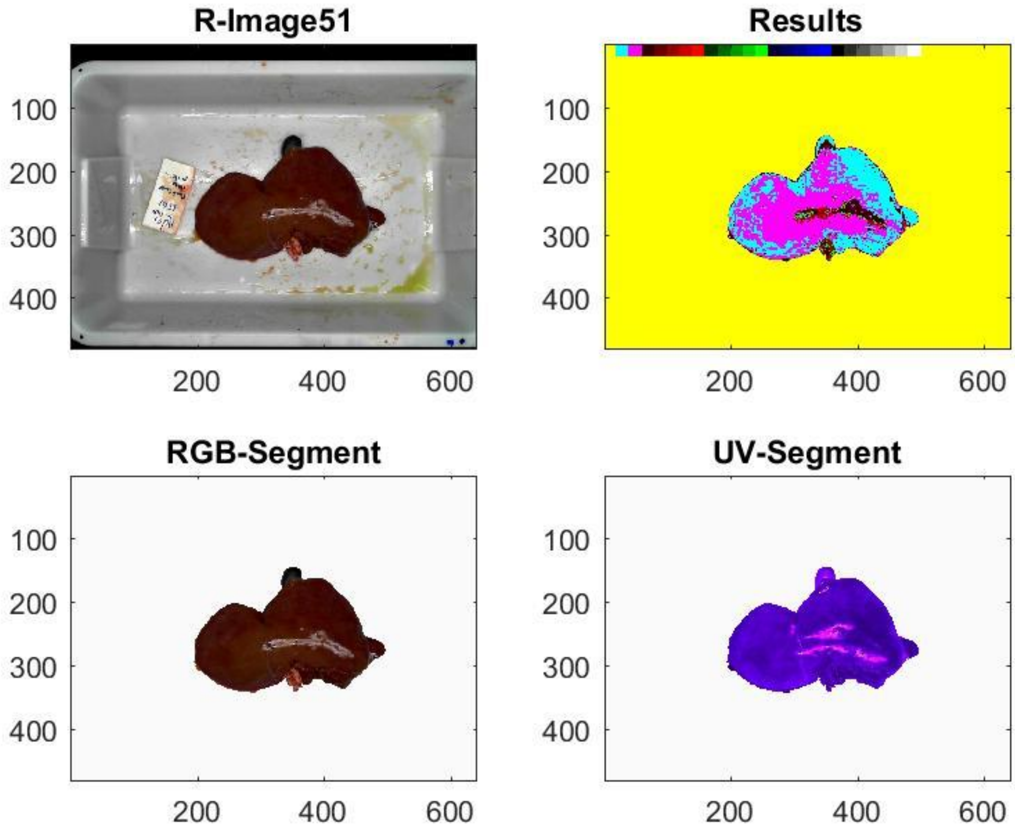

Interpretation:

Brown (least) and black (most) show regions of cirrhosis

Magenta indicates the presence of facial eczema

Aqua shows regions of healthy tissue

Comments:

This liver was condemned for “holes” along the bottom centre edge and the horizontal white region. The extent and evenness of the damage to the rest of the liver surface is consistent with facial eczema (as indicated by the magenta) but may be caused by cirrhosis

Offal 52

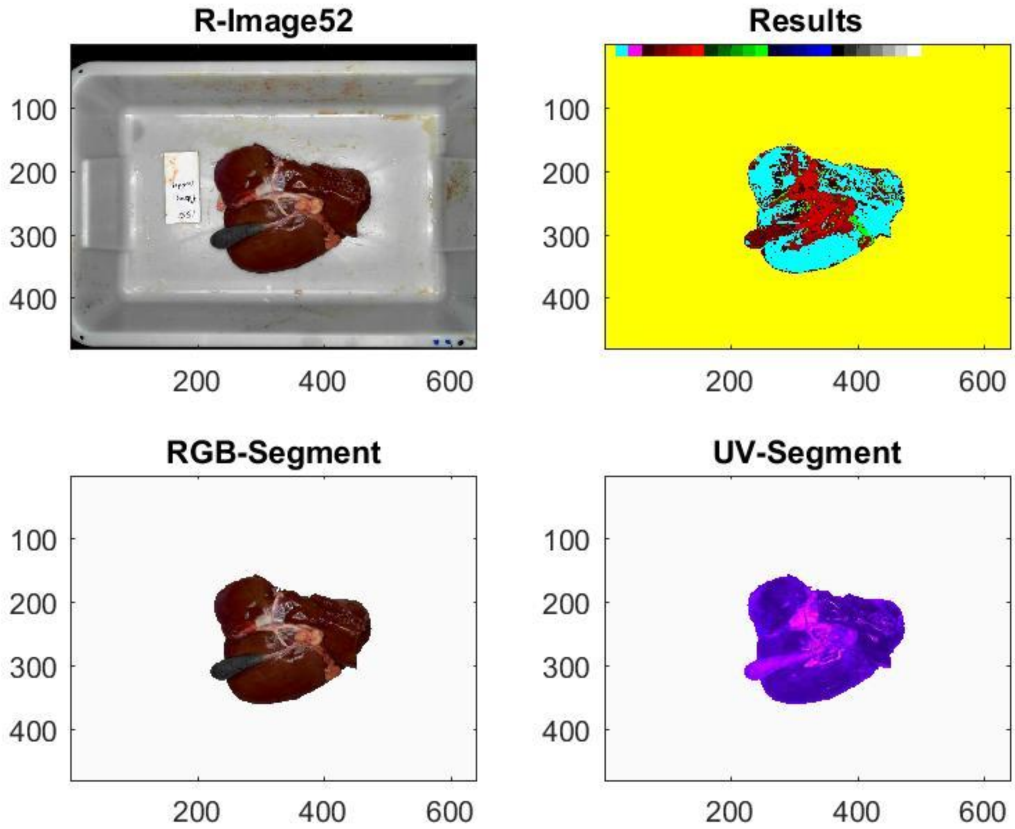

Interpretation:

Brown (least) and black (most) show regions of cirrhosis

Green shows abscesses

Aqua shows regions of healthy tissue

Comments:

This liver was condemned for abscesses in the nodules, but the presence of cirrhosis (black) was visually confirmed.

Offal 53

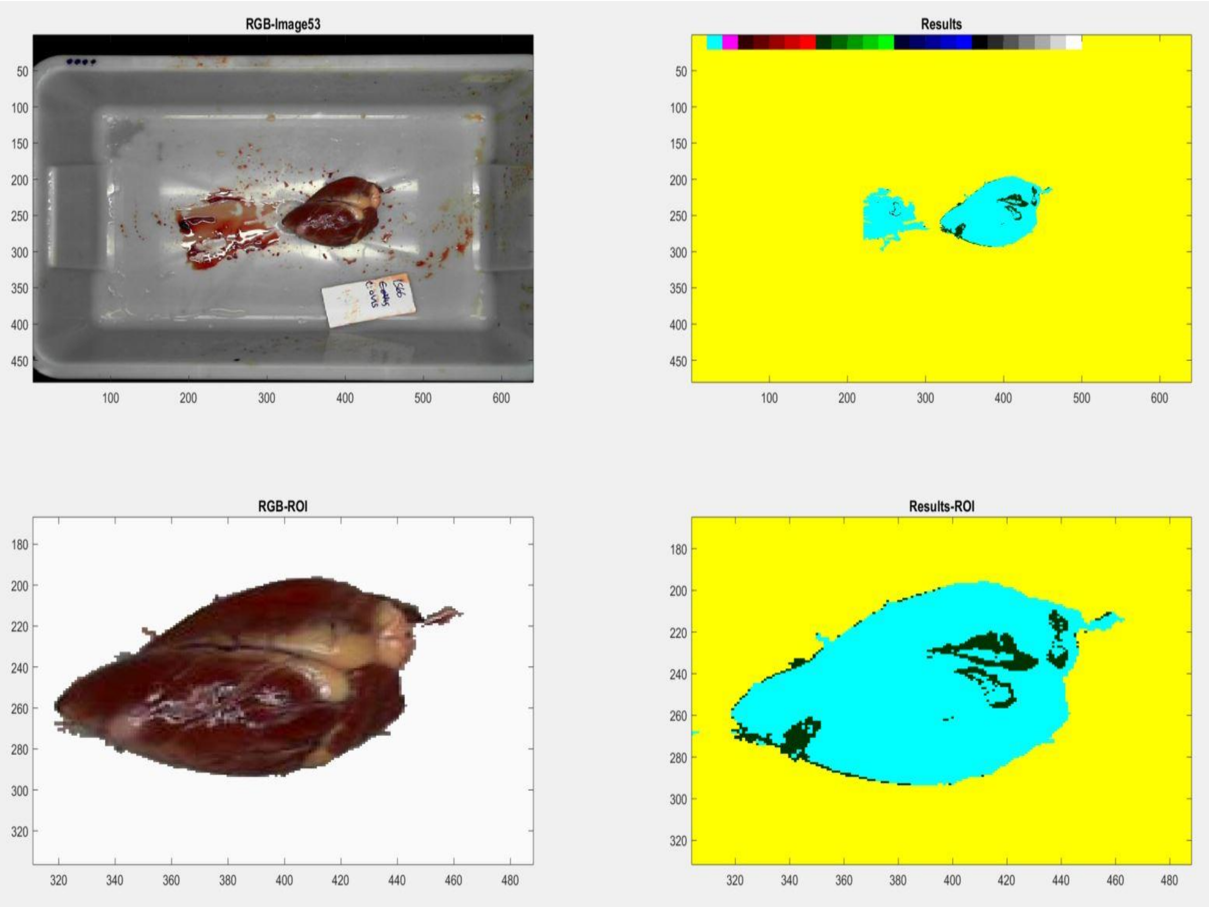

Interpretation:

Olive shows regions of c. ovis cysts

Aqua shows regions of healthy tissue

Comments:

This heart was condemned for the presence of c. ovis

Offal 54

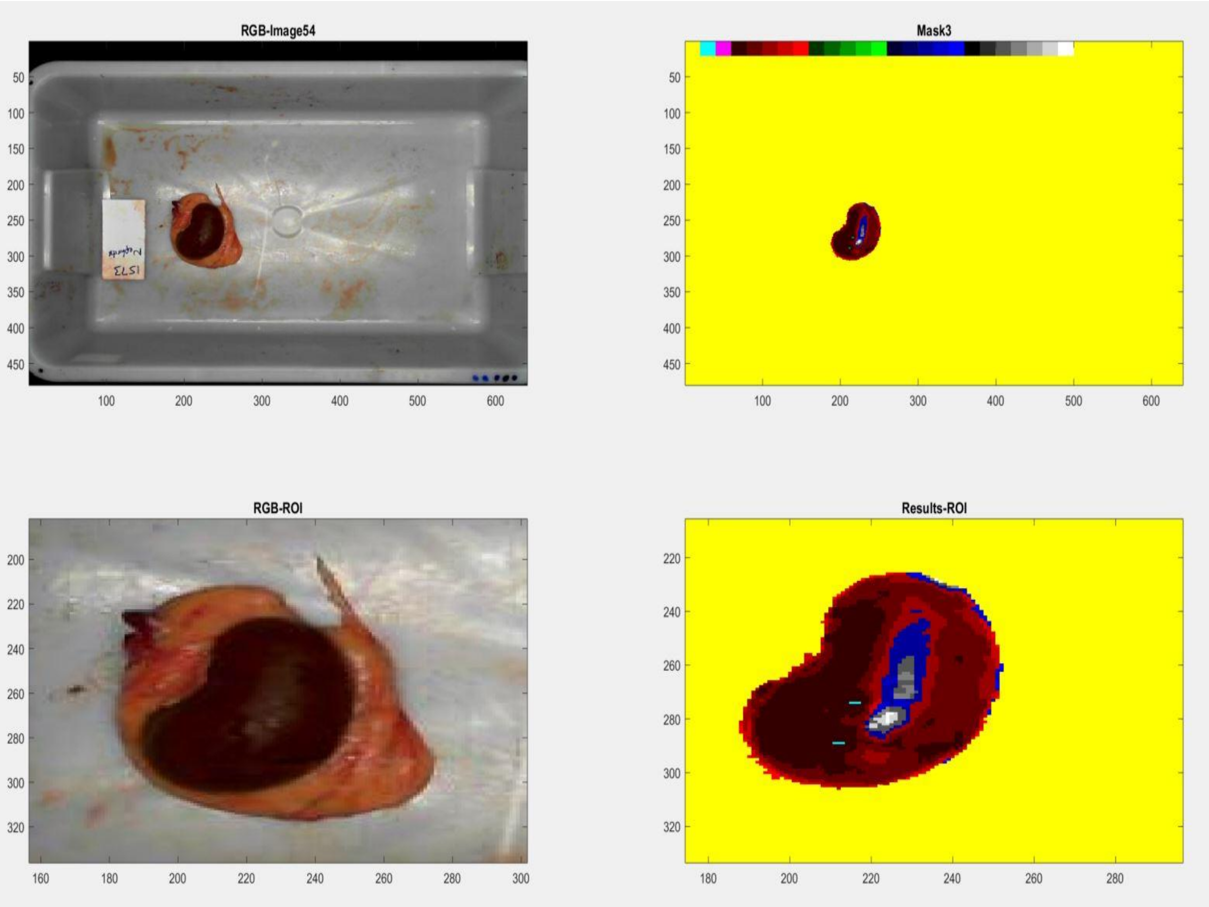

Interpretation:

Red (least), light brown, dark brown and blue (most) show regions of nephritis

White are reflective light

Aqua shows regions of healthy tissue

Comments:

This kidney was condemned for nephritis

Offal 55

Interpretation:

Not analysed

Comments:

This liver was condemned for “umbilicus adhesion”, therefore the material that needs to be detected is a thin layer of “glue” between two tissues. Thus the thin layer is not easily seen by non-penetrative imaging (i.e. cameras and hyperspectral imaging) and also does not create a strong density difference detectible by DXA X-ray imagers.

<u>Offal 56</u>

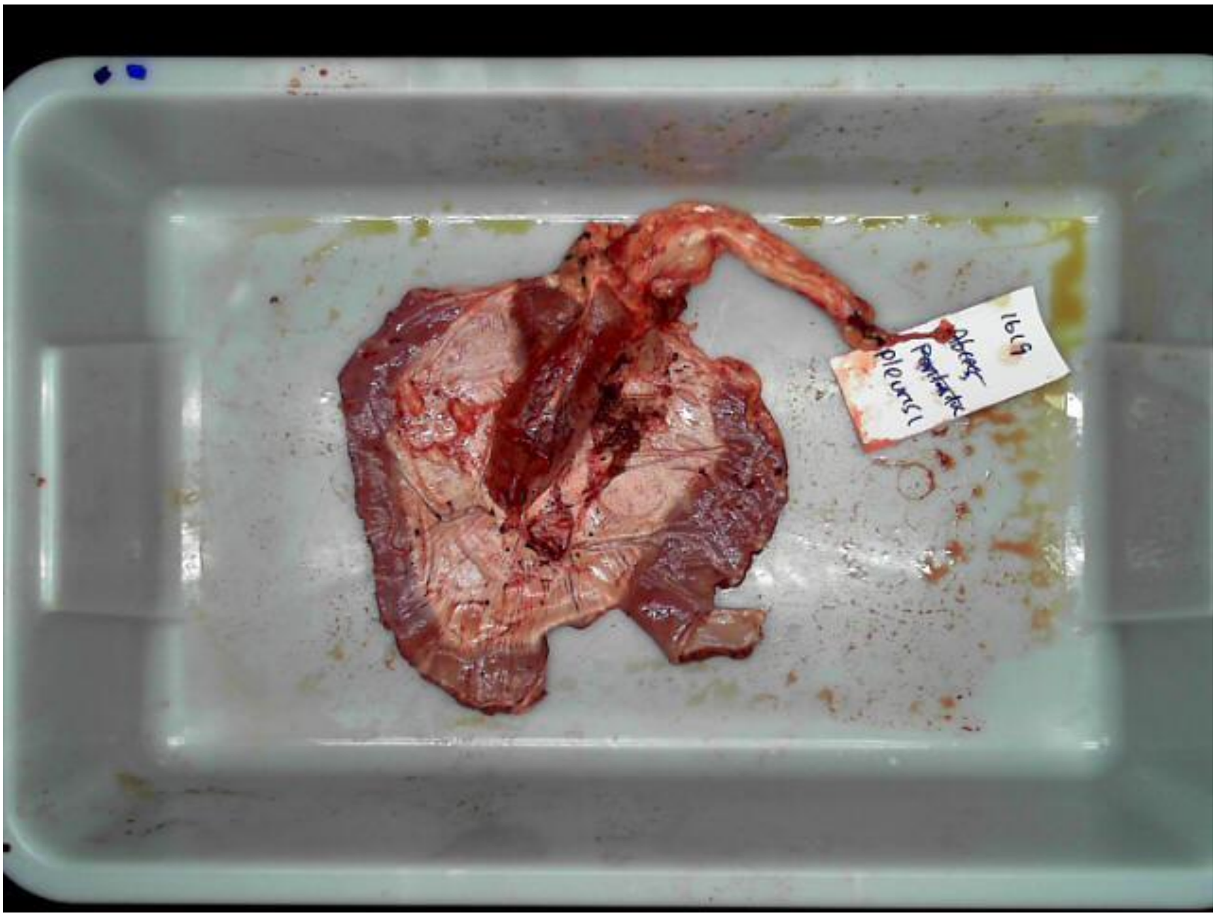

Interpretation:

Not analysed

Comments:

This pluck was condemned for pleurisy. Pleurisy is the adhesion of lung material to the diaphragm, therefore the material that needs to be detected is a thin layer of "glue" between two tissues. Thus the thin layer is not easily seen by non-penetrative imaging (i.e. cameras and hyperspectral imaging) and also does not create a strong density difference detectible by DXA X-ray imagers.

<u>Offal 57</u>

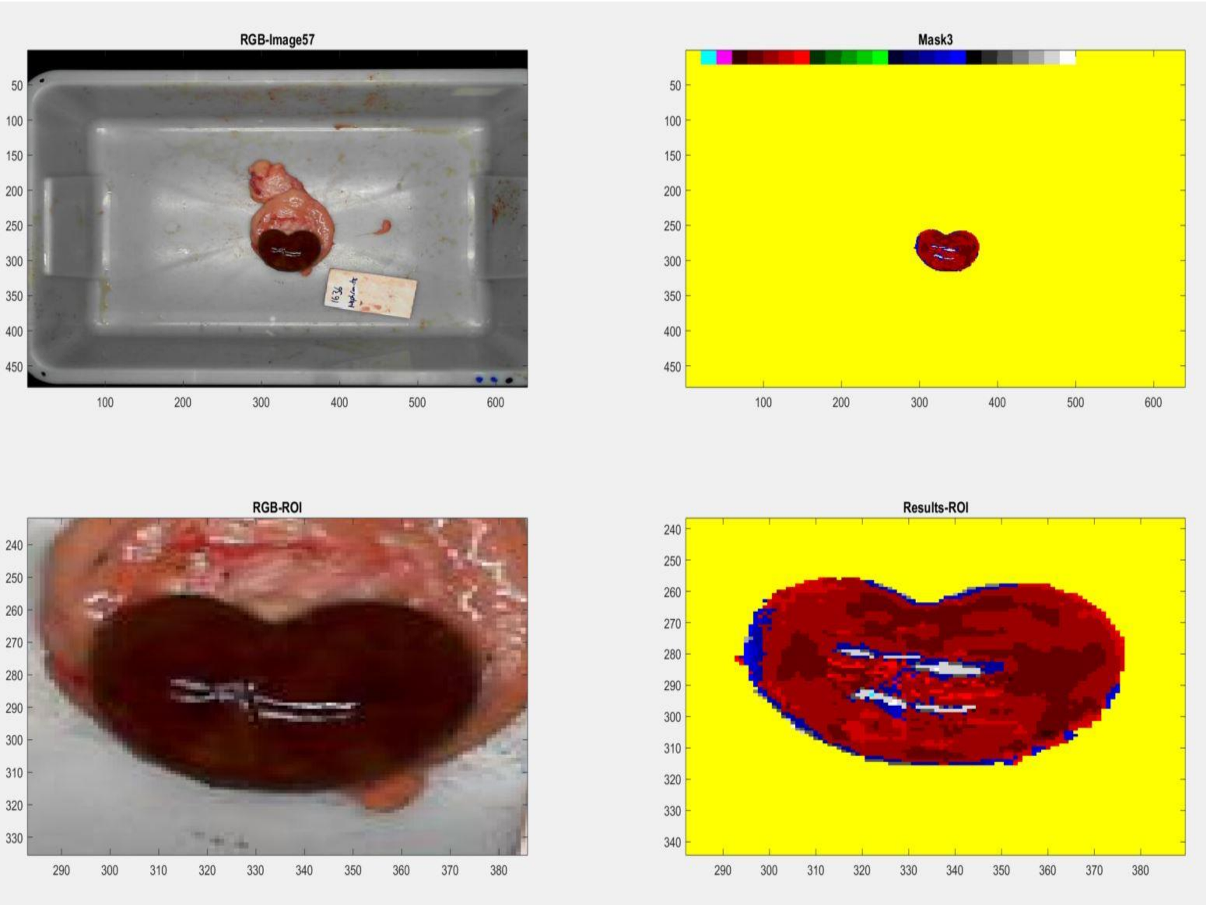

Interpretation:

Dark brown (least), light brown, red and blue (most) show regions of nephritis

White are reflective light

Aqua shows regions of healthy tissue

Comments:

This kidney was condemned for nephritis

Offal 58

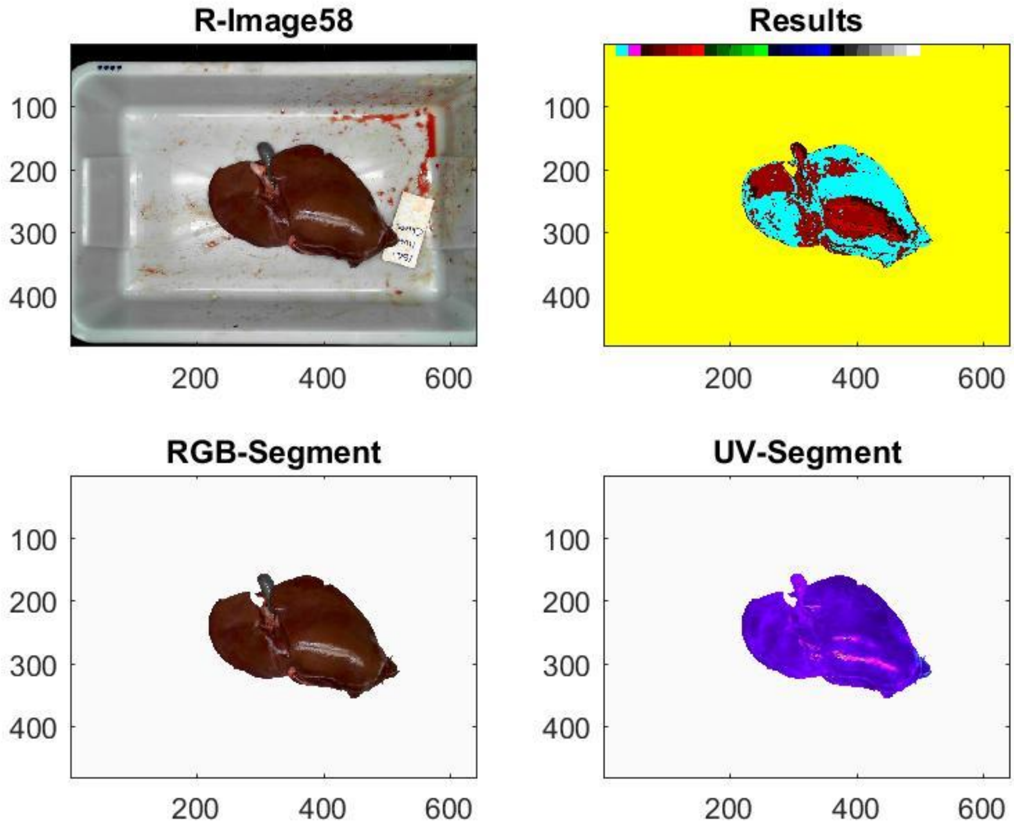

Interpretation:

Brown (least) and black (most) show regions of cirrhosis

Aqua shows regions of healthy tissue

Comments:

This liver was condemned for cirrhosis

Offal 59

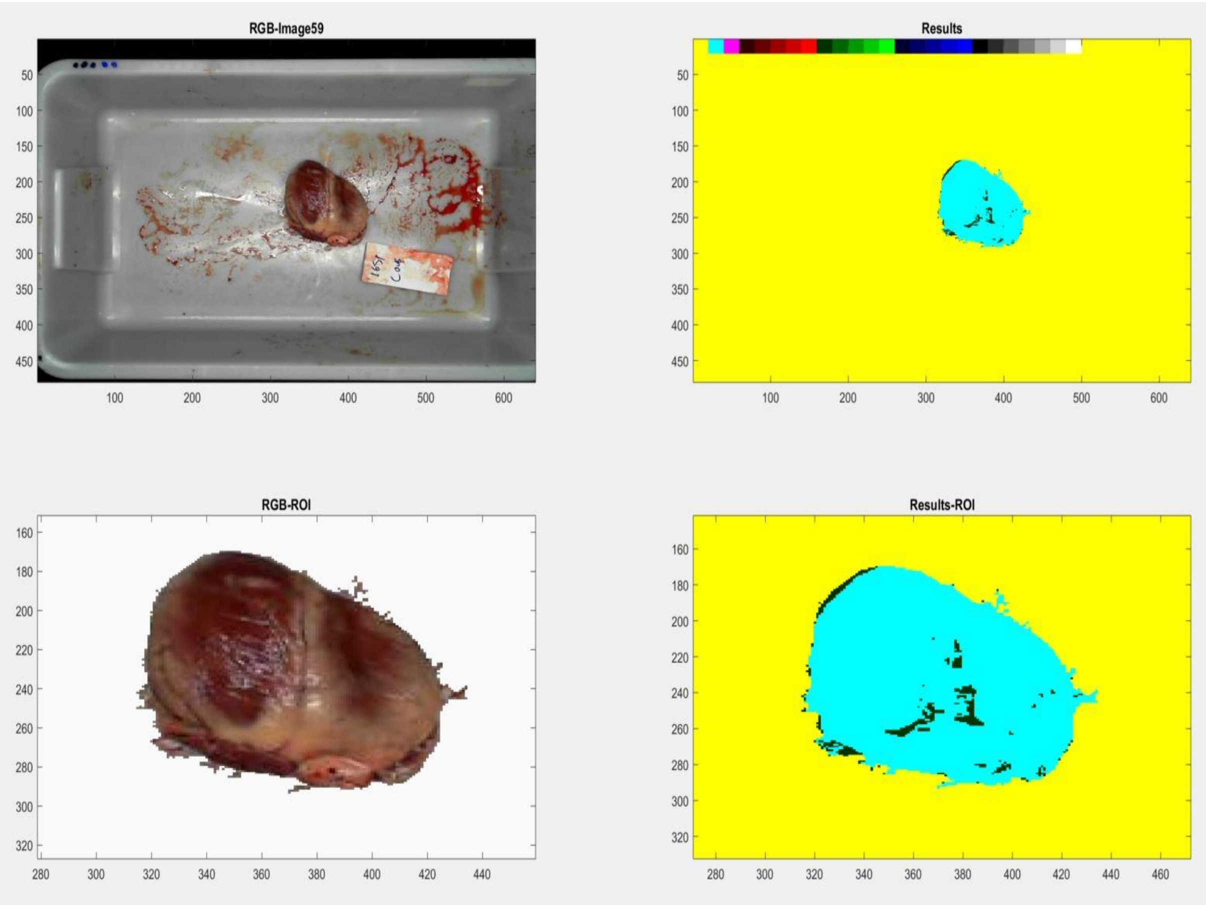

Interpretation:

Olive shows regions of c. ovis cysts

Aqua shows regions of healthy tissue

Comments:

This heart was condemned for c. ovis under the epicardial adipose tissue.

Offal 60

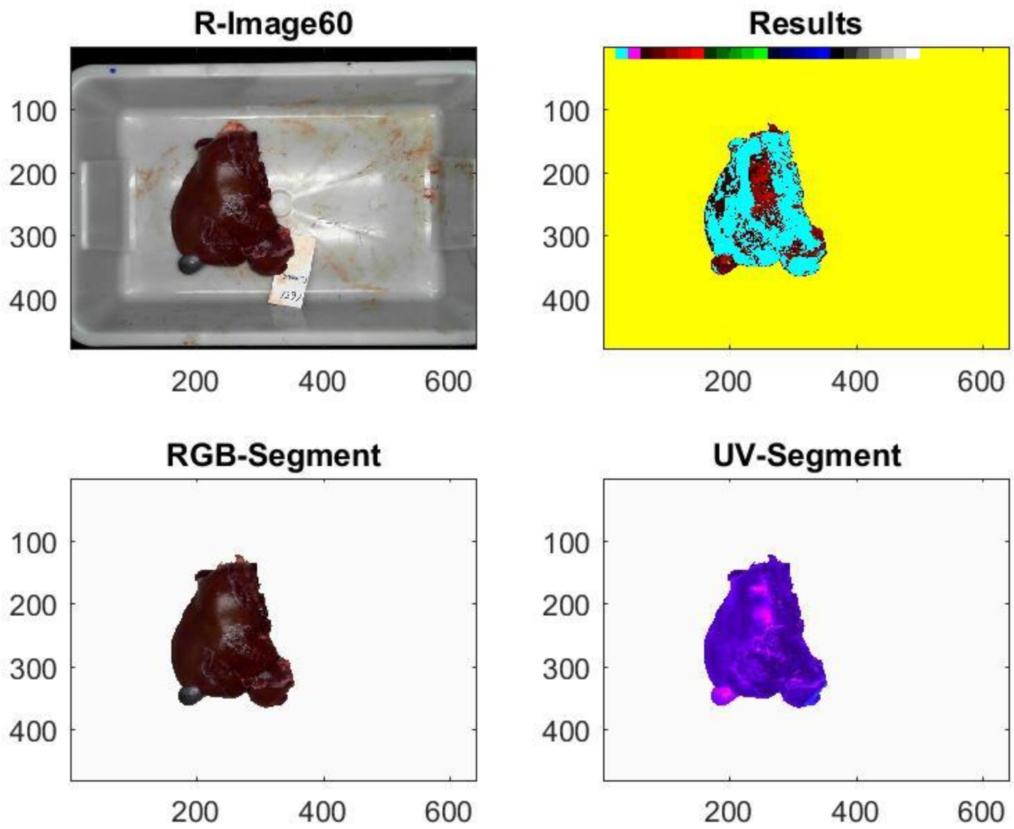

Interpretation:

Brown (least) and black (most) show regions of cirrhosis

Aqua shows regions of healthy tissue

Comments:

This liver was condemned for cirrhosis.

Offal 61

Interpretation:

Not analysed

Comments:

This pluck was condemned for pleurisy. Pleurisy is the adhesion of lung material to the diaphragm, therefore the material that needs to be detected is a thin layer of “glue” between two tissues. Thus the thin layer is not easily seen by non-penetrative imaging (i.e. cameras and hyperspectral imaging) and also does not create a strong density difference detectible by DXA X-ray imagers.

<u>Offal 62</u>

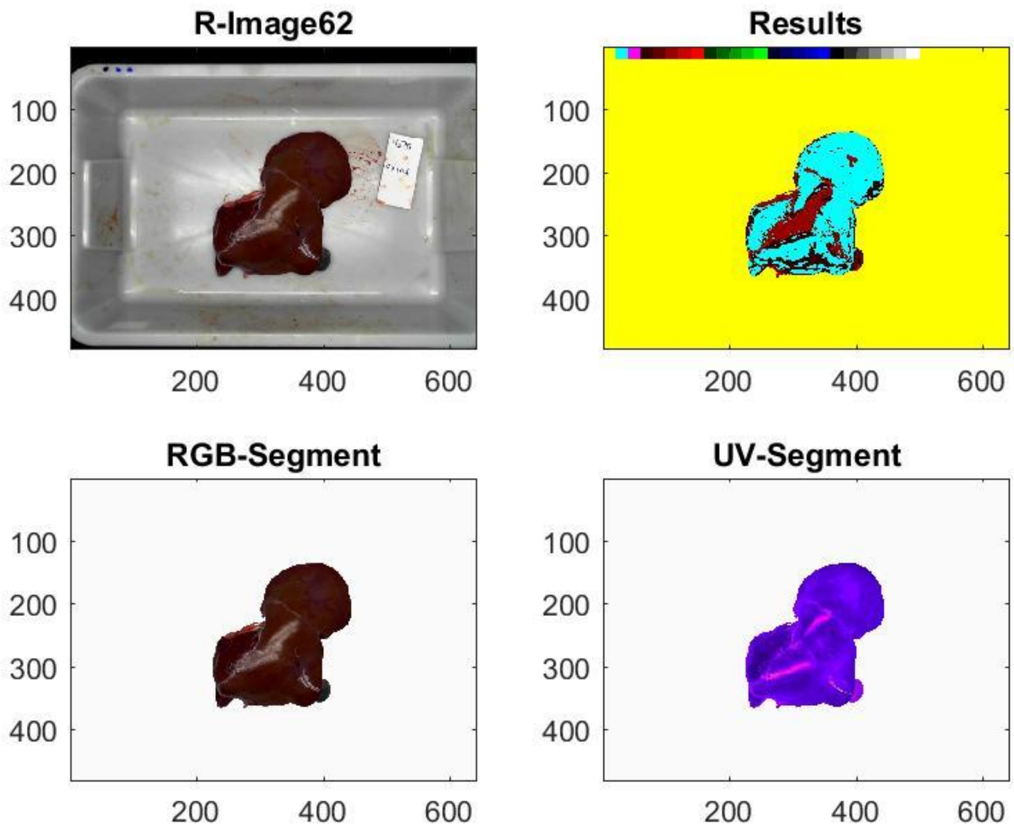

Interpretation:

Brown (least) and black (most) show regions of cirrhosis

Aqua shows regions of healthy tissue

Comments:

This liver was condemned for cirrhosis.

Offal 64

Interpretation:

Not analysed

Comments:

This pluck was condemned for pleurisy. Pleurisy is the adhesion of lung material to the diaphragm, therefore the material that needs to be detected is a thin layer of “glue” between two tissues. Thus the thin layer is not easily seen by non-penetrative imaging (i.e. cameras and hyperspectral imaging) and also does not create a strong density difference detectible by DXA X-ray imagers.

<u>Offal 64</u>

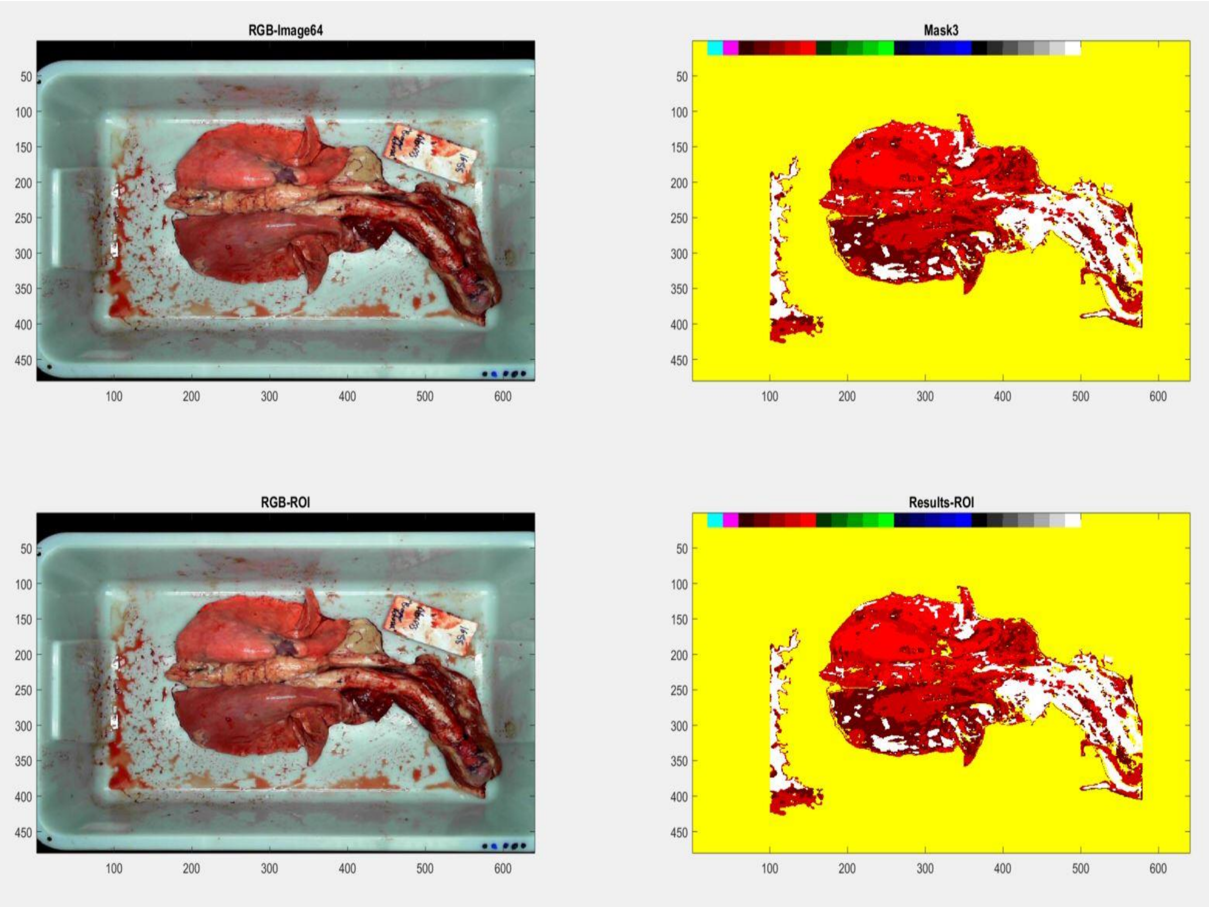

Interpretation:

Red (healthy) to light brown to dark brown (most unhealthy) lug tissue

White shows tissue not of interest.

Comments:

This lung was condemned for the presence of a "biomass adhesion" beside the trachea and top lung and also an abscess at the left edge of the lower lung. In this image the abscess was identified as very unhealthy tissue rather than being strongly differentiated.

Offal 65

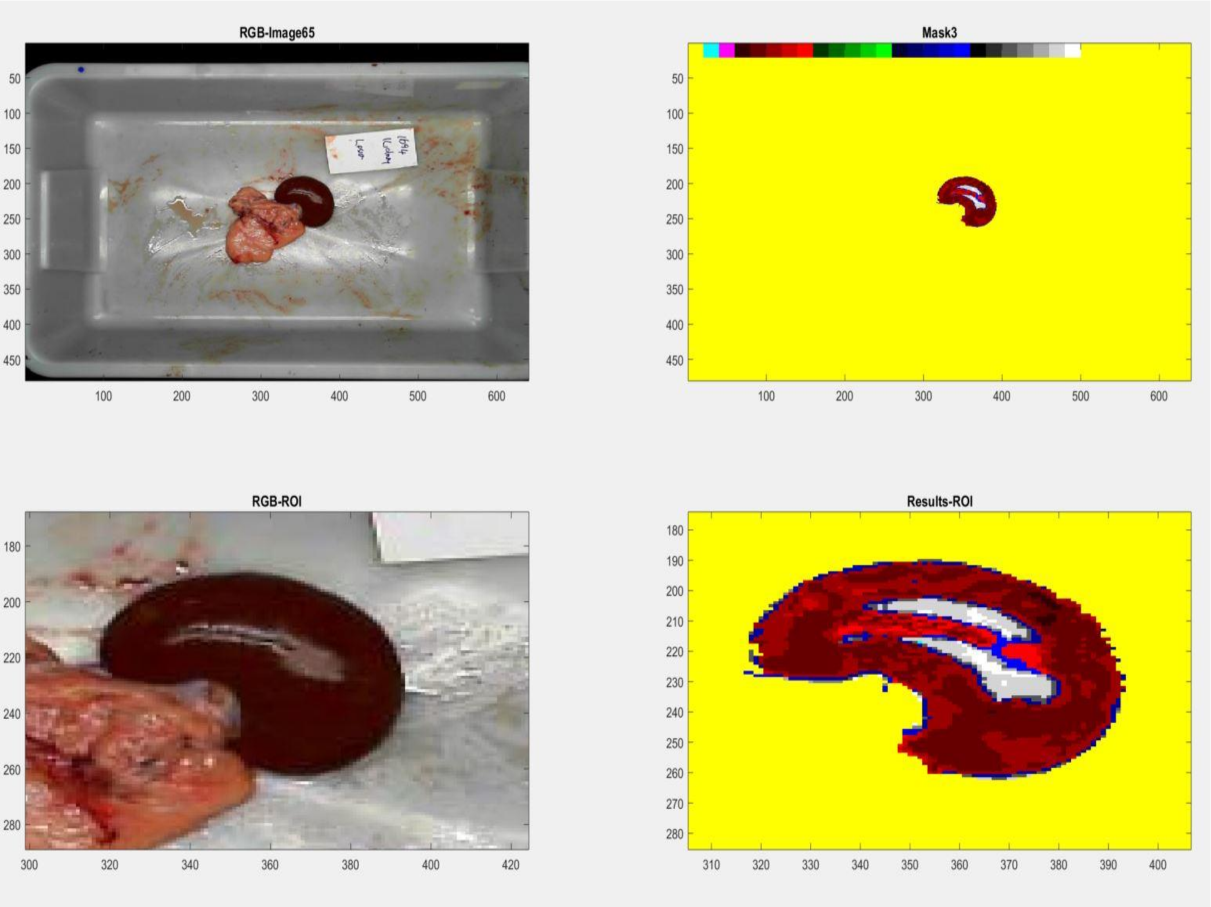

Interpretation:

Dark brown (least), light brown, red and blue (most) show regions of nephritis

White areas are reflective light

Aqua shows regions of healthy tissue

Comments:

This kidney was condemned for lesions along the bright band, with the algorithm correctly identifying the band between the reflections as highly diseased

Offal 66

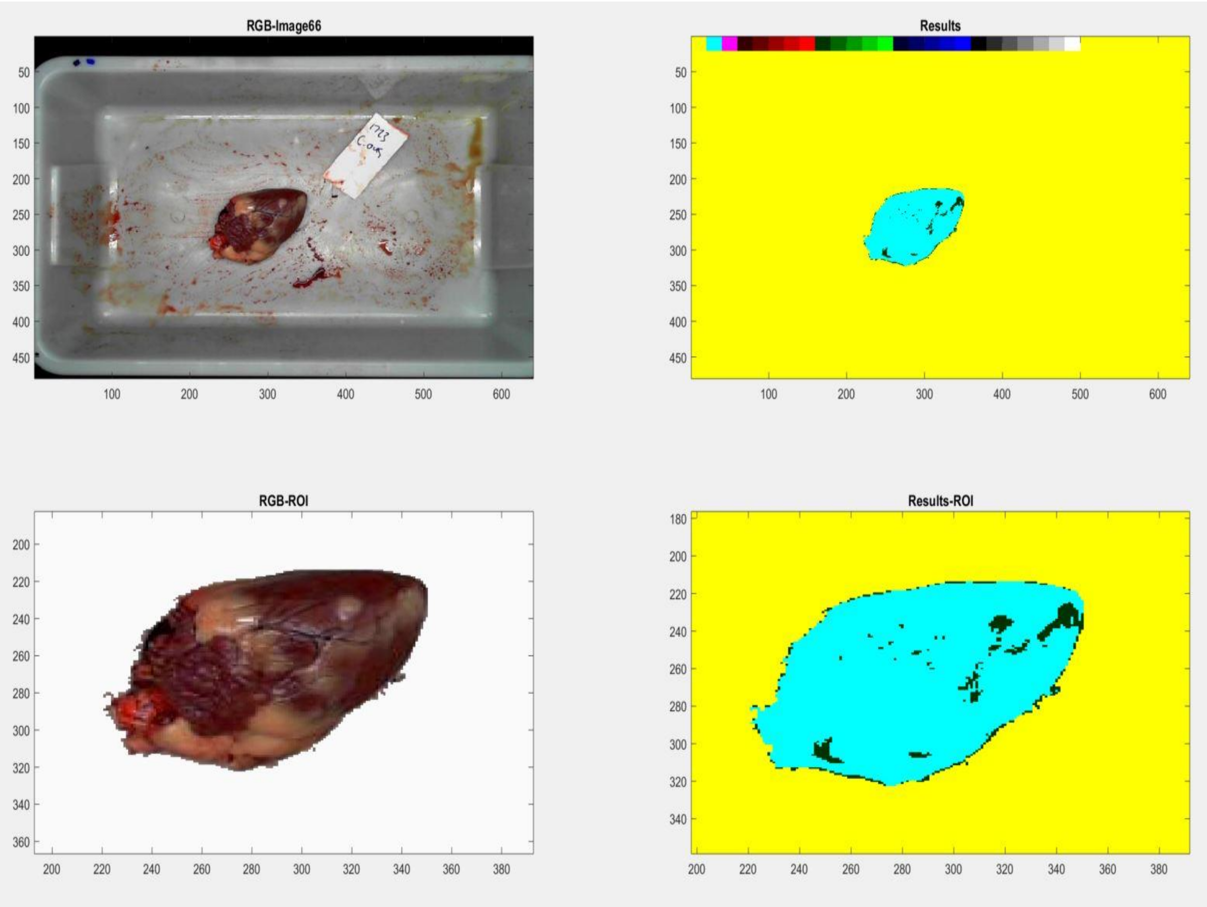

Interpretation:

Olive shows regions of c. ovis cysts

Aqua shows regions of healthy tissue

Comments:

This heart was condemned for the presence of c. ovis [300,240]

Offal 67

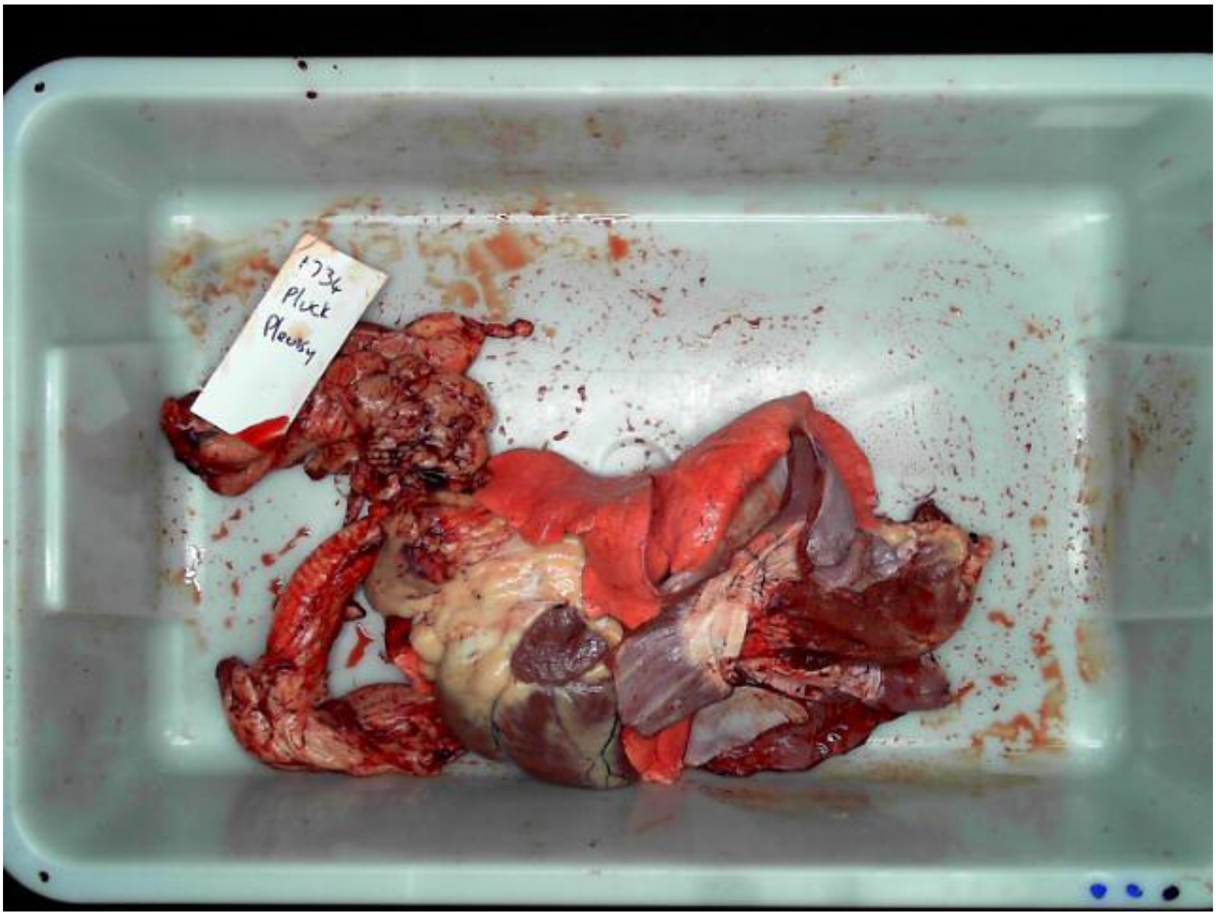

Interpretation:

Not analysed

Comments:

This pluck was condemned for pleurisy. Pleurisy is the adhesion of lung material to the diaphragm, therefore the material that needs to be detected is a thin layer of “glue” between two tissues. Thus the thin layer is not easily seen by non-penetrative imaging (i.e. cameras and hyperspectral imaging) and also does not create a strong density difference detectible by DXA X-ray imagers.

Offal 68

Interpretation:

Not analysed

Comments:

The data for this tray was taken for use in the offal identification algorithm. When used for finding condemned tissue it failed.

Offal 69

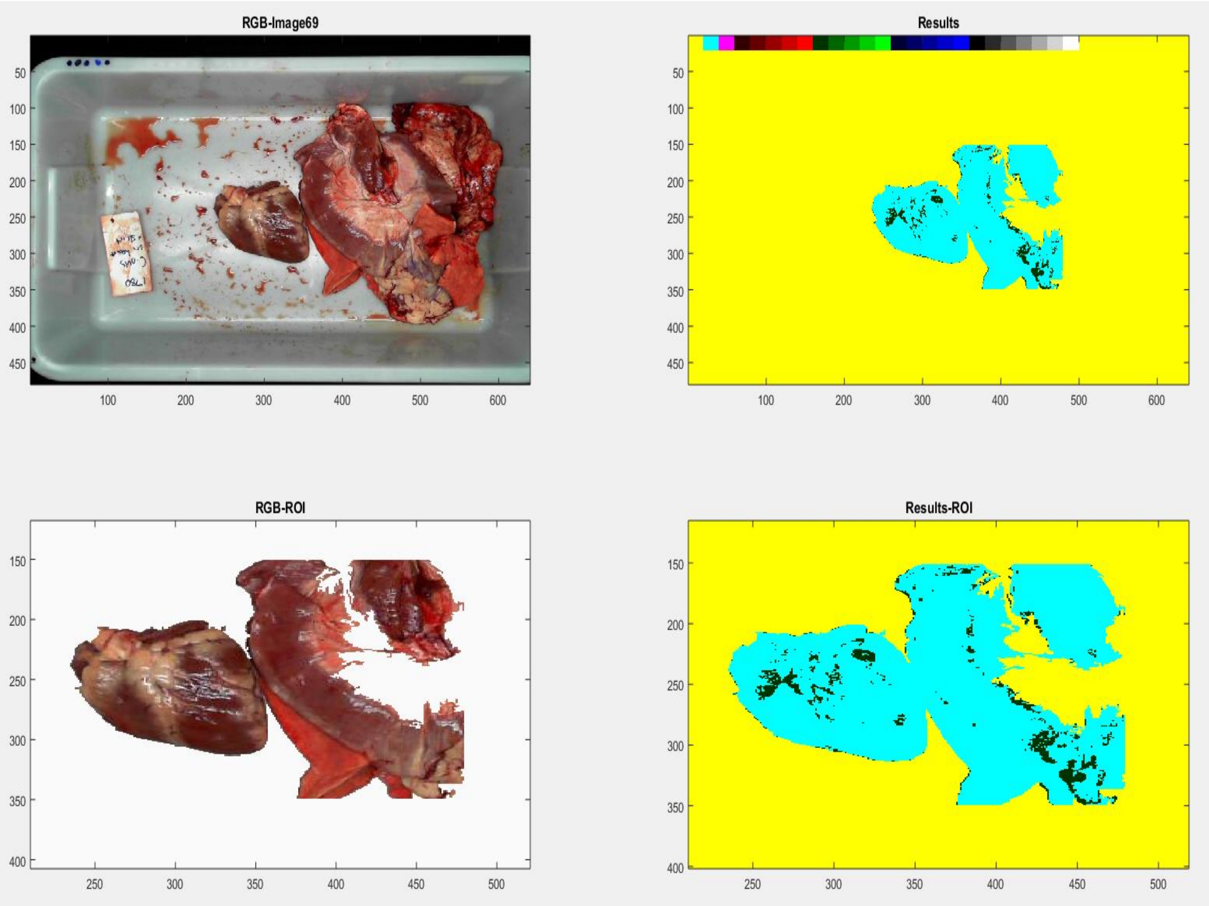

Interpretation:

Olive shows regions of c. ovis cysts

Aqua shows regions of healthy tissue

Comments:

This pluck was condemned for c. ovis on the heart and skirt. The “indicated c.ovis” on the heart is incorrect and there is no indication of c. ovis on the diaphragm (c.f. bright spot around the edge in the RGB image)

<u>Offal 70</u>

Interpretation:

Not analysed

Comments:

This pluck was condemned for pleurisy. Pleurisy is the adhesion of lung material to the diaphragm, therefore the material that needs to be detected is a thin layer of “glue” between two tissues. Thus the thin layer is not easily seen by non-penetrative imaging (i.e. cameras and hyperspectral imaging) and also does not create a strong density difference detectible by DXA X-ray imagers.

Offal 71

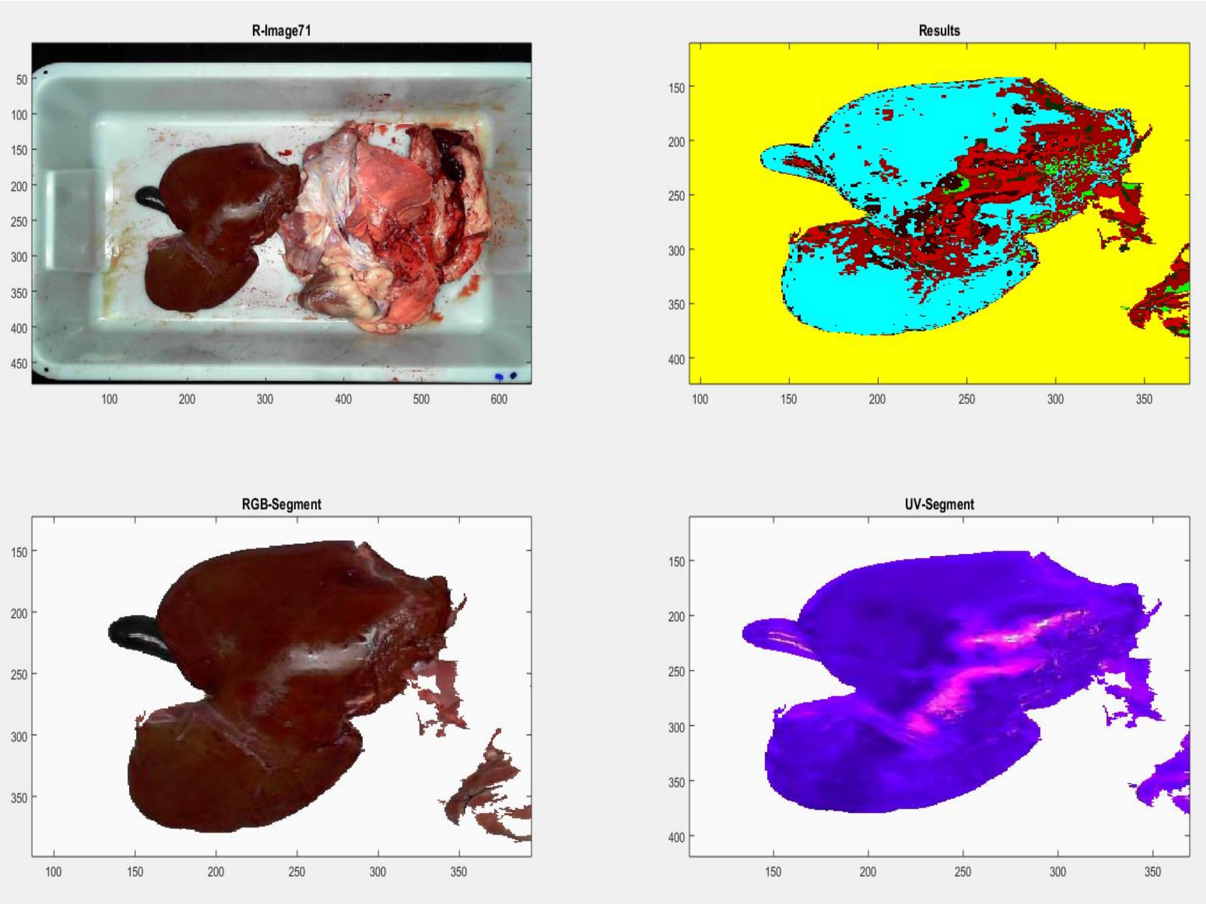

This tray comprised offal from Offal70 and a liver from Offal62

Interpretation:

Brown (least) and black (most) show regions of cirrhosis

Aqua shows regions of healthy tissue

Comments:

This liver was condemned for cirrhosis.

The lung was condemned for pleurisy.

Offal 72

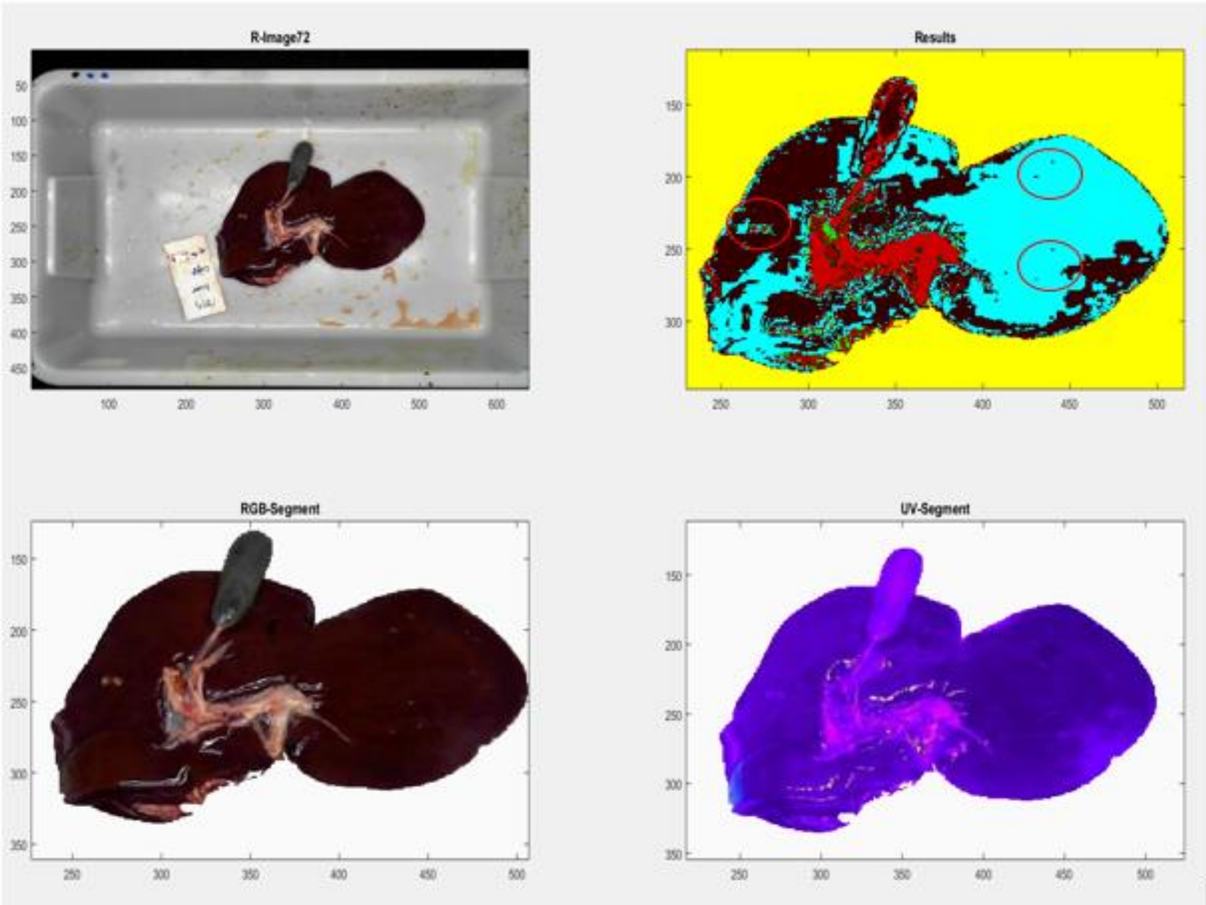

Interpretation:

Brown (least) and black (most) show regions of cirrhosis

Green shows "abnormal biomass"

Aqua shows regions of healthy tissue

Comments:

This liver was condemned for having more than 5 cysts. The cysts are identified by green/brown within the ellipses. [The identification was confirmed by blowing up the RGB image.]

<u>Offal 73</u>

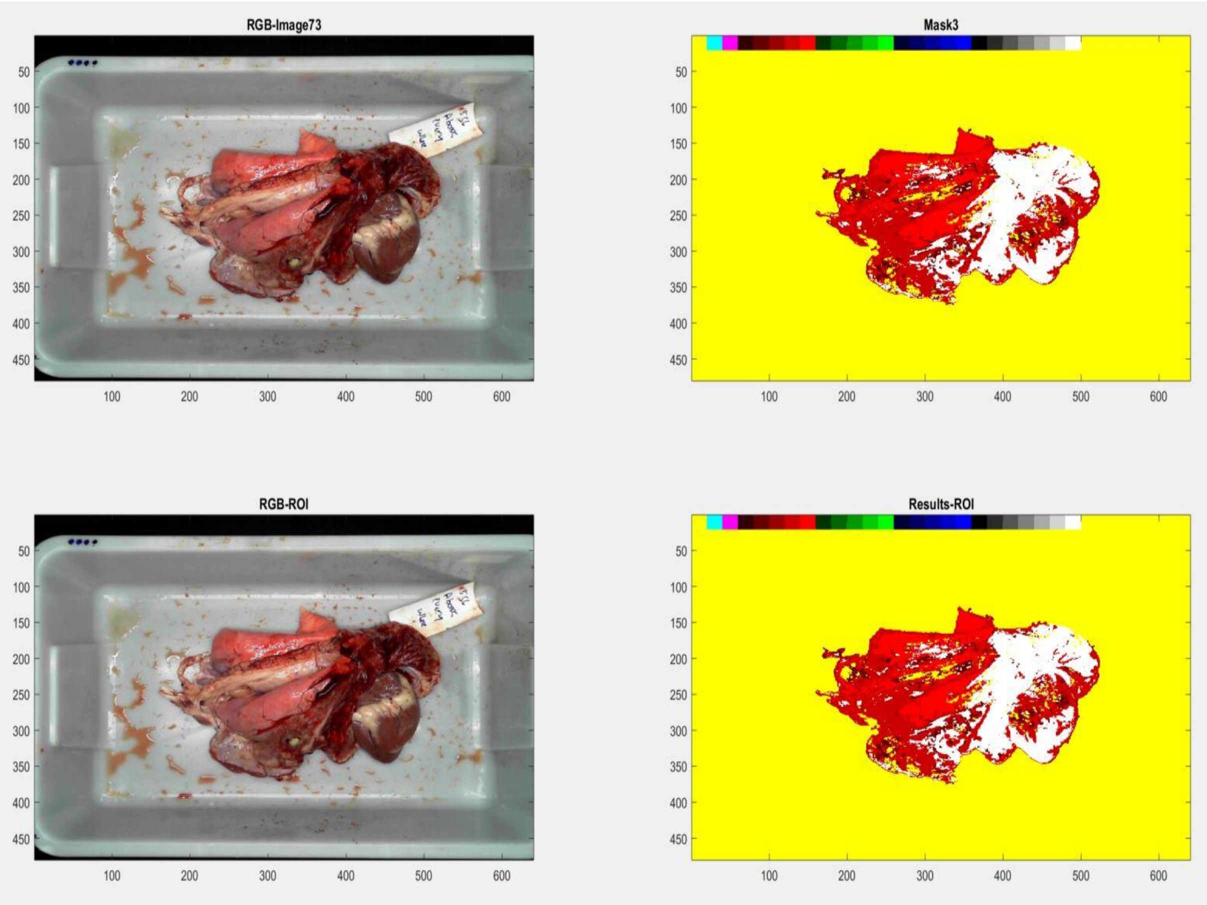

Interpretation:

Red (healthy) to light brown to dark brown (most unhealthy) lug tissue

White shows tissue not of interest.

Comments:

This lung was condemned for the presence of abscesses at the left edge of the upper lung, and also the abscess on the diaphragm. In this image the abscess was identified as unhealthy tissue rather than being strongly differentiated.

Offal 74

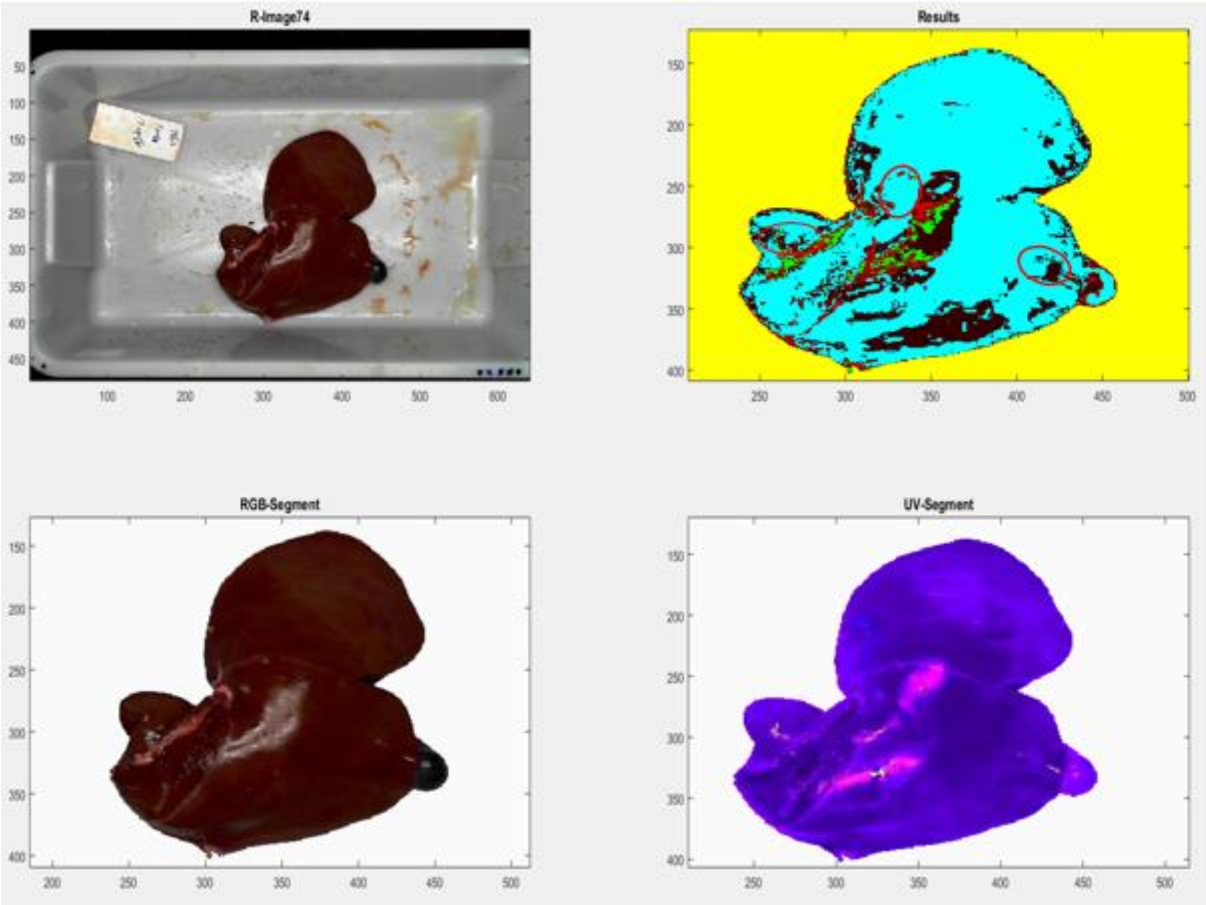

Interpretation:

Brown (least) and black (most) show regions of cirrhosis

Green shows "abnormal biomass"

Aqua shows regions of healthy tissue

Comments:

This liver was condemned for having more than 5 cysts. The cysts are identified by green/brown within the three ellipses. [The identification was confirmed by blowing up the RGB image.]

Offal 75

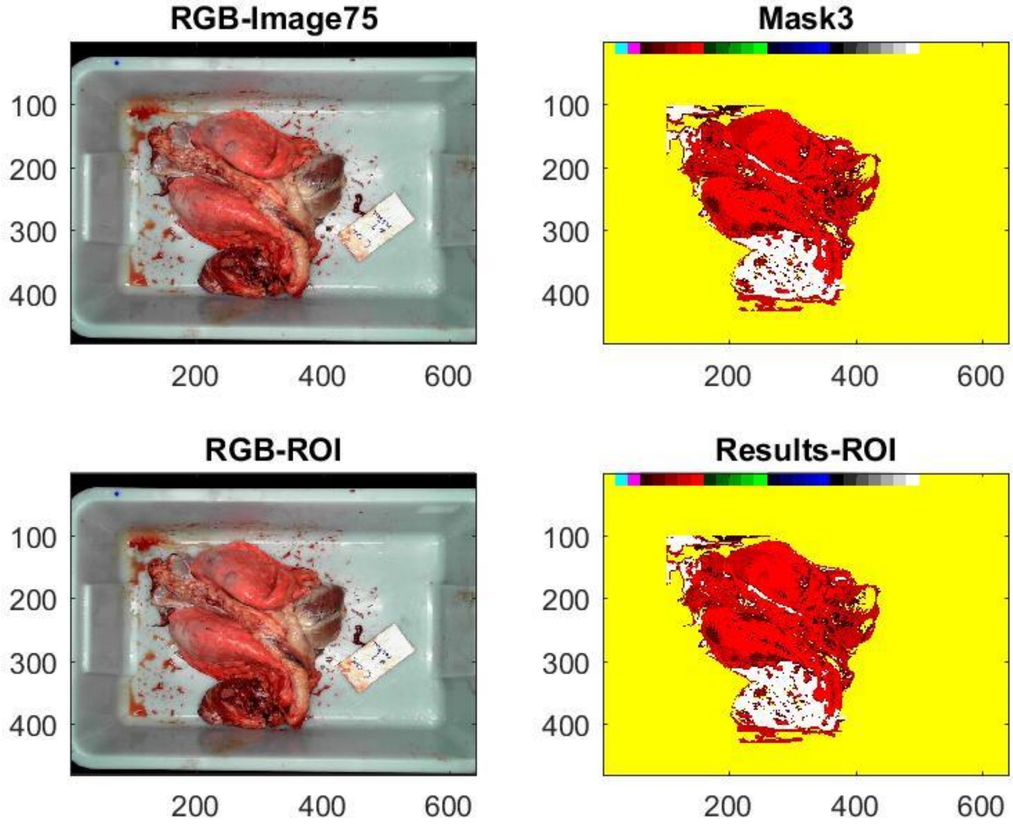

Interpretation:

Red (healthy) to light brown to dark brown (most unhealthy) lug tissue

White shows tissue not of interest.

Comments:

This lung was condemned for the presence of three abscesses at the lower lungs (upper left in the images)

The lower lung has strongly indicated, whereas the abscesses on the upper lung appear as “unhealthy tissue” only.

Offal 76

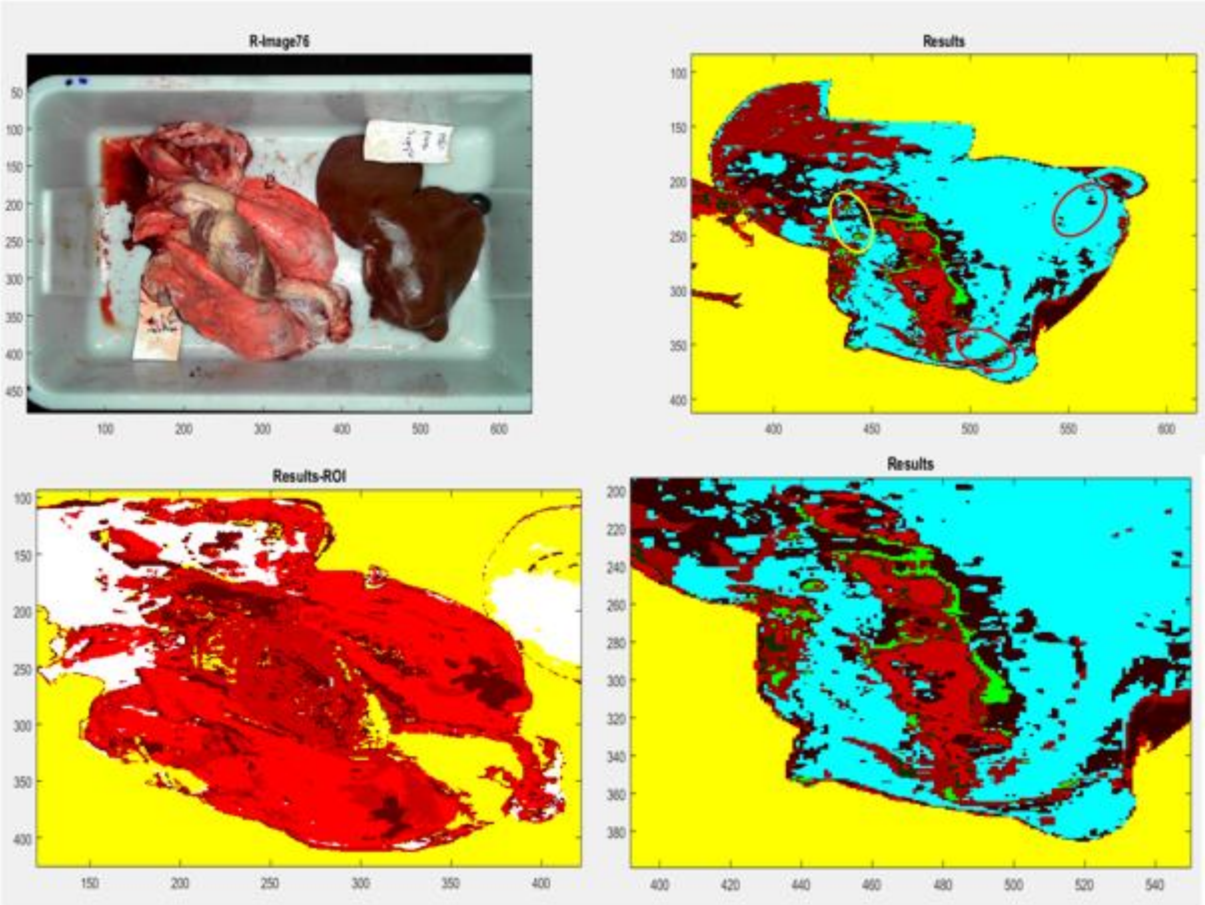

This tray is a composite of the offal in Offal 74 and 75

Interpretation:

The colours are as for Offal 74 and 75.

Comment

This set of results shows the impact of automatic camera adjustment.

- Abscesses in the lung have, ironically, become more strongly identified.
- Cysts on the liver have become more confounded.